JOURNAL OF QUATERNARY SCIENCE (2023) 1–34 ISSN 0267-8179. DOI: 10.1002/jqs.3559

JQS Journal of Quaternary Science QRA Quaternary Research Association

Biomarker proxies for reconstructing Quaternary climate and environmental change

ERIN L. MCCLYMONT,*† HELEN MACKAY,*† MARK A. STEVENSON, THALE DAMM-JOHNSEN, ELEANOR MAEDHBH HONAN, CLAIRE E. PENNY and YASMIN A. COLE
Department of Geography, Durham University, Durham, UK

Received 16 December 2022; Revised 30 June 2023; Accepted 4 July 2023

ABSTRACT: To reconstruct past environmental changes, a range of indirect or proxy approaches can be applied to Quaternary archives. Here, we review the complementary and novel insights that have been provided by the analysis of chemical fossils (biomarkers). Biomarkers have a biological source that can be highly specific (e.g. produced by a small group of organisms) or more general. We show that biomarkers are able to quantify key climate variables (particularly water and air temperature) and can provide qualitative evidence for changes in hydrology, vegetation, human–environment interactions and biogeochemical cycling. In many settings, biomarker proxies provide the opportunity to simultaneously reconstruct multiple climate or environmental variables, alongside complementary and long-established approaches to palaeoenvironmental reconstruction. Multi-proxy studies have provided rich sets of data to explore both the drivers and impacts of palaeoenvironmental change. As new biomarker proxies continue to be developed and refined, there is further potential to answer emerging questions for Quaternary science and environmental change. © 2023 The Authors *Journal of Quaternary Science* Published by John Wiley & Sons Ltd

KEYWORDS: biomarkers; palaeoclimate; palaeoenvironment; proxies; Quaternary

Introduction

To reconstruct past environmental and climate changes, indirect physical, chemical or biological signals of environmental variables ('proxies') are recovered from a range of archives (e.g. marine and lake sediments, ice cores, speleothems, peatlands). Biomarker proxies are molecular or chemical fossils with a biological origin (Eglinton and Calvin, 1967), which can be recovered, analysed and identified from palaeoenvironmental archives (Peters *et al.*, 2005). Biomarkers have emerged as valuable parts of the Quaternary science toolkit, due to both quantitative and qualitative insights into past environmental changes and because multiple biomarkers (and thus multiple environmental signals) are simultaneously recovered from single samples.

Biomarkers can either be very specific in terms of their environmental signal or biological source (e.g. individual highly branched isoprenoids indicative of sea-ice diatoms), or be more general indicators (e.g. mixtures of *n*-alkanes derived from higher plants) (Figure 1). A key strength of biomarker analysis is that biomarkers from multiple settings can be found in a single sediment sequence, since terrestrial biomarkers (from bedrock, soils or plants) may be transported by wind, rivers or ice into lakes, wetlands, caves or marine environments, allowing both the transport process and changes in different environments to be explored (e.g. Jaffé *et al.*, 2001; Ngugi *et al.*, 2017; Müller *et al.*, 2018). Biomarker transport can also be a disadvantage: advection or bioturbation may influence how biomarkers are incorporated into the sediments and can even lead to age-offsets between different proxies (e.g. Ohkouchi *et al.*, 2002). As organic molecules, biomarkers are subject to degradation processes during transport and deposition (e.g. Madureira *et al.*, 1997; Wakeham *et al.*, 1997; Thomas *et al.*, 2001). However, different classes of organic compounds have varying rates of degradation (Arndt *et al.*, 2013). Some of the most widely applied biomarkers are those which are relatively resistant to alteration (e.g. plant waxes), or where (rapid) transformation of lipids or pigments found in living biomass leaves behind a recognizable chemical signal so that the source organisms or formation processes can be determined (e.g. Harris *et al.*, 1996; Pitcher *et al.*, 2009). Biomarkers may be particularly useful in environments where other proxies (e.g. plant macrofossils) are degraded but their chemical remains can be found (e.g. Ronkainen *et al.*, 2015).

A valuable property of biomarkers is that they can be isolated from the original archive so that isotope analysis can be undertaken on individual components of organic matter with a known origin. This 'compound-specific isotope analysis' (CSIA) contrasts with the analysis of bulk samples, where changing isotope ratios could reflect varying contributions of different organic sources through time or space, as well as environmental controls over the contributing isotopic signals (e.g. Holtvoeth *et al.*, 2019; McClymont *et al.*, 2022). By knowing the origin of the biomarker, the relative impact of biological and environmental controls on stable isotope ratios can be determined (Sachse *et al.*, 2012; Holtvoeth *et al.*, 2019). CSIA has enabled, for example, separation of the contributions of C_3 and C_4 plants and isolation of hydrological controls over plant wax deuterium/hydrogen isotopes (see 'Reconstructing vegetation and hydrological change using compound-specific stable isotope analysis').

*Correspondence: Erin L. McClymont and Helen Mackay, as above.
E-mail: erin.mcclymont@durham.ac.uk and helen.mackay@durham.ac.uk
†These authors contributed equally to this work and should be considered joint first authors.

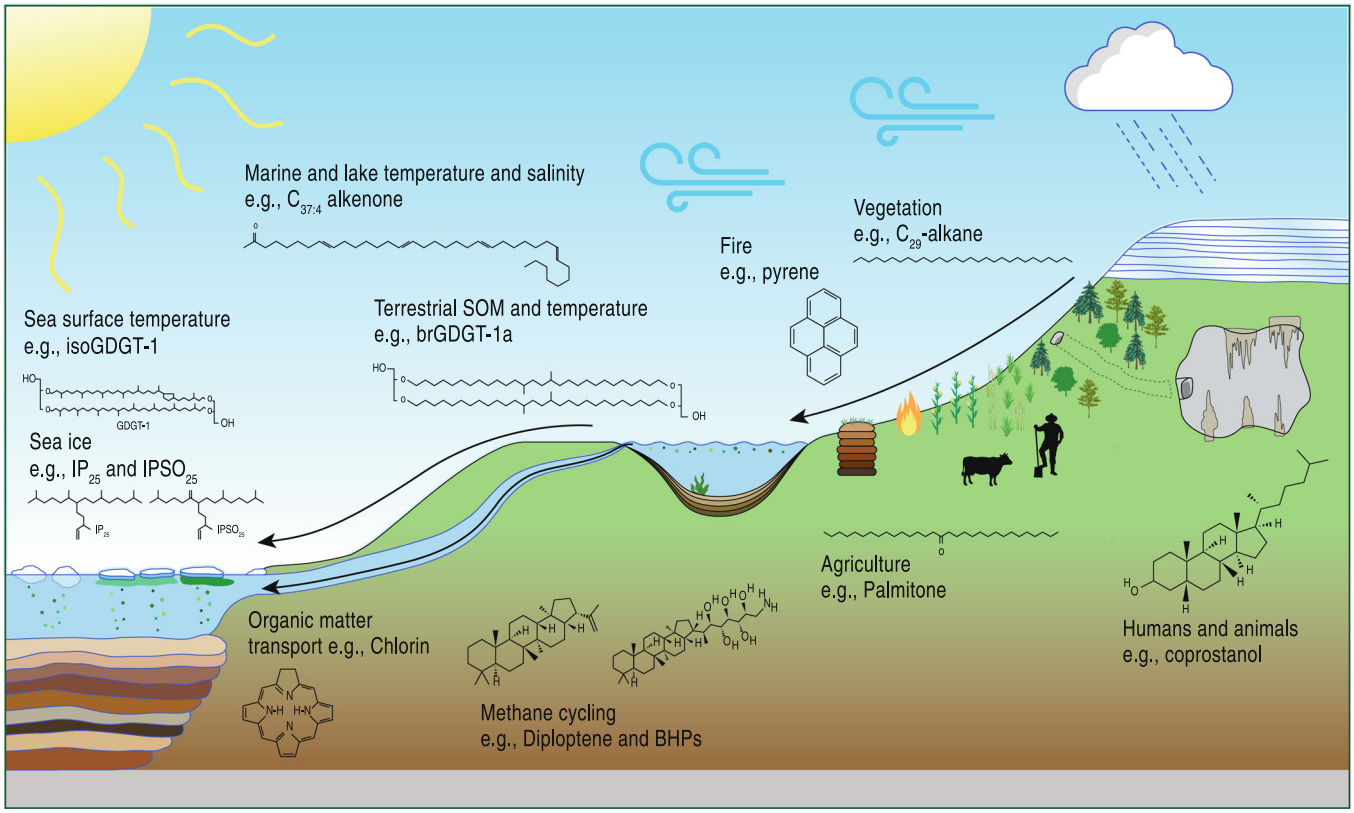

Figure 1. Using biomarkers to trace a wide range of environmental processes. Examples include biomarkers of climate change (e.g. temperature, precipitation, sea ice), ecosystem change (e.g. vegetation cover, productivity dynamics and fire regimes), biogeochemical cycling (e.g. methane production), sediment transport (e.g. soil residence time and land–ocean interactions), and human–environment interactions (e.g. presence of humans and animals and agricultural activity). Biomarkers can be transported between terrestrial ecosystems and to marine environments by rivers, surface water run-off, erosional processes, wind and melting ice. Abbreviations: IP_{25} (Ice Proxy with 25 carbon atoms), $IPSO_{25}$ (Ice Proxy Southern Ocean with 25 carbon atoms), isoGDGT (isoprenoidal glycerol dialkyl tetraether), brGDGT (branched glycerol dialkyl tetraether), BHPs (bacteriohopanepolyols). [Color figure can be viewed at wileyonlinelibrary.com]

Our aim in this review is to provide an accessible introduction to the wide range of biomarker applications in Quaternary science. Detailed reviews are also available on both biomarker synthesis and proxy development in marine sediments (Rosell-Melé, McClymont, 2007), lake sediments (Castañeda and Schouten, 2011), peatlands (Naafs *et al.*, 2019), speleothems (Blyth *et al.*, 2016; Meckler *et al.*, 2021) and geoarchaeology (Dubois and Jacob, 2016). Here, we explore a range of studies that have applied biomarker proxies and outline the novel and complementary contributions biomarkers have made to palaeoenvironmental reconstructions across a wide range of geographical regions, timescales and environments. The review was conducted using methodical keyword literature searches of the Web of Science and Google Scholar databases. The searches returned thousands of results; therefore, the scope of this review precludes citations of all relevant studies. To address our aim of providing an accessible overview of biomarkers and their applications for all Quaternary scientists, we have prioritized the inclusion of initial foundation studies alongside a diversity of examples that span different timescales, sedimentary archives, geographical locations and topics of Quaternary science. Since some biomarker proxies have been applied to multiple archives but reconstruct similar environmental variables (e.g. temperature, salinity), the review is structured according to those variables or research questions, and archive- or proxy-specific considerations are provided. Finally, we reflect on recent developments in biomarker research and consider their future potential in Quaternary science.

Introduction to biomarkers: analysis and functions

An overview of biomarker laboratory methods

Biomarkers used in Quaternary studies include water-insoluble lipids, photosynthetic pigments and macromolecules including lignin. Biomarkers are often present in very low (trace) concentrations in environmental samples (milligrams or nanograms per gram of material) and may be components of a complex matrix of organic and minerogenic materials. Isolating the biomarkers of interest requires methods that maximize recovery and minimize contamination. As multiple biomarkers are recovered simultaneously, a diverse range of environmental signals can be attained from a single sample.

Lipids and pigments are extracted from environmental or archaeological samples by using a range of organic solvents and approaches, tailored to the chemical properties of the compound(s) of interest. Ultra-sonication, microwave or accelerated solvent extraction methods are most commonly used but may have different efficiencies depending on sample size and composition (e.g. Kornilova and Rosell-Melé, 2003; Nichols, 2010; Kehelpannala *et al.*, 2020; Manley *et al.*, 2020). Lipid biomarkers are commonly extracted with dichloromethane and methanol in a ratio aligned with the expected polarity of the target marker, whereas pigments are typically extracted using acetone (e.g. Chen *et al.*, 2001) or a mixture of acetone, methanol and water (Leavitt and Hodgson, 2001). Pigment extractions can include soaking overnight at low temperatures (e.g. 20 °C) to minimize degradation (Jeffrey *et al.*, 1997).

Care is needed, because organic solvents will also extract unwanted compounds and add them to the extract, particularly plasticizers but also oils from the skin/hair of researchers handling the materials (e.g. Blyth *et al.*, 2006). As a result, subsampling cores or materials using metal spatulas, storing samples and extracts in glass jars or high-quality (low contaminant) bags, and using foil to separate samples from plastic bags or lids are effective strategies for minimizing contamination, alongside using laboratory personal protective equipment (e.g. Nichols, 2010). Inclusion of blanks during sample processing allows for contamination to be detected, monitored and isolated (Blyth *et al.*, 2016). Water can also interfere with lipid extraction efficiency and subsequent clean-up steps, and encourages oxidative degradation; the best approach is to freeze-dry samples (McClymont *et al.*, 2007; Nichols, 2010).

A common approach in palaeoenvironmental research is to recover multiple lipid biomarkers in a single extraction procedure to generate an 'extract' (Kornilova and Rosell-Melé, 2003; Nichols, 2010). The extract may then be separated into classes of compounds according to their chemistry (e.g. polarity, pH) to isolate the target biomarkers or to remove interfering compounds (Nichols, 2010). Biomarkers are then analysed using liquid (LC) or gas chromatography (GC), whereby a prepared sample is introduced to a capillary column and transferred to a detector by a flow of liquid or gas (Peters *et al.* 2005). Non-extractable material (e.g. lignins) can be introduced by pyrolysis, whereby high temperatures are used to split the large, refractory, molecules into diagnostic fragments (White *et al.*, 2004). The capillary column (usually 0.20–0.25 mm internal diameter) is coated with an internal film called the stationary phase, the chemistry of which determines how compounds are retained and released according to their chemical properties as they travel through the column. The result is a chromatogram of individual compounds separated by their chemical interaction with the column (Figure 2).

Biomarker identification usually involves the separated individual compounds being transferred directly to a mass spectrometer (LC-MS, GC-MS), which ionizes and fragments them into characteristic patterns (Peters *et al.*, 2005). Semi-quantitative analysis can be achieved by adding internal standards of known mass during the extraction steps, or a calibration curve will be derived using external standards of varying concentrations to enable absolute quantification (e.g. McGowan, 2013). However, some analysis remains qualitative where internal standards are not feasible (e.g. McClymont *et al.*, 2011). Ratios between different compounds may be more appropriate for characterizing changing biomarker distributions; for several biomarkers these ratios are defined as indices which are specifically linked to, or calibrated against, environmental variables (Tables 1 and 2).

Finally, the separation of organic matter also allows for CSIA. Not all samples or compounds are suitable: individual biomarkers need to meet higher detection limits than for GC or LC, and there needs to be excellent baseline separation between peaks. For compound-specific ^{14}C analysis, GC or LC techniques can be used to separate and then collect individual compounds or classes of compounds for subsequent analysis (Eglinton *et al.*, 1996; Yamane *et al.*, 2014; Sun *et al.*, 2020).

Biological functions of biomarkers

In this section we have selected examples to introduce the biological function of biomarkers and the mechanistic principles behind their palaeoenvironmental proxy applications. The biological function of biomarkers varies between different classes of compounds (Peters *et al.*, 2005; Bianchi and Canuel, 2011; Killops and Killops, 2013). Most lipid biomarkers used within Quaternary research can be classified as leaf wax or cell membrane lipids. Leaf wax lipids, such as *n*-alkanoic acids and *n*-alkanes, are synthesized by vegetation to act as waterproof protective barriers against the external environment and to control evaporative water loss and gas exchange (Eglinton and Hamilton, 1967; Post-Beittenmiller, 1996; Jetter *et al.*, 2006). The chain length of

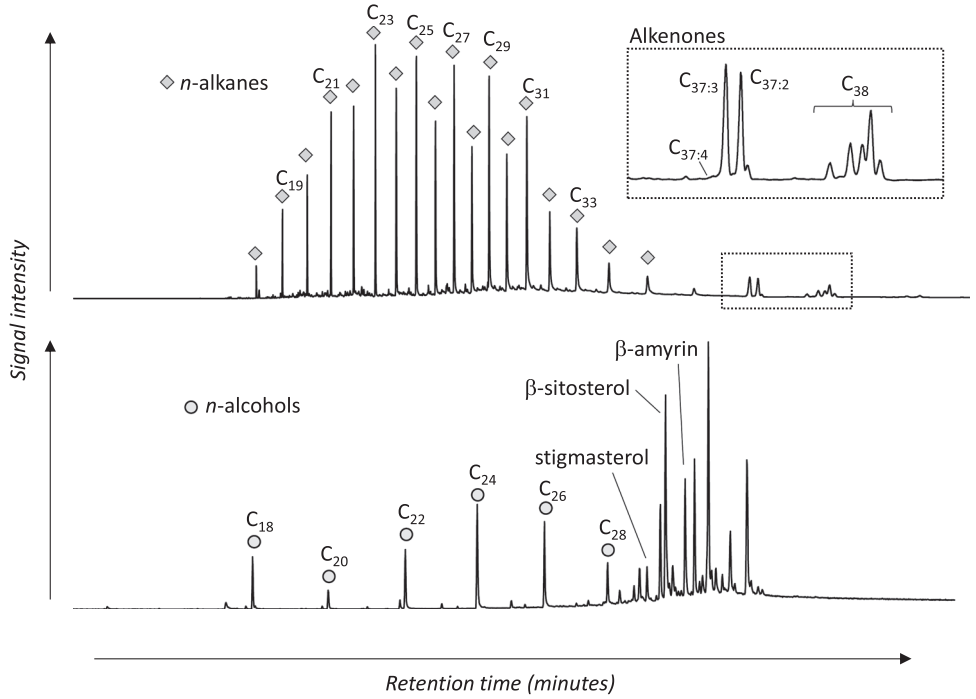

Figure 2. Two examples of biomarker distributions containing mixtures of aquatic and vascular plants. Analysis is by chromatography, whereby individual compounds are separated according to their size and chemical structures. The sample is injected at time zero, and the size of the peak corresponds to the abundance of that molecule in the sample. (a) Gas chromatogram of the apolar compounds recovered from a lake or marine sediment sample, showing a mixture of aquatic and vascular plant inputs; (b) gas chromatogram of the polar compounds recovered from a peatland sample, showing a mixture of vascular plant inputs.

Table 1. Biomarker proxies for aquatic temperatures. For the equations underpinning the listed indices please see the original publications.

Proxy	Source	Calibration	Uncertainty	Reference
Marine sea-surface temperatures (SSTs)				
U^{K}_{37}'	Ratio of long-chain (C_{37}) ketones (alkenones) synthesized by haptophyte algae	Linear core-top calibration, mean annual SST	Includes all three C_{37} alkenones but potential influence of salinity and/or sea ice over $C_{37:4}$	Brassell *et al.* (1986), Rosell-Melé (1998)
U^{K}_{37}' index	Ratio of long-chain (C_{37}) ketones (alkenones) synthesized by haptophyte algae	Linear, non-linear and Bayesian calibrations, generally to mean annual SST (core-top) or growth temperature (cultures)	Core-top calibration uncertainty 1.5 °C (1σ; linear), 1.4 °C (1σ, <23.4 °C; BAYSPLINE), up to 4.4 °C (1σ, at 29.4 °C; BAYSPLINE), Non-linearity and seasonal bias at high latitudes in Bayesian calibrations	Linear: Prahl and Wakeham (1987), Müller *et al.* (1998), Non-linear: Conte *et al.* (2006), Bayesian: Tierney and Tingley (2018)
U^{K}_{38Me}' index	Ratio of long-chain (C_{38}) ketones (alkenones) synthesized by haptophyte algae	Linear core-top calibration, mean annual SST	Core-top calibration uncertainty 1.84 °C (including sea ice samples) or 1.30 °C (excluding sea ice samples)	Novak *et al.* (2022)
TEX_{86} index	Ratio of glycerol dialkyl glycerol tetraethers (GDGTs) synthesized by Thaumarchaeota	Linear, non-linear and Bayesian calibrations, to mean annual SST or to mixed-layer temperatures (core-tops)	Potential integration of mixed-layer temperatures not just SST, Non-linear calibrations not recommended due to observed biases	Linear: Schouten *et al.* (2002), Non-linear: Kim *et al.* (2010), Bayesian: Tierney and Tingley (2014), Inglis and Tierney (2020)
Long-chain diol index (LDI)	Ratio of 1,13- and 1,15-long-chain diols, synthesized by marine eustigmatophyte algae in cultures	Linear core-top	3 °C (1σ), Not applicable to sediments where salinity <32 psu; some regional-specific non-thermal influences	Rampen *et al.* (2012), De Bar *et al.* (2020)
RAN_{13}	Ratios of the isomers of 3-hydroxy C_{13} fatty acids synthesized by bacteria	Latitudinal transect core-top calibration (NW Pacific)	2.25 °C (RMSE)	Yang *et al.* (2020)
Terrestrial temperature proxies				
U^{K}_{37}' index	Ratio of long-chain (C_{37}) ketones (alkenones) synthesized by haptophyte algae	Multiple calibrations for lake surface water temperatures, which may be calibrated to air temperatures depending on the location. Seasonal or mean annual	e.g. Freshwater lakes: 1.3 °C (spring–summer Greenland and Europe), e.g. Brackish lake cultures: 1.6 °C (RMSE) different producers and temperature sensitivities	Greenland lakes: D'Andrea *et al.* (2011), Alaskan lakes: Longo *et al.* (2016), Brackish lakes: Theroux *et al.* (2020), Reviewed by Castañeda & Schouten (2011)
TEX_{86} index	Ratio of glycerol dialkyl glycerol tetraethers (GDGTs) synthesized by Thaumarchaeota	Multiple calibrations for lake surface water temperatures, which may be calibrated to air temperatures depending on the location. Seasonal or mean annual	2.1–3.6 °C (RMSE), Mean annual air temperature, Potential for production at depth in the lake, rather than a surface water temperature	Powers *et al.* (2010), Tierney *et al.* (2010), Sinninghe Damste et al. (2022), Reviewed by Castañeda & Schouten (2011)
		Cave or surface air temperature	Connection between GDGT and surface air temperature, but some unknown influences occur. Relatively small calibration dataset needed and recognition of in-cave variables such as location and cave micro-environment	Blyth *et al.* (2016), Baker *et al.* (2019)
MBT and CBT ratios	MBT: ratio of branched GDGTs with varying numbers of methyl groups, CBT: ratio of branched GDGTs with varying numbers of cyclopentyl moieties. Synthesized by (acido)bacteria	MBT related to air temperature and precipitation. Strong impact of pH on CBT enables air temperature to be reconstructed by combining MBT and CBT	Mean annual air temperature calibrations (RMSE ~5 °C) but potential insensitivity <5 °C and >20 °C, Alternative calibrations needed in (semi-) arid soils due to temperature influence on CBT (RMSE 1.83 °C)	Weijers *et al.* (2007), Peterse *et al.* (2012), Yang *et al.* (2014)
MBT'_{5Me} index	Ratio of branched GDGTs including the 6-methyl isomers synthesized by (acido)bacterial (note that full range of source organisms remains unknown)	Global soil calibration, recovered from lakes, peats and speleothems	4.8 °C (RMSE) in soils, Mean annual air temperature	De Jonge *et al.* (2014), Baker *et al.* (2019)
Long-chain diol index (LDI)	Ratio of 1,13- and 1,15-long-chain diols, synthesized by freshwater eustigmatophyte algae in cultures	Lake surface water temperatures	Potential temperature influence, but seasonality in production and uncertainty around producers limits application	Rampen *et al.* (2014), Lattaud *et al.* (2021)
RAN_{15} and RAN_{17}	Ratios of the isomers of 3-hydroxy C_{15} and C_{17} fatty acids synthesized by bacteria	Global soil calibration, recovered from lakes and speleothems	3.5 °C RMSE in lakes, Potential influence of pH	Wang *et al.* (2021a)

Table 2. Examples of lipid ratios and compounds used to identify differences in vegetation source and environmental conditions.

Ratio or biomarker	Representation	Interpretation	Example reference(s)
Average chain length (ACL)	Weighted average indication of plant input (*n*-alkanes)	Higher values represent more higher plant inputs, which can be driven by higher temperatures and/or drier conditions	Poynter *et al.* (1989), Schefuß *et al.* (2003), Zhou *et al.* (2010)
Carbon Preference Index (CPI)	*n*-Alkanes with odd over even carbon atom preference, which reflects source material, maturity level and/or contamination	Higher values can indicate reduced decomposition (e.g. fresher material, colder/drier conditions), lower values can also be driven by petroleum or microbial inputs	Bray and Evans (1961), Zhou *et al.* (2010)
P(aqueous):, $(C_{23}+C_{25})/(C_{23}+C_{25}+C_{29}+C_{31})$ *n*-alkanes	Hydrological: submerged vascular compared withterrestrial species	Higher values indicate relatively more submerged plant input and wetter conditions	Ficken *et al.* (2000)
P(wax):, $(C_{27}+C_{29}+C_{31})/(C_{23}+C_{25}+C_{27}+, C_{29}+C_{31})$ *n*-alkanes	Hydrological: emerged species compared with total vegetation	Higher values indicated more vascular plant inputs and drier conditions	Zheng *et al.* (2007)
C_{23}/C_{31} *n*-alkanes	*Sphagnum* vs higher plants	Higher values indicate relatively more *Sphagnum* input and wetter conditions	Bingham *et al.* (2010)
C_{23}/C_{29} *n*-alkanes (peatlands)	*Sphagnum* vs non-*Sphagnum* plants	Higher values indicate relatively more *Sphagnum* input and wetter conditions	Nichols *et al.* (2006)
C_{29}/C_{33} *n*-alkanes (palaeosols)	Deciduous trees vs grasses and herbs		Trigui *et al.* (2019)
C_{27}/C_{31} *n*-alkanes (stalagmites)	Grass:tree		Xie *et al.* (2003), Blyth *et al.* (2007)
5-*n*-alkylresorcinols	Presence of sedges		Avsejs *et al.* (2002), McClymont *et al.* (2008a)
4-Isopropenylphenol (peatlands)	Analytical product of *Sphagnum* acid, specific to *Sphagnum*	Higher abundance reflects more *Sphagnum*	Boon *et al.* (1986), McClymont *et al.* (2011)
Sterols	Range of markers depending on vegetation type	E.g. lupeol, obtusifoliol, gramisterol from sedge roots in fens	Ronkainen *et al.* (2013)
Triterpenoids	Range of markers depending on vegetation type	E.g. taraxerol as an indicator of mangroves in tidal sediments or Ericaceae in peatlands, millacin as an indicator of millet	Versteegh *et al.* (2004), Jacob *et al.* (2008a, 2008b), Pancost *et al.* (2002)
Ketones	Range of markers depending on vegetation type	E.g. palmitone as an indicator of *Colocasia esculenta* (taro)	Krentscher *et al.* (2019)
Lignin phenols	Terrigenous inputs from vascular parts of plants	Identify vegetation type and extent, disentangling non-woody woody angiosperms and gymnosperm vegetation. Cannot provide species-level identification. Requires combination with pollen or macrofossil analysis if species-level information needed	Hedges *et al.* (1982), Orem *et al.* (1997), Tareq *et al.* (2011)
Polycyclic aromatic hydrocarbons (PAHs)	Incomplete combustion of organic matter	Proxy for vegetation burning. Some alkylated PAHs are also formed during thermal maturation and petrogenic processes, but ratios have been applied to distinguish between (non)pyrogenic sources and identify vegetation type	Ramdahl (1983), Reviewed by Karp *et al.* (2020), including ratio details
Levoglucosan and other monosaccharide anhydride (MA) compounds	Pyrolysis of carbohydrates such as from vegetation	Wildfire intensity indicator. Ratios of MA indicate the vegetation type involved in the burn and burn conditions. Sometimes only detectable in low abundance. Can be challenging to disentangle local from regional fire histories	Simoneit *et al.* (1999), Reviewed by Bhattarai *et al.* (2019)

leaf wax molecules varies between different plant species and hydrological conditions: aquatic (terrestrial) species are characterized by shorter (longer) chain lengths since they are adapted to wetter (drier) conditions (Cranwell *et al.*, 1987; Ficken *et al.*, 2000; Schefuß *et al.*, 2003; Table 2). Biochemical responses to environmental conditions can occur at fine scales, which should be considered during interpretation of the sedimentary record. For example, *n*-alkane chain lengths (Ronkainen *et al.*, 2013) or concentrations (Huang *et al.*, 2011) have been shown to differ between the leaves and roots of wetland species (Ronkainen *et al.*, 2013; Andersson *et al.*, 2011), and both humidity and the timing of leaf growth can impact *n*-alkane distributions even within single plants (e.g. Sachse *et al.*, 2010; Eley and Hren, 2018). There is also evidence for loss and transformation of some *n*-alkyl components within soils, although the dominant chain lengths tend to be maintained with depth (Thomas *et al.*, 2001).

Cell membrane lipids are synthesized by a range of organisms including fungi, algae, plants and animals (such as sterols, e.g. Volkman, 1986), archaea (including isoprenoidal glycerol dialkyl glycerol tetraethers [isoGDGTs], e.g. Nishihara and Koga, 1987, Sinninghe Damsté *et al.*, 2000)

and eubacteria (such as hopanoids, e.g. Innes *et al.* 1997; Ourisson *et al.* 1979). Membrane lipids are structural components of cells that provide a stable controlled environment for biogeochemical reactions. Cell membrane lipids regulate the fluidity (or permeability) of the cell membrane by altering structural features such as chain lengths, the placement of unsaturated (double) bonds and cyclic rings (Peters *et al.*, 2005; Bianchi and Canuel; 2011; Killops and Killops, 2013; Figure 3). For example, temperature changes are expressed by the number and position of methyl groups of branched GDGTs (brGDGTs; Weijers *et al.*, 2007) and the number of cyclopentane moieties of isoGDGTs (De Rosa *et al.*, 1980) (Figure 3; see next section).

The primary functions of some lipids remain unknown or poorly understood. For example, alkenones, synthesized by phytoplankton (Theroux *et al.*, 2010), were originally considered to be fluidity-influencing membrane lipids (e.g. Brassell *et al.*, 1986); however, more recent studies have demonstrated that they more probably contribute to energy storage and regulate properties such as melting point and therefore ease of lipid catabolism (e.g. Epstein *et al.*, 2001; Bakku *et al.*, 2018). Regardless of their specific function, differences in alkenone chain lengths and the degree of unsaturation (number of double bonds) can be used to reconstruct palaeotemperature (e.g. Brassell *et al.*, 1986; Figure 3; see 'Ocean and lake temperature reconstructions'). Some other types of biomarkers of interest to Quaternary scientists are transformation products that reflect environmental processes. For example, some polyaromatic hydrocarbons (PAHs) and monosaccharide anhydrides (MAs) are produced during combustion of organic matter and can therefore be used to reconstruct fire histories (see 'Biomarkers of burning and agricultural activity as indirect indicators of human activity').

Pigments can be relatively general biomarkers of photosynthetic processes (e.g. chlorophyll a/b/c and ββ-carotene are general productivity markers) or highly specific (e.g. alloxanthin is only found in cryptophytes; reviewed by McGowan, 2007). Pigment functions also vary: chlorophylls are active sites of photosynthesis, providing energy for the cell, whereas carotenoids can also help absorb light for photosynthesis (Jeffrey *et al.*, 1997) or help protect cells from ultraviolet (UV) exposure (e.g. scytonemin; McGowan, 2007). The stability of pigments is dependent on specific chemistry, the environment and presence of photoprotection (Leavitt, 1993; Cuddington and Leavitt, 1999). Some pigments are susceptible to oxidative or UV degradation, and even in environments with good preservation there can be as much as 95% degradation in the water column before sedimentation (McGowan, 2007). Pigment analysis is thus often most effective in environments where preservation is facilitated by, for example, anoxic or low light conditions (e.g. Hodgson *et al.*, 2005). Where degradation allows characteristic fragments of the original pigment to be identified, valuable information can be recovered. For example, chlorins represent the preserved central ring structure of the original chlorophyll and are frequently selected as marine productivity biomarkers over glacial–interglacial timescales (Harris *et al.*, 1996) (see 'Reconstructing biological productivity in lakes and the oceans').

Quantifying amplitudes and rates of past temperature change

Air, water and soil temperatures are important for detailing climate system response to radiative forcing, including global climate sensitivity (Masson-Delmotte *et al.*, 2021). Temperatures trace heat transfers through ocean/atmosphere circulation systems and can be informative of local conditions which may influence ecosystems. Quantification of past temperature change has been a key achievement for biomarker proxies and continues to be a frontier of biomarker proxy development. Here, we first outline insights gained from marine and lacustrine settings, before discussing emerging terrestrial records from soils, peats and speleothems.

Ocean and lake temperature reconstructions

An early biomarker proxy success was the recognition that some aquatic organisms change their cell membrane chemistry in response to water temperature, and that these signals were detectable in sediments (Brassell *et al.*, 1986; Figure 3). Multiple biomarker temperature proxies have subsequently been developed (Table 1). Biomarker temperature indices describe distributions of lipids produced by selected photosynthesizing haptophyte algae (alkenone-derived U^{K}_{37}' and U^{K}_{38Me}' indices; Prahl and Wakeham, 1987; Novak et al., 2022), ammonia-oxidizing Thaumarchaeota (isoGDGT-derived TEX_{86} index; Schouten et al., 2022), eustigmatophyte algae (long-chain alkyl diol-derived LDI; Rampen *et al.*, 2012) and bacteria (hydroxy fatty acid-derived RAN_{13} index and brGDGT-derived MBT'_{5Me} index; De Jonge *et al.*, 2014; Yang *et al.*, 2020). As each proxy has different source organisms and controls (Table 1), there is potential to generate detailed water temperature reconstructions which might include seasonality or temperature profiles with water depth. Both the U^{K}_{37}' and TEX_{86} proxies have reconstructed temperatures through the Quaternary and beyond (e.g. Herbert *et al.*, 2010); more recently developed proxies have tended to focus on the Holocene or the last glacial cycle (e.g. Powers *et al.*, 2005; Warnock *et al.*, 2018; Yang *et al.*, 2020).

Biomarker water temperature proxies are calibrated using field sampling, laboratory culture experiments and sediment core-tops (Table 1). The accuracy and precision of the temperature proxies vary, especially at the upper and lower ends of the calibrations or close to detection limits, and not all proxies are found in all settings. Many of the proxies are calibrated to mean annual surface water temperature (Table 1), but if the producers have preferred seasons or water depths, a seasonal or subsurface temperature signal may be reconstructed (D'Andrea *et al.*, 2005, 2011; Jaeschke et al., 2017; Tierney and Tingley, 2018; Inglis and Tierney, 2020; Theroux *et al.*, 2020; Spencer-Jones *et al.*, 2021). Although marine biomarkers have global calibrations (Table 1), there can also be local controls over the biomarker–temperature relationship in all aquatic settings (e.g. salinity, sea/lake ice cover, lake size). In some settings a regional temperature calibration may be more appropriate (Table 1) (e.g. Bendle *et al.*, 2005; De Jonge *et al.*, 2014; D'Andrea *et al.*, 2016; Loomis *et al.*, 2014; Longo *et al.*, 2016; De Bar *et al.*, 2020; Sinninghe Damsté *et al.*, 2022; Yao *et al.*, 2022).

A key impact of marine sea surface temperature (SST) biomarker proxies has been the generation of quantitative data to calculate amplitudes and rates of change, climate response to changing CO_2, and to facilitate data–model comparisons (e.g. Brassell *et al.*, 1986; MARGO Project Members, 2005; Martrat *et al.*, 2007; Schmittner *et al.*, 2011; Capron *et al.*, 2017; Tierney *et al.*, 2020). Relatively strong mid- and high-latitude SST responses to glacial–interglacial cycles have been demonstrated (Martrat *et al.*, 2007; Naafs *et al.*, 2013), but tropical cooling has also been reconstructed during glacials (MARGO Project Members, 2005; Herbert *et al.*, 2010; McClymont *et al.*, 2013). U^{K}_{37}' records have shown that there are regional and temporal differences in the amplitudes of interglacial warming (MARGO Project Members, 2005; Past Interglacials Working Group of PAGES, 2016) and that early ocean cooling preceded the evolution of 100-ka glacial–interglacial cycles during the mid-Pleistocene

transition (McClymont *et al.*, 2013). Recent calibration of the U^{K}_{38Me}′ index shows potential to extend the upper linear calibration limit of the U^{K}_{37}′ proxy to ~30 °C (Novak et al., 2022), reducing the reconstructed uncertainties at high SSTs (Table 1) and enabling improved reconstructions of inter-glacial warmth and glacial–interglacial variability in the low latitudes.

Differences in absolute SSTs from U^{K}_{37}′ and TEX_{86} or LDI reconstructions from the same sediment sequences have revealed circulation changes on a range of timescales

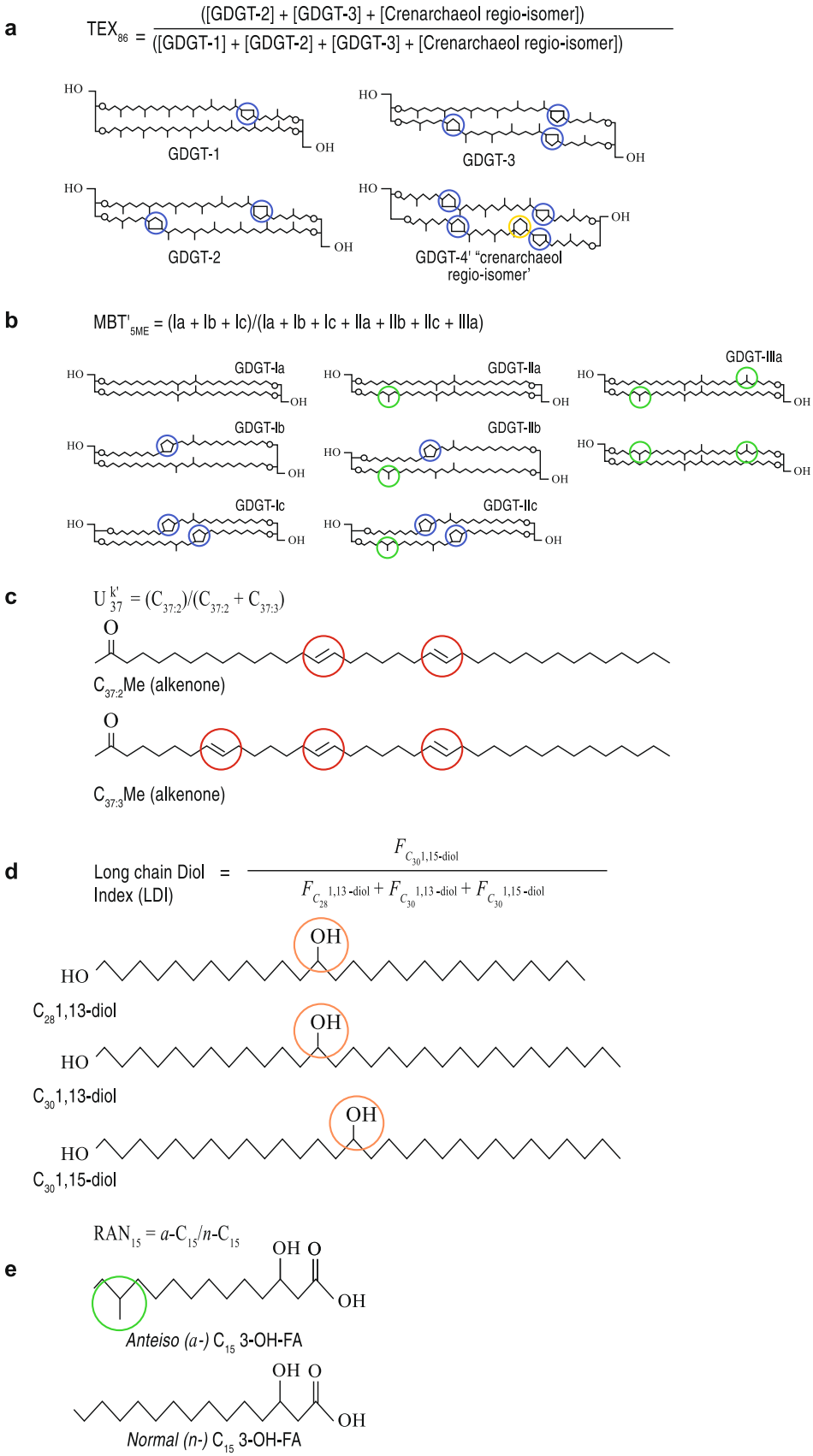

FIGURE 3 Continued.

(Figure 4). In the first TEX_{86} reconstruction spanning the last deglaciation from the South China Sea, SSTs aligned well with millennial-scale variability in Hulu Cave stalagmite $\delta^{18}O$, but exceeded and had a different trend to the U^{K}_{37}' SSTs, which may in part be explained by different seasons of production (Shintani *et al.*, 2011). In low-latitude upwelling systems, higher U^{K}_{37}' (surface) and lower TEX_{86} (subsurface) temperatures have enabled reconstructions of varying upwelling intensity spanning millennial to million-year timescales (e.g. McClymont *et al.*, 2012; De Bar *et al.*, 2018; Petrick *et al.*, 2018; Erdem *et al.*, 2021). Glacial–interglacial migrations in the latitude of the Subtropical Front in the southern hemisphere have been determined by combining U^{K}_{37}' and TEX_{86} data (Cartagena-Sierra *et al.*, 2021), and seasonally driven offsets between U^{K}_{37}', TEX_{86} and LDI temperatures identified variable Leeuwin Current strength offshore south-east Australia over the last ~135 ka (Lopes dos Santos *et al.*, 2013a). Although less widely applied, the LDI has isolated Baltic Sea cooling related to the 8.2-ka event, followed by a Holocene Thermal Maximum, and late Holocene cooling with sea-ice expansion (Warnock *et al.*, 2018). On much shorter timescales, an 'Atlantification' of waters in the Fram Strait through the 20th century was detected using U^{K}_{37}' and TEX_{86} (Tesi *et al.*, 2021; Figure 4). Here, a multi-biomarker approach, with 5–10-year resolution, enabled interactions between sea ice, ocean mixing and heat transfer to be better determined than by using the short instrumental record alone.

Lake temperature reconstructions provide valuable climate indicators for continental climate change. Early TEX_{86} records generated new constraints on temperature change in Africa: an ~2 °C increase in Lake Malawi surface water temperature occurred during the last ~100 years which exceeded variability in the preceding ~600 years (Powers *et al.*, 2005); coherence between Lake Victoria warming/cooling and rainfall occurred over the last ~14 000 years (Berke *et al.*, 2012a); and both long-term and abrupt temperature changes in Lake Tanganyika were linked to Indian Ocean SSTs across the last deglaciation (Tierney et al., 2008). However, local or regional influences over the biomarker–temperature relationships include lake size and depth (for TEX_{86}; Sinninghe Damsté *et al.*, 2022), salinity or alkalinity (for MBT'_{5Me} and alkenones; Pearson *et al.*, 2008; De Jonge *et al.*, 2014; Song *et al.*, 2016; Plancq *et al.*, 2018), nutrient availability (Toney *et al.*, 2010), and inputs of soils containing the same compounds (e.g. Loomis *et al.*, 2012; De Jonge *et al.*, 2015; Russell *et al.*, 2018). GDGT inputs from methanogens and other archaea can also complicate TEX_{86} reconstructions: at Lake Challa (Africa) reliable temperature reconstructions using lacustrine GDGTs were only possible between 25 and 13 ka, but not in the Holocene section (Sinninghe Damsté *et al.*, 2012).

The brGDGT proxy MBT'_{5Me} (de Jonge *et al.*, 2014) has been used to reconstruct millennial- and centennial-scale variations

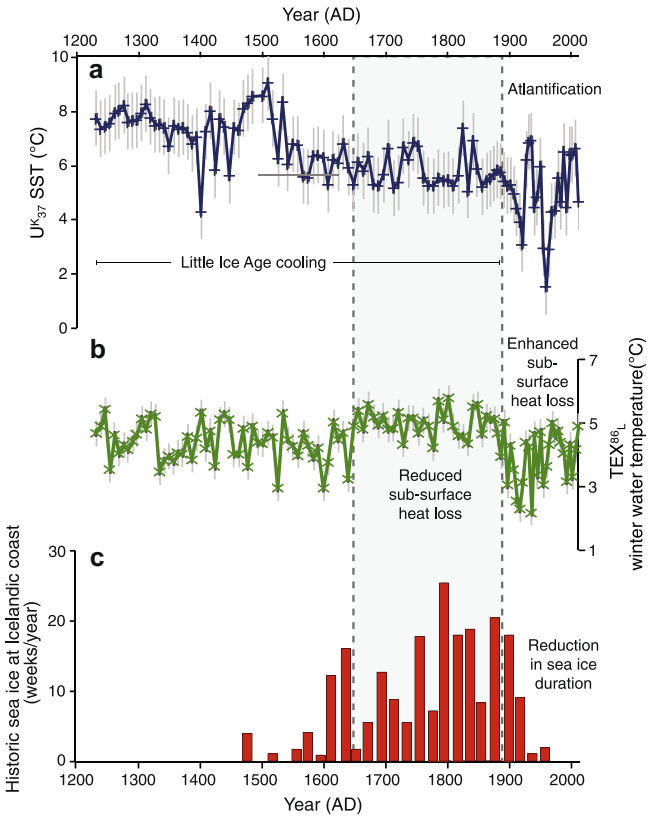

Figure 4. Biomarker insights into changes in late Holocene sea ice and expansion of Atlantic waters ('Atlantification') from reconstructed sea surface temperatures (SST) in the Fram Strait, the largest gateway to the Arctic Ocean (data from Tesi *et al.*, 2021). Surface water and subsurface water temperature reconstructions are reconstructed from the same sediment core using two different biomarker proxies (U^{K}_{37} and TEX_{86} respectively) and compared with historical records of sea ice persistence. (a) U^{K}_{37}-derived SST (standard error is shown by grey vertical lines); (b) TEX^{L}_{86}-derived water temperatures (standard error is shown by grey vertical lines); and (c) historical records of sea ice presence at Icelandic coasts (weeks/year) (Lamb, 1977). [Color figure can be viewed at wileyonlinelibrary.com]

in lake temperature, which align with stadial and interstadial events in the Iberian Peninsula (Rodrigo-Gámiz *et al.*, 2022). Although local conditions prevented application of the MBT'_{5Me} index to an Icelandic lake, the combined analysis of brGDGT distributions and U^{K}_{37}' data enabled quantification of temperature change through the Holocene which could be directly compared to reconstructed and modelled ice cap change (Harning *et al.*, 2020). Having quantified early Holocene warmth, the loss of the local ice cap by ~2050 CE was predicted (Harning *et al.*, 2020). A challenge for brGDGT reconstructions is that the calibration uncertainties (up to ~5 °C; Table 1) are of similar magnitude to some reconstructed Quaternary temperature changes. The application of MBT'_{5Me} can be

Figure 3. A selection of palaeotemperature biomarkers, detailing the different chemical properties that can be used to identify specific markers and their relationships to biological and environmental variables. (a) TEX_{86} (TetraEther indeX of tetraethers consisting of 86 carbon atoms) temperature proxy is calculated using the relative distributions of isoGDGTs (iso-GDGT-1, iso-GDGT-2 and iso-GDGT-3) and the crenarchaeol regioisomer (Schouten *et al.*, 2002). Blue circles highlight the number of cyclopentane moieties, and the yellow circle highlights the presence of a cyclohexane ring. (b) MBT'_{5Me} (Methylation of Branched Tetraethers using the 5-methyl isomers) temperature proxy in soils is calculated using the relative distributions of 5-methyl brGDGT (de Jonge *et al.*, 2014). Blue circles highlight the presence and number of cyclopentane moieties and green circles highlight the presence and number of methyl groups in the α and/or ω-5 position. (c) U^{K}_{37}' temperature proxy in freshwater and marine environments is calculated using the relative distributions of the di- and tri-unsaturated alkenone distributions (Prahl and Wakeham, 1987). The chain lengths of the two alkenones are the same (C_{37} = 37 carbon atoms), but the number of double bonds increases from two to three (highlighted by red circles). (d) LDI (long chain diol index) temperature proxy in freshwater and marine environments is calculated using the relative distributions of C_{28} and C_{30} 1,13- and C_{30} 1,15-alykl diol distributions (Rampen *et al.*, 2012; 2014). Compounds vary in terms of chain lengths (C_{28} = 28 carbons atoms and C_{30} = 30 carbons atoms) and the location of the midchain alcohol group (C_{13} or C_{15}; highlighted by the orange circles). (e) RAN_{15} temperature proxy in soils is calculated using the ratio of anteiso to normal 3-hydroxy C_{15} fatty acid (Wang et al., 2021a). Green circle highlights the methyl-substituent located on the antepenultimate carbon atom. [Color figure can be viewed at wileyonlinelibrary.com]

complex since the full range of specific bacterial sources of brGDGTs is unknown: community sequencing of laboratory cultures, environmental samples, and micro- and mesocosm studies have identified Acidobacteria as brGDGT producers; however, they currently do not account for the full distributions of brGDGTs found in sedimentary samples (e.g. Weijers et al., 2010; Sinninghe Damsté *et al.*, 2011, 2018; Martinez-Sosa and Tierney, 2019; De Jonge et al., 2021; Halamka et al., 2023).

The uncertainty surrounding the producer organisms (and whether they have changed through time), as well as limited high-latitude samples in global calibrations (Blaga et al., 2010; De Jonge *et al.*, 2014; Naafs *et al.*, 2017), has complicated the interpretation of Greenland lake data which did not align with other biomarker or macrofossil proxies (Kusch *et al.*, 2019). In the high latitudes of the southern hemisphere, accounting for distinct brGDGT distributions at low temperatures enabled the production of a regional brGDGT calibration with reduced uncertainties; in turn, millennial-scale temperature changes were identified in an Antarctic lake core spanning the last ~4000 years (Foster *et al.*, 2016). In East Africa, a regional MBT $'_{5Me}$ calibration also reduced temperature reconstruction errors to <2.5 °C (Russell *et al.*, 2018). Regional calibrations may therefore need to be considered where strong environmental impacts on lipid synthesis could occur.

Identification of key alkenone producers in North American, Greenland and Alaska lakes, with a preferred spring signal (e.g. D'Andrea, Huang, 2005; Toney *et al.*, 2010; Wang et al., 2021a), offers the potential to quantify seasonal lake temperature change in the northern high latitudes. Centennial-scale late Holocene winter–spring lake temperature changes have been quantified in Iceland, showing a strong influence from SSTs (Richter *et al.*, 2021). Holocene lake temperature changes linked to ice shelf configuration were reconstructed in northeast Greenland (Smith *et al.*, 2023). With the recent development and calibration of the 3-hydroxy-fatty acid ratios in lakes (Table 1; e.g. Wang et al., 2021a) there is also the potential for new bacteria-derived temperature proxies to be generated, but downcore applications are not yet available.

In aquatic settings where there are inputs of organic matter from the continents, and where the same biomarkers are found onshore, it is important to assess and correct (or remove) temperature data which may incorporate a mixture of both marine and terrestrial inputs, since the two environments have different biomarker–temperature calibrations (e.g. De Jonge *et al.*, 2015; Russell *et al.*, 2018; Martínez-Sosa *et al.*, 2021). For example, samples with high inputs of terrestrial brGDGTs can be flagged and removed using the BIT index (branched and isoprenoid tetraether index; Table 3 and Hopmans *et al.*, 2004), whereas two separate calibrations may be applied if there is sedimentological evidence for a switch from marine to lake environments (Smith *et al.*, 2023). Where a separation between aquatic and terrestrial lipids can be achieved, it is possible to generate terrestrial temperature records using lake/marine sediments (e.g. Blaga et al., 2010; Watson *et al.*, 2018; see subsection below).

Finally, on Quaternary timescales, there is potential for evolution to alter the biomarker–temperature relationship. Although the marine U^{K}_{37}'–SST relationship appears robust to evolutionary events in alkenone producers (McClymont *et al.*, 2005), a long-term (million year) warming in TEX_{86} at Lake El'gygytgyn in the Russian Arctic was influenced by archaeal community changes as landscape evolution influenced biogeochemical cycling (Daniels *et al.*, 2021). On shorter timescales, alkenone temperature indices in saline lakes can be impacted by shifts between the dominant haptophytes (Yao *et al.*, 2022). For example, salinity-driven changes in the haptophyte assemblage in Lake Van, Turkey, are suggested to have complicated the U^{K}_{37}'–temperature reconstructions for the oldest part of the record (~100–270 ka) (Randlett *et al.*, 2014).

Temperatures reconstructed from soils, peats and speleothems

The calibration of biomarker proxies for continental temperatures using soils, peats and speleothems has been more challenging than for aquatic settings and remains an active area of development (e.g. Weijers *et al.*, 2007; Naafs *et al.*, 2017; Meckler *et al.*, 2021). Quantified temperature data can provide a valuable backdrop to understand the rich environmental information recovered from the same archives (e.g. vegetation and hydrological change, human activity; see 'Reconstructing vegetation and hydrological change' and 'Sedimentary records of humans and animals in Quaternary landscapes').

The (acido)bacteria-produced brGDGTs, found in soils, peats and speleothems, have been explored as temperature proxies given their promise in aquatic settings ('Ocean and lake temperature reconstructions' above). The uncertainties in the brGDGT temperature calibrations for peat (~4.7 °C, Naafs *et al.*, 2017) and soils (~4.8 °C, De Jonge *et al.*, 2014; Yamamoto *et al.*, 2016) make it difficult to reconstruct low-amplitude and potentially brief Holocene temperature fluctuations. In the low latitudes, regional calibrations have been developed which have lower uncertainties (Pérez-Angel *et al.*, 2020), and loess/palaeosol sequences have required careful interpretation given unusual brGDGT distributions in semi-arid settings (Yang *et al.*, 2014). Conversion of soil or peat temperatures to overlying air temperatures has also been challenging where there are differences between the two (Dearing Crampton-Flood *et al.*, 2020). Nevertheless, in the Great Lakes region (North America) brGDGT-inferred soil/air temperatures from a lake core aligned with pollen-based temperature reconstructions associated with the Bølling–Allerød (B-A) warming, Younger Dryas cooling and Holocene warming (Watson *et al.*, 2018). Importantly, the brGDGT analysis was able to advance understanding beyond pollen-based interpretations by showing that the multi-centennial lag in warming compared to Northern Hemisphere temperature syntheses was due to the effects of continentality and regional influences of ice-sheet extent rather than a delayed vegetation response (Watson *et al.*, 2018). Where soil-derived biomarkers have been transported to different depositional settings, there can be complexity in the signature if the source regions have changed over time: shifting sediment provenance of brGDGT distributions recovered offshore of the Amazon basin over the last deglaciation impacted the reconstructed absolute air temperature time-series, due to the increasing influence of colder, higher-elevation inputs from the Andes into the Holocene (Bendle *et al.*, 2010).

In Asia, both isoGDGTs (TEX_{86}) and brGDGTs have been used in peat, loess and speleothems to explore the drivers and impacts of shifts in the summer monsoon. In peats, the combination of proxies for temperature and hydrology can be effective in considering their different drivers and the potential for (a)synchrony (e.g. Peterse *et al.*, 2014; Wang *et al.*, 2017). A 130 000-year loess–palaeosol sequence yielded high-resolution brGDGT temperature reconstructions: local insolation was the main driver of temperature change, but temperatures led brGDGT-inferred precipitation changes with a lag length which was linked to the intensity of northern hemisphere glaciation (Peterse *et al.*, 2014). Rapid brGDGT temperature changes across the Younger Dryas and ~3.2 ka in Southeast China occurred synchronously with pollen assemblage changes over

Table 3. Overview of the key proxies for palaeo-productivity and biogeochemical cycling and sediment transport.

Proxy	Source	Environmental signal	Considerations	Example reference(s)
Branched vs isoprenoidal tetraether (BIT) index from GDGTs	Archaea in soils (brGDGTs) and aquatic settings (isoGDGTs)	Indicator of soil inputs to aquatic systems	Some *in situ* water column production of branched GDGTs has been identified, complicating interpretations	Hopmans *et al.* (2004), Bechtel *et al.* (2010), Fietz *et al.* (2012)
Terrestrial to aquatic ratio (TAR)	*n*-Alkanes from higher plants (long chains) and algae (short chains)	Indicator of plant or soil inputs to aquatic systems	As well as plant inputs, soils and sedimentary rocks may also transport long-chain *n*-alkanes; multiple potential pathways	Cranwell (1973), Müller *et al.* (2014), Sanchez-Montes *et al.* (2020)
Alkenones	Ketones (alkenones) synthesized by haptophyte algae	Haptophyte algae productivity signal	Recent suggestions that alkenone abundance may link directly to total primary productivity, sea ice ($\%C_{37:4}$) or salinity ($\%C_{37:4}$)	Petrick *et al.* (2018), Cartagena-Sierra *et al.* (2021), Raja Sanchez and Rosell-Mele (2021), Wang *et al.* (2021b)
Archaeol	Produced by anaerobic archaea	Redox changes and methanogensis	Potential to record microbial activity onshore depending on source and transport pathway	Pancost *et al.* (2011)
Bacteriohopanepolyols (BHPs)	Membrane lipids produced by bacteria	Microbial processes such as methanogenesis	Potential to record microbial activity onshore depending on source and transport pathway	Talbot *et al.* (2003), Talbot and Farrimond (2007)
Chlorins	Algal productivity.	General phytoplankton productivity marker	Formed from degradation of chlorophyll to more stable tetrapyrrolic pigments. Sedimentary concentration reflects overall export to seafloor	Harris and Maxwell (1995), Zhao *et al.* (2006)
Chlorophyll and carotenoid pigments	Mainly aquatic productivity, some inputs from terrestrial plant matter	Algal production markers. Used to interpret productivity in combination with other markers	Can be susceptible to degradation, though degradation products can also be productivity markers. Generally, better preserved in lakes than ocean sediments, unless near-shore or under anoxic conditions	Leavitt (1993), Hodgson *et al.* (2003), McGowan (2013)
Highly branched isoprenoids (HBIs)	Produced by selected diatoms, including some sea-ice associated species. Arctic: IP_{25} synthesized by *Haslea* spp. Southern Ocean: $IPSO_{25}$ synthesized by the sea ice diatom *Berkeleya adelensis*	General indicators of selected diatom productivity, and for spring sea ice with $IP(SO)_{25}$	Combination of $IP(SO)_{25}$ and associated diatom HBIs or sterols can be used to distinguish between perennial sea ice (no HBIs) and open waters [no $IP(SO)_{25}$], PIP_{25}: IP_{25}/(IP_{25} + phytoplankton marker × *c*), $PIPSO_{25}$: $IPSO_{25}$/(IP_{25} + phytoplankton marker × *c*)	Belt and Muller (2013), Belt *et al.*, (2015, 2016). Vorrath *et al.* (2020)
isoGDGT-0	Methanogens are probably the dominant producers in peat	Microbial processes such as methanogenesis	Other potential source organisms may conflate the methanogensis signal	Basiliko *et al.* (2003), Pancost and Sinninghe Damsté (2003)
Isorenieratene	Algae which can fix under low-light conditions at deep water depths	Photic zone anoxia, green sulphur bacteria	Needs suitable environment for preservation	Sinninghe Damsté *et al.* (2001), Mallorquí *et al.* (2005)
Scytonemin	Protective carotenoid production by algae to avoid deleterious effects of harmful UV radiation (UVR)	Indicator of high UVR receipt. Environmental pressure for algae to protect cells during production.	Challenging to decouple UVR limitation from other limiting factors, e.g. nutrient availability	Hodgson *et al.* (2005)
Sterols (e.g. dinosterol, brassicasterol)	Produced by algae, but also present in some terrestrial material	Can be linked to groups of producers (e.g. dinosterol for dinoflagellates)	Can be degraded in the water column	Fahl and Stein (1999), Nakakuni *et al.* (2017)
Compound-specific stable carbon isotopes $\delta^{13}C$ on individual *n*-alkanes, *n*-alkanols and *n*-alkanoic acids	Wide range of sources (Table 1)	Biomarker specific: changes in C_3 to C_4 vegetation; changing productivity or producers	Can be challenging to interpret in isolation due to producer-specific influences	Huang *et al.* (2006), Tierney *et al.* (2010), McClymont *et al.* (2022)

[c]represent a constant (fixed number) in the equation, as standard mathematical nomenclature.

the last ~30 000 years in a peat sequence, and also showed asynchrony between temperature and precipitation proxies during the last deglaciation (Wang *et al.*, 2017). A 4 °C increase in mean annual air temperature was recorded by speleothem-TEX_{86} over the last deglaciation: the warming pre-dated Indian Summer Monsoon strengthening but was closely aligned with SST records (Huguet *et al.*, 2018). A pattern of early Holocene warmth followed by cooling towards the present day has been recorded by brGDGTs in peats (NE China; Zheng *et al.*, 2018) and using the more recently developed fatty acid RAN_{15} index in a Chinese speleothem (Wang *et al.*, 2018; Table 1). Given the challenges of recovering biomarkers from low organic carbon archives, and concerns about the relative influence of cave micro-environments on each record (Blyth *et al.*, 2016; Baker *et al.*, 2019), the recovery of both GDGTs and the C_{15} and C_{17} fatty acids from speleothems shows huge potential for generating new terrestrial records of cave or air temperature (e.g. Li *et al.*, 2011; Blyth *et al.*, 2016; Baker *et al.*, 2019). As speleothems can also yield fatty acid, *n*-alkanol and *n*-alkan-2-one distributions, interpreted to reflect changing soil microorganism responses to Holocene climate change (Xie *et al.*, 2003; Kalpana *et al.*, 2021), there is further potential to consider ecosystem response to temperature change (see also 'Reconstructing vegetation using biomarker distributions'), especially as analytical developments reduce sample sizes (e.g. Meckler *et al.*, 2021).

Reconstructing vegetation and hydrological change

Palaeovegetation and palaeohydrology records provide insights into drivers of climate change that impact precipitation/evaporation and terrestrial ecosystem response. Water availability is essential to the functioning of ecosystems and societies; therefore, long-term hydrological records also provide essential context for understanding changes in habitat and landcover, diets, agricultural practices, settlement dynamics and societal structures through the Quaternary. Different vegetation types have characteristic biomarker distributions and stable isotope ratios reflecting their biosynthetic pathways and biological responses to environmental conditions (Table 2, 'Biological functions of biomarkers'). When the biological source of the biomarkers is well constrained, CSIA has enabled the varying biological and environmental influences over $\delta^{13}C$ and $\delta^{2}H$ to be disentangled. CSIA has thus emerged as a powerful tool for reconstructing both past vegetation change and palaeohydrology (Castañeda and Schouten, 2011; Diefendorf and Freimuth, 2017; Holvoeth *et al.*, 2019; Inglis *et al.*, 2022).

Reconstructing vegetation using biomarker distributions

Plant-derived lipids were among the first to be characterized (Eglinton and Hamilton, 1967), and remain among the most frequently applied biomarker tools owing to their prevalence in Quaternary sequences, their relative resilience to decay, ease of analysis, and the diversity of environmental information that they contain within their distributions and isotopic compositions. Lignin-derived compounds have also been targeted as relatively well-preserved plant remains (e.g. Castañeda *et al.*, 2009b; reviewed in Jex *et al.*, 2014).

Biomarker vegetation reconstructions commonly use distributions of *n*-alkyl compounds such as *n*-alkanes, *n*-alkanols, *n*-alkanoic acids and wax esters, but may also draw upon sterols, phenols and more specific compounds (defined in Table 2). Biomarker vegetation reconstructions are usually made at the family rather than the species level, so the taxonomic detail is lower than with other vegetation proxies [pollen, plant macrofossils, and sedimentary ancient DNA (sedaDNA)]. However, the relative resistance of *n*-alkyl compounds to decay has enabled vegetation reconstructions in samples with low levels of macro- and micro-fossil preservation, particularly in wetlands (e.g. McClymont *et al.*, 2008a; Ronkainen *et al.*, 2015). Biomarkers are also considered less susceptible to the long-range transport processes that can complicate pollen analyses due to the hydrodynamic properties of the leaves they are derived from (Schwark *et al.*, 2002).

Complexity is introduced where some plants produce *n*-alkane distributions that contain peaks in both longer and shorter chain lengths. For example, some *Sphagnum* species produce a dominant *n*-alkane chain length of C_{23}, but also have elevated C_{31}, which complicates the use of the C_{23}/C_{31} ratio as a *Sphagnum* indicator (e.g. Andersson *et al.*, 2011; Bingham *et al.*, 2010; Bush and McInerney, 2013; Table 2). However, the presence of the sphagnum acid product 4-isopropenylphenol may offer a complementary assessment of the relative *Sphagnum* inputs to peat cores (e.g. Boon *et al.*, 1986; McClymont *et al.*, 2011). There may also be a bias caused by variable *n*-alkyl lipid production. For example, some conifer groups (e.g. Pinaceae) produce significantly less *n*-alkanes than broadleaf species, whereas others (e.g. Podocarpaceae) are similar (Diefendorf and Freimuth, 2017). As such, in catchments where pollen analyses indicate conifers as being the dominant vegetation type, biomarker interpretations should be part of a multi-proxy assessment: in northern Poland, this approach enabled subdecadal shifts in vegetation during the last deglaciation to be determined in detail (Aichner *et al.*, 2018).

As different vegetation types have particular moisture preferences, plant biomarkers have been used to assess palaeohydrology by reconstructing the relative contributions of different vegetation types to sedimentary archives including lake sediments (e.g. Meyers, 2003; Castañeda *et al.*, 2009b), marine sediments (Castañeda *et al.*, 2009a), peats (e.g. Pancost *et al.*, 2002; Ortiz *et al.*, 2010; Zhou *et al.*, 2010) and palaeosols (e.g. Zhang *et al.*, 2006) (Table 2). Concurrent changes in the peatland C_{23}/C_{29} *n*-alkane ratio (*Sphagnum*/vascular plants) and solar irradiance highlighted the sensitivity of north-east American hydroclimate to solar forcing, and its amplification by the Arctic/North Atlantic Oscillation since the mid-Holocene (Nichols and Huang, 2012). A key area of research has been the development of multiple records of vegetation change linked to changes in the Asian monsoon. Peatland aquatic/terrestrial vegetation reconstructions using *n*-alkanes identified Holocene intensification of the Indian Summer Monsoon in the Garwhal Himalyas, and in turn, regional heterogeneity in mid- to late Holocene monsoonal conditions in the Indian sub-continent (Bhattacharya *et al.*, 2021). Speleothem reconstructions of changing ecosystem dynamics have also been generated using a diverse suite of compounds, including *n*-alkanes (e.g. Xie *et al.*, 2003; Blyth *et al.*, 2007), sterols (e.g. Rousseau *et al.*, 1995), fatty acids (e.g. Wang *et al.*, 2019a) and lignin phenols (e.g. Blyth and Watson, 2009; Heidke *et al.*, 2019). For example, in a Chinese speleothem, ratios of long-chain *n*-alkanes and *n*-alkan-2-ones (from terrestrial vegetation) to shorter chain compounds (from soil organisms) recorded vegetation changes during the Last Glacial Maximum which could be linked to fluctuations in North Atlantic SSTs during the last deglaciation (Xie *et al.*, 2003). However, biomarker distributions (and other proxies) tend to be used as part of the evaluation of biological

and/or environmental controls over compound-specific stable carbon and hydrogen isotope ratios, rather than in isolation (e.g. Castañeda *et al.*, 2009a, 2009b).

Reconstructing vegetation and hydrological change using compound-specific stable isotope analysis

For higher plant biomarkers, stable carbon isotope analysis ($\delta^{13}C$) of individual lipids provides a powerful tool to reconstruct past vegetation changes, because different photosynthetic pathways can be distinguished by their impact on plant tissue $\delta^{13}C$ (Liu *et al.*, 2022). Thus, *n*-alkane $\delta^{13}C$ from trees and shrubs using the C_3 (Calvin–Benson) pathway is on average >10 ppm lower than in *n*-alkane $\delta^{13}C$ from plants using the C_4 (Hatch–Slack) pathway, which are mainly tropical grasses (Castañeda *et al.*, 2009a). A range of additional factors impact fractionation which may need to be considered in interpreting $\delta^{13}C$ records, including moisture availability (for C_3 plants), ecological or physiological changes and past $^{13}CO_2$ values (Diefendorf and Freimuth, 2016). A common nomenclature when presenting stable isotope ratios of individual lipids is $\delta^{13}C_{lipid}$, where 'lipid' is the chain length or the name of the lipid which has been analysed.

The long-term reliability of the leaf wax $\delta^{13}C$ vegetation proxy has been demonstrated through comparisons with pollen records from the late Pleistocene (e.g. Tierney *et al.*, 2010; Huang *et al.*, 2006). Mixing models have successfully used $\delta^{13}C$ differences to reconstruct shifts in the relative abundance of C_3 and C_4 with the caveat that bias may also be introduced by variable *n*-alkyl lipid production ('Reconstructing vegetation using biomarker distributions'; Garcin et al., 2014). In tropical Africa, $\delta^{13}C_{lipid}$ records have reconstructed variable trees/shrubs (C_3) and grasses (C_4) extending back to the early Pleistocene from both lake and marine sediments (e.g. Castañeda *et al.*, 2007; Schefuß *et al.*, 2003). In Lake Challa, Africa, $\delta^{13}C$ analysis of the C_{31} *n*-alkane ($\delta^{13}C_{31}$) reconstructed a vegetation transition from C_4-dominated plants during the glacial period to a mix of C_3/C_4 plants ~16.5 cal ka BP, which persisted during the Holocene and reflected the combined influences of increasing atmospheric CO_2 concentrations and increasing monsoon rainfall (Sinninghe Damsté *et al.*, 2011). *N*-alkane, *n*-alkanol and $\delta^{13}C_{31}$ have recorded glacial–interglacial switches between steppe vegetation (C_3) and warm season grasses (C_4) at the Chinese loess plateau over the last 170 ka (Zhang *et al.*, 2006). In Olduvai Gorge, orbitally paced $\delta^{13}C_{31}$ variations demonstrated rapid and large shifts between closed C_3 woodlands and more open C_4 grasslands ~1.9 Ma, challenging previous reconstructions of relatively stable ecosystems in the early Pleistocene (Magill *et al.*, 2013). The ecosystem variations were probably linked to SST oscillations and monsoon strength, and provide a backdrop for the emergence and dispersal of *Homo* (Magill *et al.*, 2013), as also suggested for more recent hominid migrations (e.g. Castañeda *et al.*, 2009a).

By comparing *n*-alkane flux and $\delta^{13}C$ signals across multiple glacial–interglacial timescales offshore of the Angola Basin, a decoupling between enhanced dust deposition ~900 ka and orbital variability in $\delta^{13}C_{31}$ revealed the different impacts of trade wind response to northern hemisphere ice-sheet growth (driving dust) and vegetation responses to regional SST changes (Schefuß *et al.*, 2003). Lignin phenol and *n*-alkane distributions alongside *n*-alkane $\delta^{13}C$ spanning the last 23 ka in Lake Malawi reconstructed millennial-scale variability in vegetation linked to wet conditions in south-east Africa, and a dominance of higher plant signals in bulk $\delta^{13}C$ was confirmed (Castañeda *et al.*, 2009b). However, caution is required where there may be mixed aquatic/terrestrial or local/regional inputs in the same archive: contributions of aquatic C_{27} and C_{29} *n*-alkanes to a lake sediment resulted in different $\delta^{13}C$ variations compared to the terrestrial leaf wax $\delta^{13}C_{31}$ in the same core (Liu *et al.*, 2015); varying inputs of local and more widely sourced leaf waxes to an estuarine sequence were identified by different $\delta^{13}C$ signals recorded depending upon the *n*-alkane chain length (Carr *et al.*, 2015).

A powerful and direct proxy measurement of hydroclimate comes from $\delta^{2}H$ signatures of lipids derived from plants and algae, which track the $\delta^{2}H$ of their environmental water sources (reviewed by Sachse *et al.*, 2012). D/H fractionation of meteoric water is influenced by temperature, precipitation source and amount, elevation and distance from the ocean, which results in a distinctive geographical pattern of lower $\delta^{2}H_{precipitation}$ at increasing latitude (e.g. Craig and Gordon, 1965; Bowen and Revenaugh, 2003). Several environmental and biological processes contribute to further D/H fractionation between the source water and the lipids and can complicate the interpretation of palaeohydrological $\delta^{2}H_{lipid}$ signatures (Sachse *et al.*, 2012; Sessions, 2016; Huang and Meyers, 2018): higher plant $\delta^{2}H_{lipid}$ is influenced by factors such as humidity, evapotranspiration rates, light, vegetation assemblage and plant physiological differences (e.g. Smith and Freeman, 2006; Hou et al., 2008; Liu and Yang, 2008; Yang *et al.*, 2009; Kahmen *et al.*, 2013), whilst algal $\delta^{2}H_{lipid}$ is influenced by metabolic processes, growth rate and phase, nutrients and temperature (e.g. Schouten *et al.*, 2006; Sachse and Sachs, 2008; Wolhow et al., 2009; Zhang *et al.*, 2009). Salinity also influences source water $\delta^{2}H$ and D/H fractionation of both plant and algal lipids, facilitating the application of $\delta^{2}H_{lipid}$ as a palaeosalinity proxy (discussed in the next section).

Palaeohydrological $\delta^{2}H_{lipid}$ reconstructions developed from terrestrial and marine sediment archives (e.g. Sauer *et al.*, 2001; Xie *et al.*, 2000; Huang *et al.*, 2004; Schefuß *et al.*, 2005) have provided insight into diverse aspects of the Quaternary climate system and its impacts on palaeohydrology. Applications have included reconstructions of changes in the Inter-Tropical Convergence Zone and El Niño/Southern Oscillation (ENSO) (e.g. Atwood and Sachs, 2014; Massa *et al.*, 2021), the South Pacific Convergence Zone (e.g. Maloney *et al.*, 2022), the Southern Annular Mode (e.g. van der Bilt *et al.*, 2022), monsoonal activity (e.g, Seki *et al.*, 2009; Basu *et al.*, 2019), seismic activity (e.g. Norström *et al.*, 2018), insolation forcing (e.g. Lupien *et al.*, 2022) and meltwater dynamics (e.g. Aichner *et al.*, 2022). By comparing terrestrial and aquatic *n*-alkane $\delta^{2}H$ signatures, variations in evapotranspiration of lake environments (e.g. Sachse *et al.*, 2004, 2006), climate-driven lake level changes (e.g. Günther *et al.*, 2016; Saini *et al.*, 2017; Aichner *et al.*, 2019) and seasonality of precipitation (e.g. Kjellman *et al.*, 2020; Katrantsiotis *et al.*, 2021) have been determined. Another approach to disentangling the impact of lake water evaporation from precipitation changes is coupling $\delta^{2}H$ and $\delta^{18}O$ reconstructions, as demonstrated using $\delta^{2}H$ of *n*-alkanes and $\delta^{18}O$ of sugar biomarkers to develop a Lateglacial–Holocene palaeohydrological reconstruction from Himalayan Nepal (Hepp *et al.*, 2015). Reconstructed palaeohydrology from $\delta^{2}H_{lipid}$ has also provided climatic contexts for human evolution (as reviewed by Patalano *et al.*, 2021) and human settlements (e.g. Sharifi *et al.*, 2015; Balascio *et al.*, 2020).

Care is needed to disentangle changes in *n*-alkane $\delta^{2}H$ that are driven by biological fractionation or vegetation change rather than hydroclimate (e.g. Liu *et al.*, 2006; Wang *et al.*, 2013; Griepentrog, *et al.*, 2019). This can be effectively

achieved by reconstructing vegetation change using pollen, biomarker distributions, leaf wax $\delta^{13}C$ or sedaDNA. At Meerfelder Maar, western Europe, the influences of vegetation change and hydroclimate were assessed using *n*-alkane distributions, pollen and *n*-alkane δ^2H, demonstrating that cooler and wetter conditions were established ~2.8 ka BP (Rach *et al.*, 2017). Contrasting late Holocene $\delta^2H_{dinosterol}$ hydroclimate reconstructions from paired lakes in the western tropical Pacific showcases the importance of multi-site and multi-proxy data to distinguish between climate and other limnological drivers of hydrological change (Maloney *et al.*, 2022). By combining *n*-alkane and *n*-acid distributions with *n*-alkane $\delta^{13}C$ and δ^2H, both vegetation ($\delta^{13}C_{31}$ and $\delta^{13}C_{33}$) and precipitation (δ^2H_{C29}) were recorded and could be separated (Wang *et al.*, 2013). Under arid conditions in the Qinling Mountains, China, a strong correlation between altitude and δ^2H_{lipid} (but not $\delta^{13}C_{lipid}$) highlights the potential to reconstruct and evaluate palaeoelevation and its interaction with local hydroclimate (Liu, 2021). These studies demonstrate both the complexity but also the valuable and detailed environmental issue which can be recovered using CSIA.

Where temperature and hydroclimate reconstructions are available from the same archive, the synchroneity or links between both larger and smaller scale climate drivers can be interrogated (e.g. Berke *et al.*, 2014; Tierney et al., 2008; Muñoz *et al.*, 2020; Stockhecke *et al.*, 2021). In Lake Victoria, Africa, coherence between leaf wax δ^2H hydroclimate and GDGT-inferred temperature records ('Quantifying amplitudes and rates of past temperature change') provided clear evidence for orbitally forced tropical climate since the Late Pleistocene, and highlighted the role of ENSO-related teleconnections in shaping climatic events such as the Younger Dryas (Figure 5) (Berke *et al.*, 2012b). In Lake Elsinore (California), abrupt changes recorded by leaf wax δ^2H in the Lateglacial (32–20 ka) were independent of GDGT-inferred temperature shifts and were attributed to changes in storm tracks (Feakins *et al.*, 2019). In a marine sediment core offshore Sumatra, leaf wax δ^2H challenged previous views of increased precipitation over the Indo-Pacific Warm Pool during the Last Glacial Maximum, which was attributed to regional differences in deglacial sea level and coastline configuration (Niedermeyer *et al.*, 2014). In turn, new Holocene oscillations in the Indian Ocean precipitation could be linked to rainfall in East Africa via a 'precipitation dipole', rather than by ENSO (Niedermeyer *et al.*, 2014). These examples are important for demonstrating that we can extend our understanding of the Lateglacial climate instability beyond ice and ocean dynamics, to include hydroclimate and atmospheric variability, especially in the low latitudes.

Reconstructing salinity using lake and marine sediments

Palaeosalinity reconstructions in the oceans and in lakes may provide an indication of changes in circulation (e.g. through changing water masses or currents) or hydroclimate (e.g. where enhanced freshwater inputs or increased evaporation can lead to lake salinity changes). In estuarine or coastal settings, salinity variations may also reflect changes in river discharge or the relative contribution of marine and freshwater as influenced by local changes in relative sea level. In this section we outline both biomarker distributions and CSIA which have detailed changes in salinity either in marine or lacustrine settings.

Sea-surface salinity as an indicator of circulation or sea-level changes

During the early U^K_{37}'-SST calibration work ('Ocean and lake temperature reconstructions'), a potential salinity or polar water mass influence over the abundance of the haptophyte algae $C_{37:4}$ alkenone was determined (Rosell-Melé, 1998; Bendle *et al.*, 2005), noting that this alkenone is not part of the U^K_{37}' index (Table 1). Subsequently, high $C_{37:4}$ values have been used to track expansion of (sub)polar water masses in the Atlantic, Pacific, and Southern Oceans across glacial–interglacial and million-year timescales (McClymont *et al.*, 2008b; Martínez-Garcia *et al.*, 2010). Elevated $C_{37:4}$ alkenone abundances (low salinity) have identified meltwater from Heinrich event icebergs reaching the Iberian Peninsula (Martrat *et al.*, 2007), and glacial meltwater reaching the north-east Pacific (Sánchez-Montes *et al.*, 2020). Although not specific salinity markers, terrestrially derived biomarkers in the iceberg-rafted debris (IRD)-rich Heinrich layers (Madureira *et al.*, 1997; Rosell-Melé *et al.*, 1997; van der Meer, 2007) confirmed the release of IRD and meltwater to the North Atlantic Ocean. Alternatively, large inputs of heavily altered carotenoids to southern Greenland, in the absence of IRD, suggested that an outburst flood occurred during the last interglacial (Nicholl *et al.*, 2012).

More direct records of sea-surface salinity draw on the impact of changing salinity on D/H fractionation in seawater and during biosynthesis (e.g. Sauer *et al.*, 2001; Englebrecht and Sachs, 2005; Schouten *et al.*, 2006). Cultured haptophyte algae show that $\delta^2H_{alkenone}$ records salinity change (Englebrecht and Sachs, 2005; Schouten *et al.*, 2006), and may even be used to identify the source regions of alkenones transported to sediment drift sites (Englebrecht and Sachs, 2005). An early application in the eastern tropical Pacific used instrumental records to show that $\delta^2H_{alkenone}$ fluctuations recorded rainfall and river discharge in Columbia, and revealed reduced runoff during the last glacial compared to the Holocene (Pahnke *et al.*, 2007). Combined $\delta^2H_{alkenone}$ and dinoflagellate cyst analysis showed substantial freshening of the Black Sea over the last ~3000 years, and refuted a hypothesis that salinity changes were responsible for changes to the haptophyte assemblage (van der Meer *et al.*, 2008). In the south-east Atlantic, a decoupling of SST and salinity across multiple deglaciations has been recognized, whereby salinity ($\delta^2H_{alkenone}$) increased earlier than ocean warming (U^K_{37}' index); both changes pre-date the onset of deglaciation and may even play a role in triggering or facilitating ocean circulation change during glacial–interglacial transitions (Kasper *et al.*, 2014; Petrick *et al.*, 2015). In the Mediterranean Sea, $\delta^2H_{alkenone}$ confirmed a large drop in surface salinity at the onset of a Last Interglacial sapropel, supporting the hypothesis that these organic-rich layers were the result of precession-driven monsoon rains disrupting the circulation (van der Meer *et al.*, 2007). As for leaf wax δ^2H ('Reconstructing vegetation and hydrological change using compound-specific stable isotope analysis'), care is needed to assess whether salinity change is the primary signal being recorded by sedimentary δ^2H_{lipid}, since it could also be impacted by factors including variations in growth rate (Wolhowe *et al.*, 2009) and the algal species/genera (Schouten *et al.*, 2006; van der Meer *et al.*, 2008; Nelson and Sachs, 2014).

In coastal systems, salinity change can be a reflection of relative sea-level change. A fall in $C_{37:4}$ abundance (increased salinity) was used to identify relative sea-level rise in a Scottish isolation basin following the last deglaciation (Bendle *et al.*, 2009). The relative contribution of mangrove species biomarkers (e.g. taraxerol) to intertidal sediments has also been explored as an alternative indicator of sea-level change

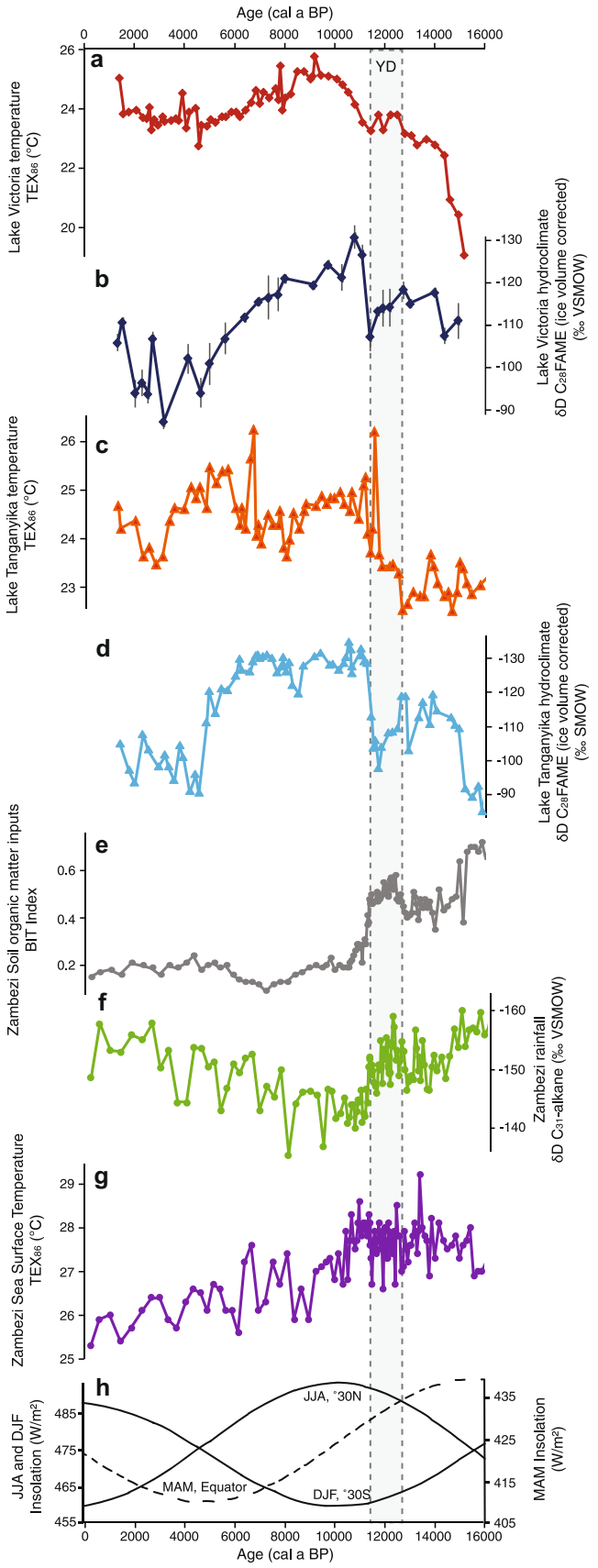

Figure 5. Terrestrial and marine biomarker reconstructions of environmental change in east Africa since the late Pleistocene. (a,b) Palaeoclimate reconstructions from Lake Victoria (Berke et al., 2012): (a) TEX_{86} palaeotemperatures and (b) palaeoprecipitation record from ice volume-corrected δ^2H of the C_{28} leaf wax fatty acid methyl ester (FAME) with error bars (grey lines) representing the mean error of replicated analyses for each sample. (c,d) Palaeoclimate reconstructions from Lake Tanganyika (Tierney et al., 2008); (c) TEX_{86} palaeotemperatures and (d) palaeoprecipitation record from ice volume-corrected δ^2H of the C_{28} leaf wax FAME. (e–h) Palaeoclimate reconstructions from a marine sediment core off the mouth of the Zambezi River (Schefuß et al., 2011): (e) BIT (branched and isoprenoid tetraether) index representing soil organic matter inputs; (f) palaeprecipitation record from δ^2H of C_{31} alkane; (g) TEX_{86} sea surface temperatures; and (h) insolation curves for June–July–August (JJA) and December–January–February (DJF) for the Northern (30°N) and Southern (30°S) Hemisphere (solid lines) and March–April–May (MAM) insolation at the equator (dashed line). [Color figure can be viewed at wileyonlinelibrary.com]

(Versteegh *et al.*, 2004; Koch *et al.*, 2011), but local influences on sedimentation patterns and biomarker degradation require further investigation (He *et al.*, 2018; Sefton, 2020). Both *n*-alkane and taraxerol δ^2H in mangrove systems show potential for isolating a biological response to changes in salinity (Ladd and Sachs, 2015). A salinity impact on mangrove water-use efficiency was also indicated by *n*-alkane $\delta^{13}C$ in Australia (Ladd and Sachs, 2013). A challenge in low-latitude settings is to isolate a sea-level-driven salinity change from a hydroclimate impact on precipitation or seawater δ^2H (e.g. Pahnke *et al.*, 2007; Tamalavage *et al.*, 2020). However, by combining pollen analysis with plant wax distributions and δ^2H from a mangrove system in the Bahamas, the time-varying influences of changes in vegetation assemblage and precipitation could be disentangled for the Holocene (Tamalavage *et al.*, 2020). Multi-proxy analyses thus show great potential for evaluating the relative influences of vegetation change, hydroclimate and sea-level-driven salinity variability in mangrove environments.

Lake salinity as an indicator of hydrological change

As observed in the marine environment (subsection above), high abundances of the haptophyte–algae $C_{37:4}$ alkenone have been recorded with low salinity in modern calibration studies of saline lakes (Liu *et al.*, 2008, 2011; Song *et al.*, 2016; He *et al.*, 2020) and in comparisons between lake reconstructions and instrumental data (He *et al.*, 2013). Qualitative palaeosalinity reconstructions using $C_{37:4}$ abundance in lake sediments have reconstructed late Holocene moisture fluctuations on the Northern Tibetan Plateau linked to solar irradiance (He *et al.*, 2013), and identified the transition between marine and lake environments associated with ice-shelf expansion in north-east Greenland (Smith *et al.*, 2023). However, not all lakes have recorded the $C_{37:4}$ alkenone (e.g. Toney *et al.*, 2010), and seasonal biases in alkenone production may influence the reconstructions (He *et al.*, 2020). Combined analysis of alkenone distributions and phylogenetic analysis in a suite of saline Chinese lakes (Yao *et al.*, 2022) indicates that $C_{37:4}$ alkenone may reflect changing haptophyte groups rather than salinity, since the detected groups occupied different ecological niches. The presence of another salinity-sensitive indicator, the alkenone $C_{38:3Me}$, was detected during times of haptophyte assemblage changes consistent with fresher surface waters in a Pleistocene record from Lake Van, Turkey (Randlett *et al.*, 2014). Palaeosalinity indices, such as the RIK_{37} (ratio of isomeric ketones of C_{37} chain length) index (Longo *et al.*, 2016), capture salinity-driven shifts in haptophyte species composition and are reliable salinity proxies in oligohaline environments (Longo *et al.*, 2016).

Salinity is also reflected in lake water δ^2H and the biosynthesis of algal lipids: field calibration laboratory culture studies have demonstrated that the salinity is inversely related to the D/H fractionation of algal lipids (e.g. Sessions *et al.*, 1999; Schouten *et al.*, 2006; Sachse and Sachs, 2008; Schwab and Sachs, 2011; Ladd and Sachs, 2012; Nelson and Sachs, 2014; Englebrecht and Sachs, 2015; see 'Reconstructing vegetation

and hydrological change using compound-specific stable isotope analysis' for discussions of other controls on δ^2H_{lipids}). Mid-Holocene changes to the Indian Summer Monsoon have been detected using biomarker δ^2H in a saline–alkaline lake in the core 'monsoon zone' of central India (Sarkar *et al.*, 2015): more enriched δ^2H in terrestrial leaf waxes and cyanobacteria, alongside increased abundance of the biomarker tetrahymanol (generated under saline conditions; Romero-Viana *et al.*, 2012) reconstructed increased salinity and a lowering of lake levels after 6 cal ka BP (Sarkar *et al.* 2015).

Archaeal GDGTs have also been used as palaeosalinity indicators based on ratios of archaeol, a biomarker for hypersaline archaea, and caldarchaeol, a cosmopolitan isoGDGT that is produced across a range of salinity conditions. The Archaeol and Caldarchaeol Ecometric (ACE) index (Turich and Freeman, 2011) has since been used as a qualitative lacustrine palaeosalinity proxy, showing that salinity increased due to a reduced water balance during periods of higher Lateglacial temperatures in southern California (Feakins *et al.*, 2019). However, a study of 55 lakes in mid-latitude Asia has identified a threshold response in the ACE index, which suggests that it may only be effective in high lake salinity ranges (60 000–100 000 mg L^{-1}) (He *et al.*, 2020).

Reconstructing changes in sea ice extent

Early identification of elevated concentrations (>5–10%) of the abundant haptophyte algae $C_{37:4}$ alkenone in high-latitude marine samples suggested that low temperatures and/or low salinity in (sub)polar waters were important (see 'Sea-surface salinity as an indicator of circulation or sea-level changes'). Subsequently, DNA analyses have demonstrated that high $C_{37:4}$ abundances can be more specifically linked to sea ice-associated haptophyte algae (Wang *et al.*, 2021b). With further testing, this new evidence offers the potential for both sea ice and SST information to be simultaneously retrieved from alkenone data in the high latitudes.

Two related sea-ice biomarker proxies have been more extensively developed: specific highly branched isoprenoids (HBIs) usually synthesized in spring by particular ice-associated diatoms (see detailed review by Belt, 2018). In the Arctic, the mono-unsaturated alkene containing 25 carbon atoms is used ('IP_{25}', Belt *et al.*, 2007) but this is not present in the Southern Ocean. Instead, the di-unsaturated HBI ('$IPSO_{25}$') is applied (Belt *et al.*, 2016) (Table 3). Extensive evaluation of the HBIs, especially IP_{25}, against diatom proxy data gives confidence in their ability to reconstruct sea-ice changes (Massé et al., 2008; Weckström *et al.*, 2013). $IPSO_{25}$ is a relatively specific environmental indicator, reflecting the tendency for its producer, *Berkeleya adeliensis*, to live in platelet ice and the bottom layer of land-fast ice (Belt *et al.*, 2016; Riaux-Gobin *et al.*, 2000), and thus shows a strong signal of coastal production (Massé *et al.*, 2011; Rontani *et al.*, 2019). However, since HBIs have also been determined beyond the continental shelf edge, in the Scotia Sea (Collins *et al.*, 2013), further investigation is required to fully evaluate the interpretation of $IPSO_{25}$ beyond the coastal regions.

A challenge for both HBI proxies is how to interpret the sea ice signal when IP_{25} or $IPSO_{25}$ is absent. Absence could reflect compound degradation within the sea ice, water column or sediments (Belt, 2018), although recent work has confirmed IP_{25} in pre-Quaternary sediments (Knies *et al.*, 2014; Clotten *et al.*, 2018). Alternatively, productivity by ice-dwelling diatoms may be minimal or absent under permanent sea ice cover if photosynthesis is restricted (Belt, 2018). To address the latter concern, the relative abundance of IP_{25} or $IPSO_{25}$ can be compared with open-ocean productivity biomarkers (e.g. HBI III or brassicasterol for diatoms, dinosterol for dinoflagellates). Revised 'PIP_{25}' or '$PIPSO_{25}$' indices have been proposed to describe this ratio (Table 3): an absence of both the sea-ice and open-ocean biomarkers yields a $PIP(SO)_{25}$ value of zero ('perennial sea ice'), whereas open-ocean only biomarkers yield a $PIP(SO)_{25}$ value of 1; values in between reflect seasonal sea ice presence (Belt & Müller, 2013).

IP_{25} records have been important in assessing the role of sea ice in past climate changes. Relatively short historical sea ice records have been extended (Tesi *et al.*, 2021). By filling in intervals of sparse historical data, abrupt changes in sea ice have been reconstructed for the last millennium (Massé et al., 2008). Millennial-scale fluctuations in spring sea-ice cover occurred to the north of Iceland during the Holocene and the last glacial–interglacial cycle (e.g. Müller *et al.*, 2009; Hoff *et al.*, 2016; Stein *et al.*, 2017; Xiao *et al.*, 2017; Sadatzki *et al.*, 2020), including contrasting sea-ice conditions between the early/mid- and late Younger Dryas close to northern Norway (Cabedo-Sanz *et al.* 2013). Regional differences between the timing of expanded sea-ice cover were proposed to have contributed to millennial-scale variability in deep-water formation across the deglaciation (Figure 6) (Xiao *et al.*, 2017). In the longer term, an increase in Bering Sea sea-ice cover and development of the seasonal advance and retreat of the sea ice margin occurred alongside the mid-Pleistocene transition ~1 Ma, which might have been important for influencing ice-sheet growth and increased deep ocean storage of carbon during glacial stages (Detlef *et al.*, 2018). The transition from the warm Pliocene epoch into the Quaternary also saw an expansion of Arctic sea ice alongside the intensification of northern hemisphere glaciation ~2.7 Ma (Knies *et al.*, 2014; Clotten *et al.*, 2018). Although preservation over long timescales is promising, concerns have also been raised about the inherent instability of HBIs, meaning caution needs to be applied to interpretation of their presence/absence (Sinninghe Damsté *et al.*, 2007).

$IPSO_{25}$ records have been integrated within several multi-proxy studies. Expanded seasonal sea ice cover occurred during the last glacial stage in the Scotia Sea (Collins *et al.*, 2013), and millennial-scale evolution of perennial and seasonal sea ice was recorded over the last deglaciation in the Amundsen Sea (Lamping *et al.*, 2020). Multiple $IPSO_{25}$ records detail expansion and retreat of sea ice during the Holocene (Barbara *et al.*, 2010, 2016; Etourneau *et al.*, 2013; Denis *et al.*, 2010; Tesi *et al.*, 2020; Ashley *et al.*, 2021; Johnson *et al.*, 2021). High-resolution analyses of the last ~400 years have shown that $IPSO_{25}$ can identify trends and cyclicity in seasonal and perennial sea ice cover, and links to ocean or atmospheric forcings (e.g. Campagne *et al.*, 2015; Barbara *et al.*, 2016; Vorrath *et al.*, 2020). Differences in Holocene sea-ice histories between sites probably indicate the influence of local and regional circulation systems (Lamping *et al.*, 2020; Vorrath *et al.*, 2020), which are also expressed in the instrumental record (e.g. Parkinson, 2019).

Tracing biological productivity and biogeochemical cycling

Biomarker proxies implicitly record the flux of organic matter between different reservoirs of the Earth system. In this section, we outline biomarkers which have been used qualitatively to explore biogeochemical cycles in more detail by either detecting specific environmental conditions (e.g. biomarkers for methanogenic or methanotrophic micro-organisms) or for

tracing changes in productivity and degradation (e.g. fluxes of biomarkers linked to specific producers).

Reconstructing biological productivity in lakes and the oceans

The source-specific nature of biomarkers allows for groups of producers to be traced in sedimentary systems, and to assess whether their productivity has changed in the past (Tables 2 and 3). When comparing the relative abundances of productivity markers, it is important to assess the potential impacts of bioturbation, remineralization and degradation of organic matter; these can be rapid and effective in oxic settings and could bias the target productivity signal (e.g. Leavitt, 1993; Arndt *et al.*, 2013; Jessen *et al.*, 2017). Intact pigments are particularly vulnerable to oxidation, UV radiation and associated processes of degradation, and usually have very low preservation in marine sequences (Reuss *et al.*, 2005; McGowan, 2013). Better preservation may be recorded in lake sediments, but still more successfully with anoxic water columns, or with minimal sinking depths and benthic algae coverage (Leavitt, 1993; Hodgson *et al.*, 2005; McGowan, 2013).

Pigment analysis has detected lake productivity oscillations in central Italy linked to warm–cold oscillations in the North Atlantic between ~15.0 and 28.0 cal ka BP (Chondrogianni *et al.*, 2004), and changes in lake level linked to the onset of the African Humid Period in Ethiopia (Loakes *et al.*, 2018). In East Antarctica, recolonization and succession of marine flora has been determined as the ice sheet and sea ice interacted through the Holocene (Hodgson *et al.*, 2003). A distinctive pigment is isorenieratene (Table 3), a carotenoid pigment synthesized by green sulphur bacteria, making it a biomarker for a relatively uncommon but specific environment: photic zone euxinia (both anoxic and sulphidic) (Sinninghe Damsté *et al.*, 2001). Isorenieratene has been instrumental in demonstrating that euxinic conditions developed during the Last Interglacial in the Mediterranean Sea associated with the formation of sapropels (Marino *et al.*, 2007). Significantly, the co-recorded proxy data illustrated the role of increased runoff in altering Mediterranean circulation (see 'Sea-surface salinity as an indicator of circulation or sea-level changes') (Marino *et al.*, 2007).

It is more common to find pigment degradation products in marine sediments, often alongside lipid biomarkers for other producers or degradation pathways (Table 3). Chlorophyll degradation products, chlorins ('Biological functions of biomarkers'), have been used to reconstruct export production, i.e. the organic matter which is removed from the surface ocean and stored longer term in the deep ocean or sediments (e.g. Petrick *et al.*, 2018). Chlorins, alkenones, sterols and diols have reconstructed intensification or shifts in export production across multiple glacial–interglacial cycles linked to coastal upwelling systems (Petrick *et al.*, 2018), highly productive oceanographic fronts (Cartagena-Sierra *et al.*, 2021), sea-ice extent (Fahl and Stein, 1999) and changing nutrient inputs (e.g. Martínez-Garcia *et al.*, 2011; Sánchez-Montes *et al.*, 2022). In the Subantarctic Atlantic Ocean, a consistent pattern of elevated higher plant *n*-alkanes during glacial intervals aligned closely with dust peaks in Antarctic ice cores (Martínez-Garcia *et al.*, 2009). In turn, lower SSTs and higher primary productivity (both reconstructed from alkenones) demonstrated close connections between ocean and atmosphere circulation, nutrient supply and potential glacial-stage CO_2 drawdown by the ocean through the Quaternary (Martínez-Garcia *et al.*, 2011). A recent global-scale analysis of seafloor sediments flags the potential that alkenone concentrations may be dominated by primary productivity, and thus provide a potentially quantitative reconstruction of production over Quaternary timescales (Raja and Rosell-Melé, 2021).

Reconstructing sediment, organic matter and nutrient cycling

The presence of terrestrial biomarkers in marine sediments can enable an assessment of the links between ocean circulation and environmental change onshore as detailed above, but may also give insights into the transport pathways of terrestrial organic material and identify important connections between nutrient cycles and productivity alongside palaeohydrology. For example, flood events have been identified in estuarine sediments by increases to the C_{31}/C_{17} *n*-alkane ratio (Meyers, 2003), which were consistent with historical records of the Minjiang River, China, since the 1800s CE (Wang *et al.*, 2014). A 'terrestrial to aquatic organic matter *n*-alkane ratio' (TAR, Table 3) has been used to record both dust and glacier-derived sediment inputs to the North Atlantic and Gulf of Alaska across multiple glacial–interglacial cycles (Naafs *et al.*, 2012; Lang *et al.*, 2014; Müller *et al.*, 2018) with potential impacts on marine productivity (Müller *et al.*, 2018; Sánchez-Montes *et al.*, 2020). Biomarker fingerprinting of sediments eroded by the circum-Atlantic ice sheets has added to this detail, and determined the asynchroneity of IRD or meltwater release between different ice sheets (e.g. Stein *et al.*, 2009; Rosell-Melé *et al.*, 2011; Naafs *et al.*, 2013; Hefter *et al.*, 2017).

As well as tracing these land–ocean and land–lake transfers of organic matter, and describing or quantifying lake/ocean export productivity (subsection above), biomarkers can be used to trace biogeochemical cycling in two ways: (i) the presence of biomarkers generated under specific environmental conditions, e.g. anoxic settings; or (ii) the presence of diagenetic products of the original biosynthesized molecule, where the environmental controls on diagenesis are known. Although used to qualitatively describe organic matter formation, transport and reworking, there is emerging potential to consider biomarker concentrations or transformations as a way to quantify carbon burial and biogeochemical interactions including nutrient and oxygen availability.

In peatlands, biomarker tracers of biogeochemical cycling have been explored, due to the close links between peat water table depth, oxygen availability and the associated generation of greenhouse gases. For example, elevated concentrations of the anaerobic archaea-produced archaeol reflect rising water tables in peat sequences (Pancost *et al.*, 2011) or enhanced methanogenesis during warm periods of the late Pleistocene and Holocene in Siberian permafrost (Bischoff *et al.*, 2013). Methanogens are also probably the main source of isoGDGT-0 in peats (Basiliko *et al.*, 2003, Pancost and Sinninghe Damsté, 2003); by comparing iso-GDGT-0 and archaeol accumulation rates in a 16-kyr-old peat sequence from Hani, China, the long-term link between elevated levels of methanogenesis, high temperatures and high summer insolation was demonstrated (Zheng *et al.*, 2019).

Biohopanoids are largely biomarkers of aerobic bacteria (Rohmer *et al.*, 1992; Talbot *et al.*, 2016), and include relatively simple C_{30} hopanoids (e.g. diploptene), or more complex versions with additional side chains (bacteriohopanepolyols or BHPs; reviewed by Kusch and Rush, 2022). BHPs have a wide range of sources including methanotrophs, heterotrophs and phototrophs (reviewed by Talbot *et al.* 2016; Inglis *et al.*, 2018; Kusch and Rush, 2022). Quaternary applications of BHPs in the Congo fan have demonstrated the correlation between elevated aerobic methane oxidation

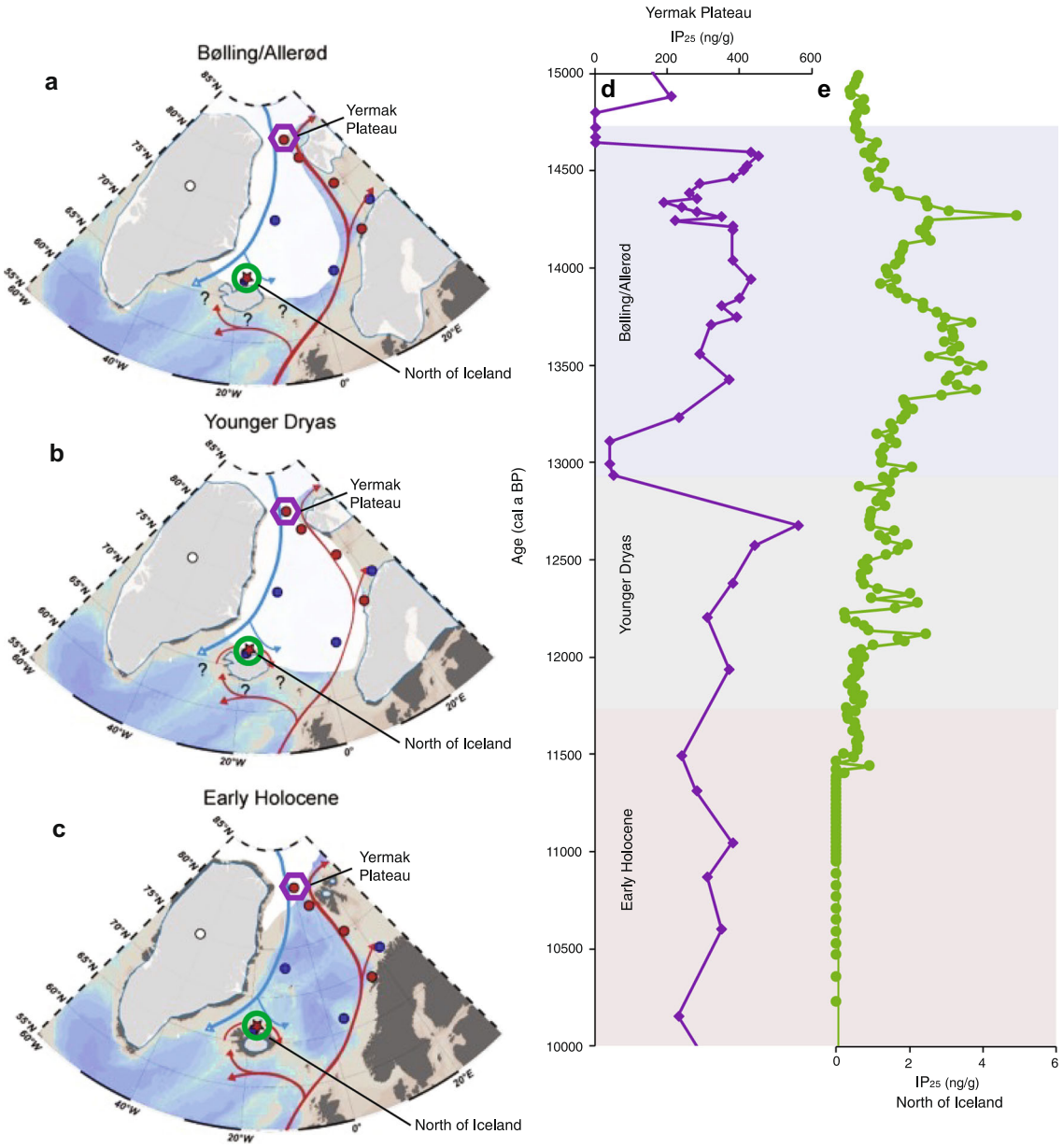

Figure 6. Schematic illustration of biomarker- (IP_{25}) inferred changes in spring/summer sea ice extent (white shadings) between (a) the Bølling/Allerød, (b) Younger Dryas and (c) Early Holocene (adapted from Xiao *et al.*, 2017; see the original figure for the detailed map key). Atlantic Water advection is represented by red arrows and cold Polar waters from the Arctic Ocean are represented by blue arrows. (d,e) Examples of the IP_{25} records used to develop the sea ice maps in a–c. (d) Most northerly IP_{25} record of sea ice presence (Yermak Plateau, denoted in purple; Müller *et al.*, 2009) and (e) most southerly IP_{25} record of sea ice presence (north of Iceland, denoted in green; Xiao *et al.*, 2017) included in the schematic maps. [Color figure can be viewed at wileyonlinelibrary.com]

in the wetlands onshore and late Quaternary interglacial climates (Talbot *et al.*, 2014) as well as a longer term shift ~1 Ma (Spencer-Jones *et al.*, 2017). Variations in archaeol and diploptene $\delta^{13}C$ values suggested links between the strength of the Asian monsoon and fluctuations in atmospheric methane concentrations (Zheng *et al.*, 2014). Low $\delta^{13}C_{diploptene}$ have also traced the presence and small-scale spatial heterogeneity of methane-oxidizing bacteria (MOB), and therefore methane oxidation, in Alaskan thermokarst lakes (Davies *et al.*, 2016).

Long-term insights into the nitrogen cycle have been developed using the bacteriohopanetetrol stereoisomer (BHT-*x*), a tracer of anaerobic oxidation of ammonium (anammox) (Rush *et al.*, 2014). For example, BHT-*x* demonstrated the link between higher temperatures and the intensification of oxygen deficiency zones in the Late Pleistocene in the Gulf of Alaska (Zindorf *et al.*, 2020). Their study indicated that, unlike redox-sensitive trace metals, BHT-*x* is not impacted by dilution effects of high sedimentation rates. Ammonium oxidation has also been reconstructed using ratios of isoGDGT [2]/[3], indicating the presence of the archaea *Thaumarchaeota*: in the South China Sea, interglacials were shown to be characterized by concurrent increases in ammonium oxidation and $\delta^{15}N$-inferred N_2 fixation (Dong *et al.*, 2019).

Transformation of the original biosynthesized compounds into recognizable products, under specific redox conditions, has also allowed changes in aerobic/anaerobic conditions to be traced in a range of environments. Interlinked changes to pH and water table explained the presence and down-core variations of an unusual hopanoid (the C_{31} 17α,21β(H)-homohopane) in Holocene peats, which is usually only found in thermally mature organic matter (Pancost *et al.*, 2003; McClymont *et al.*, 2008a; Inglis *et al.*, 2018). Transformation of sterols into stanols at the interface between oxic and anoxic conditions (Wakeham, 1989; Naafs *et al.*, 2019) has also been used to qualitatively assess Holocene changes in peat redox

conditions and water table depth (Naafs *et al.*, 2019). In a marine sediment core, the different resistance to oxygenation of a plant wax *n*-alcohol and *n*-alkane was exploited to identify bottom current strength and thus duration of organic matter exposure to oxygenated waters across multiple millennial-scale and glacial–interglacial cycles (Martrat *et al.*, 2007).

To assess the impacts of biogeochemical cycles on atmospheric CO_2, the $\delta^{13}C_{alkenone}$ biomarker proxy showed early promise, drawing on the fractionation of stable carbon isotopes during haptophyte photosynthesis (Bidigare et al., 1997). However, recent work has demonstrated that CO_2 uptake by haptophytes is different at low CO_2 concentrations (Badger *et al.*, 2019), indicating the need for careful interpretation of alkenone-based CO_2 reconstructions during the Quaternary.

Sedimentary records of humans and animals in Quaternary landscapes

Lipid biomarker analyses of sedimentary archives are increasingly used to characterize the presence, activities and impacts of humans and animals in the landscape, either as independent reconstructions or as complementary evidence in support of archaeological and palaeoecological anthropogenic reconstructions. Biomarkers also offer an alternative approach when levels of preservation are low or where archaeological excavation is not possible due to time, financial or logistical constraints (discussed in Brown *et al.*, 2022). Biomarkers in archaeological remains contain a wealth of information about the origin of artefacts and deposits and their associated use (reviewed by Evershed, 2008); however, here we focus on sedimentary biomarker proxies that provide both direct and indirect evidence for the presence and environmental impacts of human and animals. For more information, we direct readers to the dedicated review of anthropic biomarkers in sediment archives (Dubois and Jacob, 2016).

Faecal biomarkers as direct sedimentary indicators of human and animals

Faecal steroid biomarkers (5β-stanols, bile acids), which are produced in the digestive tracts of mammals and deposited via excrement into the environment, present an opportunity to directly identify both animals and humans from sedimentary archives (reviewed by Bull *et al.*, 2002). These compounds are well preserved within sedimentary archives over Holocene timescales (e.g. Simpson *et al.*, 1998; D'Anjou *et al.*, 2012; White *et al.*, 2019; Schroeter *et al.*, 2020; Brown *et al.*, 2021). Different species produce different diagnostic distributions of faecal steroids due to differences in diets, digestive processes and gut bacteria (e.g. Leeming *et al.*, 1996). Steroid ratios have therefore been used to distinguish between source organisms in investigations of modern faeces and archaeological deposits (e.g. Prost *et al.*, 2017; Zocatelli *et al.*, 2017; Shillito *et al.*, 2020; Kemp *et al.*, 2022), including through multivariate statistical analysis (Harrault *et al.*, 2019). The presence of 5β-stanols is not conclusive evidence of faecal deposition, since small amounts can be produced through the reduction of cholesterol in sedimentary environments (e.g. Gaskell and Eglinton, 1975; Bethell *et al.*, 1994), but the application of sterol ratios and the tandem analysis of sterols and bile acids can be used to confirm faecal input and improve faecal source assignment (e.g. Prost *et al.*, 2017). Identification of faecal sources is improved by characterizing steroid distributions of local reference dung to correct for within-species variability of sterol threshold values (Larson *et al.*, 2022) and reference soils to account for *in situ* sterol transformation (e.g. Bull *et al.*, 2002; Birk *et al.*, 2012).

Interactions between seabirds and their environment have been particularly effective using faecal steroids as indicators of nearby colonies (reviewed by Duda *et al.*, 2021). The changing impacts of penguin colonies and vegetation types (e.g. mosses vs lichens) on the West Antarctic Peninsula over the last 2400 years have been assessed from lake sediments (Wang *et al.*, 2007). Local declines of northern common eider (*Somateria mollissima borealis*) populations in Arctic Canada and Greenland have been linked to changes in sea-ice concentrations during the Little Ice Age (Hargan *et al.*, 2019), and Holocene little auk (*Alle alle*) population changes have been linked to the availability and stability of open waters (polynyas) in the sea ice (Ribeiro *et al.*, 2021).

New insights into the presence and impacts of humans in past landscapes have occurred where faecal steroids have refined the timings of human arrival and settlement activities in locations such as northern Norway (D'Anjou *et al.*, 2012), the North Atlantic Faroe Islands (Curtin *et al.*, 2021), the Azores Archipelago (Raposeiro et al., 2021), the Pacific Cook Islands (Sear *et al.*, 2020) and New Zealand (Argiriadis *et al.*, 2018). Faecal steroids have also reconstructed the presence of humans and/or livestock (e.g. White *et al.*, 2018; Vachula *et al.*, 2019; McWethy et al., 2020; Elliott Arnold et al., 2021; Keenan *et al.*, 2021; Ortiz et al., 2022), characterized long-term animal husbandry practices and land use (e.g. Mackay *et al.*, 2020; Schroeter *et al.*, 2020; Birk *et al.*, 2021), and the diets of extinct species (e.g. van Geel *et al.*, 2008; Sistiaga *et al.*, 2014). Comprehensive modern characterization of east African megafauna also illustrates the potential for faecal sterol applications to inform conservation palaeobiology (Kemp *et al.*, 2022).

Robust sedimentary faecal biomarker identifications of human presence in past landscapes are developed in combination with other sedimentary markers of anthropogenic activity such as pollen, charcoal, fire-derived lipid biomarkers (e.g. D'Anjou *et al.*, 2012; Battistel *et al.*, 2016; Section 8.2) and/or domesticated mammal sedaDNA (e.g. Brown *et al.*, 2022), and are integrated with the existing historical and/or archaeologyical context. Current uncertainties associated with within-species variability of steroid distributions, contributions from environmentally transformed 5β-stanols, and steroid transportation, storage, secondary deposition and degradation processes (e.g. Birk *et al.*, 2021; Keenan *et al.*, 2021; Davies *et al.*, 2022; Lawson et al., 2022) present a range of opportunities for further analysis to refine steroid identification of faecal sources and enhance their applications as anthropogenic and mammalian tracers in Quaternary science.

Biomarkers of burning and agricultural activity as indirect indicators of human activity

Pyrogenic biomarkers can enhance understanding of fire histories since their signatures and concentrations record information on the fuel type and conditions during the fire such as burn intensity and moisture content, as demonstrated through modern burning experiments (e.g. Oros and Simoneit, 2001; Karp *et al.*, 2020) and palaeo-comparisons with macro- and micro-charcoal (e.g. Elias *et al.*, 2001; Schreuder *et al.*, 2019a).

PAHs are produced during the incomplete combustion of biomass (reviewed by Richter and Howard (2000) and Lima *et al.* (2005)). PAH compound distributions represent combustion conditions, vegetation fuel type and transport pathways

(Karp *et al.*, 2020) and can be used to distinguish between local and regional burning events (e.g. Vachula *et al.*, 2022). Many PAHs can be atmospherically transported across thousands of kilometres, although some compounds, such as benzo[a]pyrene, have lower modelled half-life transport distances of ca. 500 km (Halsall et al., 2001). PAHs are produced by a wide range of burn temperatures (ca. 200–700 °C; Lu *et al.*, 2009), but higher concentrations are produced under high-intensity burning temperatures of 400–500 °C and during the combustion of woody rather than grassy vegetation (Karp *et al.*, 2020). Palaeo-PAH records may therefore be biased towards wildfires and sensitive to changes in fuel type and/or fire regime. Whilst PAHs can be released from petrogenic sources (e.g. Wakeham *et al.*, 1980), pyrogenic inputs can be identified using relative distributions of PAHs (e.g. Stogiannidis and Laane, 2015) or through comparisons with other fire proxies (e.g. Ruan *et al.*, 2020; Tan *et al.*, 2020). Long-term records of PAH fire histories have tracked human settlement and activity in the late Holocene in northern Norway (D'Anjou *et al.*, 2012), East Africa (Battistel *et al.*, 2016) and New Zealand (Argiriadis *et al.*, 2018) and characterized the advent of hominin pyrotechnology in the Middle Palaeolithic (Brittingham *et al.*, 2019). PAHs from lake sediments have also tracked industrial emissions such as combustion of coal (e.g. Meyers, 2003) and other fossil fuels (e.g. Guo *et al.*, 2022); anthropogenic pollution contributions must be considered if using PAHs to reconstruct fire histories over the industrial period.

Levoglucosan and its isomers (mannosan and galactosan) are monosaccharide anhydride (MA) compounds that are specific palaeo-fire proxies (reviewed by Simoneit, 2002 and Bhattarai *et al.*, 2019) since they are exclusively formed during the combustion of cellulose (Simoneit *et al.*, 1999) at burn temperatures of ca. 150–350 °C (e.g. Kuo *et al.*, 2008). MAs can travel hundreds to thousands of kilometres transported by wind and rivers (e.g. Mochida *et al.*, 2010; Zennaro *et al.*, 2014). Ratios of levoglucosan, mannosan and galactosan can reveal the type of biomass involved in burning events (e.g. Fabbri *et al.*, 2009; Kirchgeorg *et al.*, 2014) and combustion conditions (e.g. Kuo *et al.*, 2011). Lake sediment comparisons of macroscopic charcoal and MAs from the Mayan Lowlands, Guatemala, demonstrated the advances of combining these fire proxies to enhance understanding of palaeo-fire regimes at different spatial scales (Schüpbach *et al.*, 2015). Offshore levoglucosan records have confirmed vegetation changes associated with the late Quaternary megafaunal extinction in south-eastern Australia (Lopes dos Santos *et al.*, 2013b) and demonstrated increased burning linked to vegetation change and human settlement in sub-Saharan north-west Africa 60–50 ka (Schreuder *et al.*, 2019b). MA records from ice cores have been successfully applied to track post-Last Glacial Maximum and Holocene fire intensity and burning type at regional to semi-hemispheric scales (e.g. Zennaro *et al.*, 2014; Battistel *et al.*, 2018; Segato *et al.*, 2021; Chen *et al.*, 2022). Combustion-derived derivatives of lignin phenols, monosaccharide molecules and diterpenoids are also major components of smoke particulate matter and can be detected in sediment archives (Oros and Simoneit, 2001).

Evidence of crop cultivation and processing can characterize the timings of human presence and the types of activities taking place in past landscapes. Although not every cultivar has known specific lipid biomarkers, millacin is a marker of the introduced broomcorn millet in well-defined botanical settings (e.g. Jacob *et al.*, 2008a, 2008b; Bossard *et al.*, 2013). Fluxes of millacin detected in lake sediments have, for example, traced the introduction, intensification and failure of millet cultivation since the Bronze Age in the French Alps, and comparisons with contemporary palaeohydrological reconstructions have demonstrated climatically driven downturns in millet cultivation in the Hallstatt period (Jacob *et al.*, 2008a). Other cultivar biomarkers include cannabinol, a marker of hemp that can be used to identify processing activities (retting) from sediment archives (e.g. Lavrieux *et al.*, 2013; Schmidt *et al.*, 2020; Rull *et al.*, 2022), and palmitone, a marker of *Colocasia esculenta* Schott (taro) (e.g. Krentcher et al., 2019).

Conclusions and future outlook

Biomarkers have emerged as valuable parts of the Quaternary science toolkit, due to both quantitative and qualitative insights into past environmental changes, and because multiple biomarkers (and thus multiple environmental signals) can be recovered from single samples. Analytical developments and improved understanding of the processes underpinning the wide range of biomarker proxies outlined here have also led to data that have been both novel and complementary to more established Quaternary science approaches.

The major impacts of biomarker analyses have so far come from the quantification of temperature changes, and detailed assessments of the interactions between vegetation change and hydroclimate. The results are important in spanning a wide range of timescales, from annual/decadal through to the long-term evolution of Quaternary climates at glacial–interglacial and longer timescales. In considering future climate projections, both the quantitative and the qualitative insights gained from biomarker reconstructions have enabled data–model comparison and data–model assimilation to be undertaken across a wide range of timescales, including the pre-Quaternary (Tierney *et al.*, 2020; Masson-Delmotte *et al.*, 2021). In addition to providing valuable palaeoclimatic insights, biomarkers are increasingly being used to directly identify human impacts on the environment both pre-dating and through the Industrial era, thereby providing essential long-term context to advance our understanding of the resilience of ecosystems and societies.

Continued efforts to better constrain quantitative calibrations of temperature, salinity, sea ice and precipitation will further enhance our biomarker reconstructions. Community-wide collaborations have been important for advancing our understanding and application of palaeoenvironmental proxies and their uncertainties (e.g. Schouten *et al.*, 2013 for TEX_{86}; Belt *et al.*, 2014 for IP_{25}); similar approaches could assist with advancing our understanding of more recently developed or more qualitative biomarker proxies (e.g. anthropogenic markers). With the increasing application of (seda)DNA approaches to identify and understand the biomarker producers (e.g. Wang *et al.*, 2019b; Theroux *et al.*, 2020), more nuanced interpretations of past temperature or other environmental changes are also likely to result from reduced uncertainty estimates and through advances in our understanding of signals related to key producers and their potentially varied responses to factors including seasonality and nutrient availability. There is therefore the potential to add to the rich environmental information provided by both biomarkers and other geochemical and palaeoecological proxies, with new assessments of biogeochemical cycling, sea ice evolution and human–environment interactions, as well as new data on how that organic matter has been preserved, recycled and transported through palaeoenvironments.

In this review, we have outlined some of the many, diverse ways in which biomarkers have advanced understanding of Quaternary environments. The biomarker toolkit is continually evolving, aided by advances in instrument capabilities which are

presenting new opportunities to analyse smaller sample sizes and a greater diversity of Quaternary archives. For example, improvements in detection limits facilitated by high-resolution mass spectrometry present opportunities to expand the suite of palaeoenvironmental proxies that can be analysed from a single sample, and extend applications where sample sizes are limited and/or biomarker concentrations may be low (e.g. varved sediments, ice cores and/or highly resolved sedimentary records). In turn, untargeted analysis of environmental mass spectrometry spectral data, such as hierarchical clustering (e.g. Bale *et al.*, 2021) and the application of information theory and molecular networking (e.g. Ding *et al.*, 2021), yields highly detailed molecular information, with the potential to provide unprecedented levels of information about environmental contributions as well the identification of as yet unknown biomarkers, which may prove to be of ecological and environmental significance. In addition, there is great potential to expand compound-specific analyses, which have already yielded detailed insights into past hydroclimate, productivity and CO_2, by extending the range of biomarkers that can be analysed. A rapidly advancing area of biomarker research is radiocarbon analysis of individual lipids, or groups of lipids, which has already demonstrated that different pools of organic matter are being (re)worked and transported through river systems today (e.g. Galy & Eglinton, 2011; Eglinton *et al.*, 2021; Feng *et al.*, 2013) and have been in the past (Bliedtner *et al.*, 2020). Biomarker radiocarbon analysis shows great potential to not only enhance our understandings of Quaternary sedimentary environments and processes, but also to improve chronological controls through compound-specific radiocarbon analysis. Biomarkers have therefore made a wealth of contributions to Quaternary science, and the continued advances in this field of research offer many opportunities to extend our understandings of Earth systems in the past, present and future.

Acknowledgments. We thank Chris Orton for drafting Figs 1 and 3, Tommaso Tesi for access to data to generate Fig. 4, and Melissa Berke and George Swann for reflections on earlier manuscript drafts. We thank the Leverhulme Trust (RL-2019-23) and European Research Council (ANTSIE, grant no. 864637) for funding support.

Funding. Funding support has been provided by the Leverhulme Trust (Research Leadership Award 2019-023, E.L.M., T.D.J., C.P.) and the European Research Council H2020 (ANTSIE, grant no. 864637, E.L.M., M.S., E.M.H., Y.C.).

Conflict of interest statement—E.L.M. declares membership of the *Journal of Quaternary Science* Editorial Board. No other conflicts of interest are declared by the authors.

Data availability statement

Only published data and materials are referred to in this paper.

Ethics approval statement. No ethical approvals were requested as this paper reviews existing published data.

Patient consent statement. Not applicable.

Permission to reproduce material from other sources. We have applied to the publisher for permission to present the maps we adapted in Fig. 5.

Abbreviations. ACE index, Archaeol and Caldarchaeol Ecometric index; B-A, Bølling–Allerød; BHPs, bacteriohopanepolyols; BHT-*x*, bacteriohopanetetrol stereoisomer; BIT index, ratio describing relative abundance of isoGDGTs and brGDGTs; brGDGTS, branched glycerol dialkyl glycerol tetraethers; CSIA, compound-specific stable isotope analysis; D/H, deuterium/hydrogen; ENSO, El Niño/Southern Oscillation; GC, gas chromatography; GDGT, glycerol dialkyl glycerol tetraethers; HBI, highly branched isoprenoid; IP_{25}, ice proxy with 25 carbon atoms; $IPSO_{25}$, ice proxy for the Southern Ocean with 25 carbon atoms; isoGDGTs, isoprenoidal glycerol dialkyl glycerol tetraethers; ITCZ, Inter-Tropical Convergence Zone; LC, liquid chromatography; LDI, ratio describing relative abundance of 1,13- and 1,15-long-chain diols; MAs, monosaccharide anhydrides; MBT $'_{5Me}$ index, ratio describing relative abundance of brGDGTs with varying degrees of methylation; MS, mass spectrometry; PAHs, polyaromatic hydrocarbons; PIP_{25}, phytoplankton and ice proxy with 25 carbon atoms; $PIPSO_{25}$, phytoplankton and ice proxy for the Southern Ocean with 25 carbon atoms; RAN_{13} index, ratio describing relative abundance of isomers of the C_{13} 3-hydroxy fatty acids; sedaDNA, sedimentary ancient DNA; SST, sea surface temperature; TEX_{86} index, ratio describing relative abundance of the isoGDGTs; U^K_{37} index, ratio describing relative abundance of the $C_{37:4}$, $C_{37:3}$ and $C_{37:2}$ alkenones; U^K_{37}' index, ratio describing relative abundance of the $C_{37:3}$ and $C_{37:2}$ alkenones; U^K_{38Me}' index, ratio describing relative abundance of the C_{38} alkenones with methyl groups; UV, ultraviolet.

References

Aichner, B., Makhmudov, Z., Rajabov, I., Zhang, Q., Pausata, F.S.R., Werner, M. *et al.* (2019) Hydroclimate in the Pamirs Was Driven by Changes in Precipitation-Evaporation Seasonality Since the Last Glacial Period. *Geophysical Research Letters*, 46, 13972–13983. Available at: https://doi.org/10.1029/2019GL085202

Aichner, B., Ott, F., Słowiński, M., Noryśkiewicz, A.M., Brauer, A. & Sachse, D. (2018) Leaf wax *n*-alkane distributions record ecological changes during the Younger Dryas at Trzechowskie paleolake (northern Poland) without temporal delay. *Climate of the Past*, 14(11), 1607–1624. Available at: https://doi.org/10.5194/cp-14-1607-2018

Aichner, B., Wünnemann, B., Callegaro, A., van der Meer, M.T.J., Yan, D., Zhang, Y. *et al.* (2022) Asynchronous responses of aquatic ecosystems to hydroclimatic forcing on the Tibetan Plateau. *Communications Earth & Environment*, 3, 3, Available at: https://doi.org/10.1038/s43247-021-00325-1.

Andersson, R.A., Kuhry, P., Meyers, P., Zebühr, Y., Crill, P. & Mörth, M. (2011) Impacts of paleohydrological changes on n-alkane biomarker compositions of a Holocene peat sequence in the Eastern European Russian Arctic. *Organic Geochemistry*, 42, 1065–1075. Available at: https://doi.org/10.1016/j.orggeochem.2011.06.020

Argiriadis, E., Battistel, D., McWethy, D.B., Vecchiato, M., Kirchgeorg, T., Kehrwald, N.M. *et al.* (2018) Lake sediment fecal and biomass burning biomarkers provide direct evidence for prehistoric human-lit fires in New Zealand. *Scientific Reports*, 8, 12113, Available at: https://doi.org/10.1038/s41598-018-30606-3.

Arndt, S., Jørgensen, B.B., LaRowe, D.E., Middelburg, J.J., Pancost, R.D. & Regnier, P. (2013). Quantifying the degradation of organic matter in marine sediments: A review and synthesis. *Earth-Science Reviews*, 123, 53–86. Available at: https://doi.org/10.1016/j.earscirev.2013.02.008

Ashley, K.E., McKay, R., Etourneau, J., Jimenez-Espejo, F.J., Condron, A., Albot, A. *et al.* (2021) Mid-Holocene Antarctic sea-ice increase driven by marine ice sheet retreat. *Climate of the Past*, 17, 1–19. Available at: https://doi.org/10.5194/cp-17-1-2021.

Atwood, A.R. & Sachs, J.P. (2014) Separating ITCZ- and ENSO-related rainfall changes in the Galápagos over the last 3 kyr using D/H ratios of multiple lipid biomarkers. *Earth and Planetary Science Letters*, 404, 408–419. Available at: https://doi.org/10.1016/j.epsl.2014.07.038

Avsejs, L.A., Nott, C.J., Xie, S., Maddy, D., Chambers, F.M. & Evershed, R.P. (2002) 5-n-Alkylresorcinols as biomarkers of sedges in an ombrotrophic peat section. *Organic Geochemistry*, 33(7), 861–867. Available at: https://doi.org/10.1016/S0146-6380(02)00046-3

Badger, M.P.S., Chalk, T.B., Foster, G.L., Bown, P.R., Gibbs, S.J., Sexton, P.F. *et al.* (2019) Insensitivity of alkenone carbon isotopes to atmospheric CO_2 at low to moderate CO_2 levels. *Climate of the Past*, 15, 539–554. Available at: https://doi.org/10.5194/cp-15-539-2019,2019

Baker, A., Blyth, A.J., Jex, C.N., Mcdonald, J.A., Woltering, M. & Khan, S.J. (2019) Glycerol dialkyl glycerol tetraethers (GDGT) distributions from soil to cave: Refining the speleothem paleothermometer. *Organic Geochemistry*, 136, 103890, Available at: https://doi.org/10.1016/j.orggeochem.2019.06.011.

Bakku, R.K., Araie, H., Hanawa, Y., Shiraiwa, Y. & Suzuki, I. (2018) Changes in the accumulation of alkenones and lipids under nitrogen limitation and its relation to other energy storage metabolites in the haptophyte alga Emiliania huxleyi CCMP 2090. *Journal of Applied Phycology*, 30(1), 23–36. Available at: https://doi.org/10.1007/s10811-017-1163-x

Balascio, N.L., Anderson, R.S., D'Andrea, W.J., Wickler, S., D'Andrea, R.M. & Bakke, J. (2020) Vegetation changes and plant wax biomarkers from an ombrotrophic bog define hydroclimate trends and human–environment interactions during the Holocene in northern Norway. *The Holocene*, 30, 1849–1865. Available at: https://doi.org/10.1177/0959683620950456

Bale, N.J., Ding, S., Hopmans, E.C., Arts, M.G.I., Villanueva, L., Boschman, C. *et al.* (2021) Lipidomics of Environmental Microbial Communities. I: Visualization of Component Distributions Using Untargeted Analysis of High-Resolution Mass Spectrometry Data. *Frontiers in Microbiology*, 12, 659302, Available at: https://doi.org/10.3389/fmicb.2021.659302.

Barbara, L., Crosta, X., Leventer, A., Schmidt, S., Etourneau, J., Domack, E. *et al.* (2016) Environmental responses of the Northeast Antarctic Peninsula to the Holocene climate variability. East Antarctic Peninsula climate history. *Paleoceanography*, 31, 131–147. Available at: https://doi.org/10.1002/2015PA002785

Barbara, L., Crosta, X., Massé, G. & Ther, O. (2010) Deglacial environments in eastern Prydz Bay, East Antarctica. *Quaternary Science Reviews*, 29, 2731–2740. Available at: https://doi.org/10.1016/j.quascirev.2010.06.027

Basiliko, N., Yavitt, J.B., Dees, P.M. & Merkel, S.M. (2003) Methane biogeochemistry and methanogen communities in two northern peatland ecosystems, New York State. *Geomicrobiology Journal*, V. 20, 563–577. Available at: https://doi.org/10.1080/713851165

Basu, S., Sanyal, P., Pillai, A.A.S. & Ambili, A. (2019) Response of grassland ecosystem to monsoonal precipitation variability during the Mid-Late Holocene: Inferences based on molecular isotopic records from Banni grassland, western India. *PLoS One*, 14, e0212743. Available at: https://doi.org/10.1371/journal.pone.0212743

Battistel, D., Argiriadis, E., Kehrwald, N., Spigariol, M., Russell, J.M. & Barbante, C. (2016) Fire and human record at Lake Victoria, East Africa, during the Early Iron Age: Did humans or climate cause massive ecosystem changes? *The Holocene*, 27(7), 997–1007. Available at: https://doi.org/10.1177/0959683616678466

Battistel, D., Kehrwald, N.M., Zennaro, P., Pellegrino, G., Barbaro, E., Zangrando, R. *et al.* (2018) High-latitude Southern Hemisphere fire history during the midto late Holocene (6000–750 BP). *Climate of the Past*, 14, 871–886. Available at: https://doi.org/10.5194/cp-14-871-2018

Bechtel, A., Smittenberg, R.H., Bernasconi, S.M. & Schubert, C.J. (2010) Distribution of branched and isoprenoid tetraether lipids in an oligotrophic and a eutrophic Swiss lake: Insights into sources and GDGT-based proxies. *Organic Geochemistry*, 41(8), 822–832. Available at: https://doi.org/10.1016/j.orggeochem.2010.04.022

Belt, S.T. (2018) Source-specific biomarkers as proxies for Arctic and Antarctic sea ice. *Organic Geochemistry*, 125, 277–298. Available at: https://doi.org/10.1016/j.orggeochem.2018.10.002

Belt, S.T., Brown, T.A., Ampel, L., Cabedo-Sanz, P., Fahl, K., Kocis, J.J. *et al.* (2014) An inter-laboratory investigation of the Arctic sea ice biomarker proxy IP_{25} in marine sediments: key outcomes and recommendations. *Climate of the Past*, 10, 155–166. Available at: https://doi.org/10.5194/cp-10-155-2014

Belt, S.T., Cabedo-Sanz, P., Smik, L., Navarro-Rodriguez, A., Berben, S.M.P., Knies, J. *et al.* (2015) Identification of paleo Arctic winter sea ice limits and the marginal ice zone: Optimised biomarker-based reconstructions of late Quaternary Arctic sea ice. *Earth and Planetary Science Letters*, 431, 127–139. Available at: https://doi.org/10.1016/j.epsl.2015.09.020

Belt, S.T., Massé, G., Rowland, S.J., Poulin, M., Michel, C. & LeBlanc, B. (2007) A novel chemical fossil of palaeo sea ice: IP25. *Organic Geochemistry*, 38(1), 16–27. Available at: https://doi.org/10.1016/j.orggeochem.2006.09.013

Belt, S.T. & Müller, J. (2013) The Arctic sea ice biomarker IP25: a review of current understanding, recommendations for future research and applications in palaeo sea ice reconstructions. *Quaternary Science Reviews*, 79, 9–25. Available at: https://doi.org/10.1016/j.quascirev.2012.12.001

Belt, S.T., Smik, L., Brown, T.A., Kim, J.H., Rowland, S.J., Allen, C.S. *et al.* (2016) Source identification and distribution reveals the potential of the geochemical Antarctic sea ice proxy IPSO25. *Nature Communications*, 7, 12655, Available at: https://doi.org/10.1038/ncomms12655.

Bendle, J., Rosell-Melé, A. & Ziveri, P. (2005) Variability of unusual distributions of alkenones in the surface waters of the Nordic seas. *Paleoceanography*, 20(2), n/a. Available at: https://doi.org/10.1029/2004PA001025

Bendle, J.A., Weijers, J.W.H., Maslin, M.A., Sinninghe Damsté, J.S., Schouten, S., Hopmans, E.C. *et al.* (2010) Major changes in glacial and Holocene terrestrial temperatures and sources of organic carbon recorded in the Amazon fan by tetraether lipids. *Geochemistry, Geophysics, Geosystems*, 11(12), n/a. Available at: https://doi.org/10.1029/2010GC003308

Bendle, J.A.P., Rosell-Melé, A., Cox, N.J. & Shennan, I. (2009) Alkenones, alkenoates, and organic matter in coastal environments of NW Scotland: Assessment of potential application for sea level reconstruction: Biomarkers in coastal environments. *Geochemistry, Geophysics, Geosystems*, 10(12), n/a. Available at: https://doi.org/10.1029/2009GC002603

Berke, M.A., Johnson, T.C. & Werne, J.P. (2012a) Molecular records of climate variability and vegetation response since the Late Pleistocene in the Lake Victoria basin, East Africa. *Quaternary Science Reviews*, 55, 59–74. Available at: https://doi.org/10.1016/j.quascirev.2012.08.014

Berke, M.A., Johnson, T.C., Werne, J.P. et al (2012b) A mid-Holocene thermal maximum at the end of the African Humid Period. *Earth and Planetary Science Letters*, 351–352, 95–104. Available at: https://doi.org/10.1016/j.epsl.2012.07.008

Berke, M.A., Johnson, T.C., Werne, J.P., Livingstone, D.A., Grice, K., Schouten, S. *et al.* (2014) Characterization of the last deglacial transition in tropical East Africa: Insights from Lake Albert. *Palaeogeography, Palaeoclimatology, Palaeoecology*, 409, 1–8. Available at: https://doi.org/10.1016/j.palaeo.2014.04.014

Bethell, P.H., Goad, L.J., Evershed, R.P. & Ottaway, J. (1994) The study of molecular markers of human activity: the use of coprostanol in the soil as an indicator of human faecal material. *Journal of Archaeological Science*, 21(5), 619–632. Available at: https://doi.org/10.1006/jasc.1994.1061

Bhattacharya, S., Kishor, H., Ankit, Y., Mishra, P.K. & Srivastava, P. (2021) Vegetation History in a Peat Succession Over the Past 8,000 years in the ISM-Controlled Kedarnath Region, Garhwal Himalaya: Reconstruction Using Molecular Fossils. *Frontiers in Earth Science*, 9, 703362, Available at: https://doi.org/10.3389/feart.2021.703362.

Bhattarai, H., Saikawa, E., Wan, X., Zhu, H., Ram, K., Gao, S. *et al.* (2019) Levoglucosan as a tracer of biomass burning: Recent progress and perspectives. *Atmospheric Research*, 220, 20–33. Available at: https://doi.org/10.1016/j.atmosres.2019.01.004

Bianchi, T.S. & Canuel, E.A. (2011) Chemical Biomarkers in Aquatic Ecosystems, *Chemical Biomarkers in Aquatic Ecosystems*. Princeton University Presshttps://doi.org/10.1515/9781400839100

Bingham, E.M., McClymont, E.L., Väliranta, M., Mauquoy, D., Roberts, Z., Chambers, F.M. *et al.* (2010) Conservative composition of n-alkane biomarkers in Sphagnum species: Implications for palaeoclimate reconstruction in ombrotrophic peat bogs. *Organic Geochemistry*, 41, 214–220. Available at: https://doi.org/10.1016/j.orggeochem.2009.06.010

Birk, J.J., Dippold, M., Wiesenberg, G.L.B. & Glaser, B. (2012) Combined quantification of faecal sterols, stanols, stanones and bile acids in soils and terrestrial sediments by gas chromatography–mass spectrometry. *Journal of Chromatography A*, 1242, 1–10. Available at: https://doi.org/10.1016/j.chroma.2012.04.027

Birk, J.J., Reetz, K., Sirocko, F., Wright, D.K. & Fiedler, S. (2021) Faecal biomarkers as tools to reconstruct land-use history in maar sediments in the Westeifel Volcanic Field, Germany. *Boreas*, 51, 637–650. Available at: https://doi.org/10.1111/bor.12576

Bischoff, J., Mangelsdorf, K., Gattinger, A., Schloter, M., Kurchatova, A.N., Herzschuh, U. *et al.* (2013) Response of methanogenic archaea to Late Pleistocene and Holocene climate changes in the Siberian Arctic: methanogenic response to climate changes. *Global Biogeochemical Cycles*, 27, 305–317. Available at: https://doi.org/10.1029/2011GB004238

Bliedtner, M., von Suchodoletz, H., Schäfer, I., Welte, C., Salazar, G., Szidat, S. *et al.* (2020) Age and origin of leaf wax *n*-alkanes in fluvial sediment–paleosol sequences and implications for paleoenvironmental reconstructions. *Hydrology and Earth System Sciences*, 24, 2105–2120. Available at: https://doi.org/10.5194/hess-24-2105-2020

Blyth, A.J., Asrat, A., Baker, A., Gulliver, P., Leng, M.J. & Genty, D. (2007) A new approach to detecting vegetation and land-use Change using high-resolution lipid biomarker records in stalagmites. *Quaternary Research*, 68, 314–324. Available at: https://doi.org/10.1016/j.yqres.2007.08.002

Blyth, A.J., Farrimond, P. & Jones, M. (2006) An optimised method for the extraction and analysis of lipid biomarkers from stalagmites. *Organic Geochemistry*, 37(8), 882–890. Available at: https://doi.org/10.1016/j.orggeochem.2006.05.003

Blyth, A.J., Hartland, A. & Baker, A. (2016) Organic proxies in speleothems – New developments, advantages and limitations. *Quaternary Science Reviews*, 149, 1–17. Available at: https://doi.org/10.1016/j.quascirev.2016.07.001

Blyth, A.J. & Watson, J.S. (2009) Thermochemolysis of organic matter preserved in stalagmites: A preliminary study. *Organic Geochemistry*, 40, 1029–1031. Available at: https://doi.org/10.1016/j.orggeochem.2009.06.007

Boon, J.J., Dupont, L. & De Leeuw, J.W. (1986) Characterization of a peat bog profile by Curie Point pyrolysis-mass spectrometry combined with multivariant analysis and by pyrolysis gas chromatography–mass spectrometry. In: Fuchsman, C.H., (Ed.) *Peat and Water*. Elsevier Applied Science Publishers Ltd. pp. 215–219.

Bossard, N., Jacob, J., Le Milbeau, C., Sauze, J., Terwilliger, V., Poissonnier, B. *et al.* (2013) Distribution of miliacin (olean-18-en-3β-ol methyl ether) and related compounds in broomcorn millet (Panicum miliaceum) and other reputed sources: Implications for the use of sedimentary miliacin as a tracer of millet. *Organic Geochemistry*, 63, 48–55. Available at: https://doi.org/10.1016/j.orggeochem.2013.07.012

Bowen, G.J. & Revenaugh, J. (2003) Interpolating the isotopic composition of modern meteoric precipitation. *Water Resources Research*, 39(10), 1299. Available at: https://doi.org/10.1029/2003WR002086

Brassell, S.C., Eglinton, G., Marlowe, I.T., Pflaumann, U. & Sarnthein, M. (1986) Molecular stratigraphy: a new tool for climatic assessment. *Nature*, 320, 129–133. Available at: https://doi.org/10.1038/320129a0

Bray, E.E. & Evans, E.D. (1961) Distribution of n-paraffins as a clue to recognition of source beds. *Geochimica et Cosmochimica Acta*, 22, 2–15. Available at: https://doi.org/10.1016/0016-7037(61)90069-2

Brittingham, A., Hren, M.T., Hartman, G., Wilkinson, K.N., Mallol, C., Gasparyan, B. *et al.* (2019) Geochemical Evidence for the Control of Fire by Middle Palaeolithic Hominins. *Scientific Reports*, 9, 15368, Available at: https://doi.org/10.1038/s41598-019-51433-0.

Brown, A.G., Fonville, T., van Hardenbroek, M., Cavers, G., Crone, A., McCormick, F. *et al.* (2022) New integrated molecular approaches for investigating lake settlements in north-western Europe. *Antiquity*, 96, 1179–1199. Available at: https://doi.org/10.15184/aqy.2022.70

Brown, A.G., Van Hardenbroek, M., Fonville, T., Davies, K., Mackay, H., Murray, E. *et al.* (2021) Ancient DNA, lipid biomarkers and palaeoecological evidence reveals construction and life on early medieval lake settlements. *Scientific Reports*, 11, 11807, Available at: https://doi.org/10.1038/s41598-021-91057-x.

Bull, I.D., Lockheart, M.J., Elhmmali, M.M., Roberts, D.J. & Evershed, R.P. (2002) The origin of faeces by means of biomarker detection. *Environment International*, 27, 647–654. Available at: https://doi.org/10.1016/S0160-4120(01)00124-6

Bush, R.T. & McInerney, F.A. (2013) Leaf wax n-alkane distributions in and across modern plants: Implications for paleoecology and chemotaxonomy. *Geochimica et Cosmochimica Acta*, 117, 161–179. Available at: https://doi.org/10.1016/j.gca.2013.04.016

Cabedo-Sanz, P., Belt, S.T., Knies, J. & Husum, K. (2013) Identification of contrasting seasonal sea ice conditions during the Younger Dryas. *Quaternary Science Reviews*, 79, 74–86. Available at: https://doi.org/10.1016/j.quascirev.2012.10.028

Campagne, P., Crosta, X., Houssais, M.N., Swingedouw, D., Schmidt, S., Martin, A. *et al.* (2015) Glacial ice and atmospheric forcing on the Mertz Glacier Polynya over the past 250 years. *Nature Communications*, 6, 6642, Available at: https://doi.org/10.1038/ncomms7642.

Capron, E., Govin, A., Feng, R., Otto-Bliesner, B.L. & Wolff, E.W. (2017) Critical evaluation of climate syntheses to benchmark CMIP6/PMIP4 127 ka Last Interglacial simulations in the high-latitude regions. *Quaternary Science Reviews*, 168, 137–150. Available at: https://doi.org/10.1016/j.quascirev.2017.04.019

Carr, A.S., Boom, A., Chase, B.M., Meadows, M.E. & Grimes, H.L. (2015) Holocene sea level and environmental change on the west coast of South Africa: evidence from plant biomarkers, stable isotopes and pollen. *Journal of Paleolimnology*, 53, 415–432. Available at: https://doi.org/10.1007/s10933-015-9833-7

Cartagena-Sierra, A., Berke, M.A., Robinson, R.S., Marcks, B., Castañeda, I.S., Starr, A. *et al.* (2021) Latitudinal Migrations of the Subtropical Front at the Agulhas Plateau Through the Mid-Pleistocene Transition. *Paleoceanography and Paleoclimatology*, 36(7), e2020PA004084. Available at: https://doi.org/10.1029/2020PA004084

Castañeda, I.S., Mulitza, S., Schefuß, E. et al (2009a) Wet phases in the Sahara/Sahel region and human migration patterns in North Africa. *Proc. Natl. Acad. Sci. U.S.A.* 106, 20159–20163. Available at: https://doi.org/10.1073/pnas.0905771106

Castañeda, I.S. & Schouten, S. (2011) A review of molecular organic proxies for examining modern and ancient lacustrine environments. *Quaternary Science Reviews*, 30, 2851–2891. Available at: https://doi.org/10.1016/j.quascirev.2011.07.009

Castañeda, I.S., Werne, J.P., & Johnson, T.C. (2007) Wet and arid phases in the southeast African tropics since the Last Glacial Maximum. *Geology*, 35(9), 823–826. Available at: https://doi.org/10.1130/G23916A.1.

Castañeda, I.S., Werne, J.P., Johnson, T.C., & Filley, T.R. (2009b) Late Quaternary vegetation history of southeast Africa: The molecular isotopic record from Lake Malawi. *Palaeogeography, Palaeoclimatology, Palaeoecology*, 275, 100–112. Available at: https://doi.org/10.1016/j.palaeo.2009.02.008.

Chen, A., Yang, L., Kang, H., Gao, Y. & Xie, Z. (2022) Southern hemisphere fire history since the late glacial, reconstructed from an Antarctic sediment core. *Quaternary Science Reviews*, 276, 107300, Available at: https://doi.org/10.1016/j.quascirev.2021.107300.

Chen, N., Bianchi, T.S., McKee, B.A. & Bland, J.M. (2001) Historical trends of hypoxia on the Louisiana shelf: application of pigments as biomarkers. *Organic Geochemistry*, 32(4), 543–561. Available at: https://doi.org/10.1016/S0146-6380(00)00194-7

Chondrogianni, C., Ariztegui, D., Rolph, T., Juggins, S., Shemesh, A., Rietti-Shati, M. *et al.* (2004) Millennial to interannual climate variability in the Mediterranean during the Last Glacial Maximum. *Quaternary International*, 122, 31–41. Available at: https://doi.org/10.1016/j.quaint.2004.01.029

Clotten, C., Stein, R., Fahl, K. & De Schepper, S. (2018) Seasonal sea ice cover during the warm Pliocene: Evidence from the Iceland Sea (ODP Site 907). *Earth and Planetary Science Letters*, 481, 61–72. Available at: https://doi.org/10.1016/j.epsl.2017.10.011

Collins, L.G., Allen, C.S., Pike, J., Hodgson, D.A., Weckström, K. & Massé, G. (2013) Evaluating highly branched isoprenoid (HBI) biomarkers as a novel Antarctic sea-ice proxy in deep ocean glacial age sediments. *Quaternary Science Reviews*, 79, 87–98. Available at: https://doi.org/10.1016/j.quascirev.2013.02.004

Conte, M.H., Sicre, M.-A., Rühlemann, C., Weber, J.C., Schulte, S., Schulz-Bull, D. *et al.* (2006) Global temperature calibration of the alkenone unsaturation index ($U^{K'}_{37}$) in surface waters and comparison with surface sediments: alkenone unsaturation index. *Geochemistry, Geophysics, Geosystems*, 7, n/a. Available at: https://doi.org/10.1029/2005GC001054

Craig, H. & Gordon, L.I. (1965) Deuterium and oxygen 18 variations in the ocean and marine atmosphere. Proceedings of a Conference on Stable Isotopes in Oceanographic Studies and Paleotemperatures, V. Lischi & Figli, Pisa, Spoleto, Italy (1965), pp. 9-130.

Cranwell, P.A. (1973) Chain-length distribution of n-alkanes from lake sediments in relation to post-glacial environmental change. *Freshwater Biology*, 3(3), 259–265. Available at: https://doi.org/10.1111/j.1365-2427.1973.tb00921.x

Cranwell, P.A., Eglinton, G. & Robinson, N. (1987) Lipids of aquatic organisms as potential contributors to lacustrine sediments—II. *Organic Geochemistry*, 11, 513–527. Available at: https://doi.org/10.1016/0146-6380(87)90007-6

Cuddington, K. & Leavitt, P.R. (1999) An individual-based model of pigment flux in lakes: implications for organic biogeochemistry and paleoecology. *Canadian Journal of Fisheries and Aquatic Sciences*, 56, 1964–1977. Available at: https://doi.org/10.1139/f99-108

Curtin, L., D'Andrea, W.J., Balascio, N.L., Shirazi, S., Shapiro, B., de Wet, G.A. *et al*. (2021) Sedimentary DNA and molecular evidence for early human occupation of the Faroe Islands. *Communications Earth & Environment*, 2, 253, Available at: https://doi.org/10.1038/s43247-021-00318-0.

Damsté, J.S.S., Hopmans, E.C., Pancost, R.D., Schouten, S. & Geenevasen, J.A.J. (2000) Newly discovered non-isoprenoid glycerol dialkyl glycerol tetraether lipids in sediments. *Chemical Communications*, 17, 1683–1684. Available at: https://doi.org/10.1039/B004517I

D'Andrea, W.J. & Huang, Y. (2005) Long chain alkenones in Greenland lake sediments: Low δ13C values and exceptional abundance. *Organic Geochemistry*, 36, 1234–1241. Available at: https://doi.org/10.1016/j.orggeochem.2005.05.001

D'Andrea, W.J., Huang, Y., Fritz, S.C. & Anderson, N.J. (2011) Abrupt Holocene climate change as an important factor for human migration in West Greenland. *Proceedings of the National Academy of Sciences*, 108, 9765–9769. Available at: https://doi.org/10.1073/pnas.1101708108.

D'Andrea, W.J., Theroux, S., Bradley, R.S. & Huang, X. (2016) Does phylogeny control U 37 K -temperature sensitivity? Implications for lacustrine alkenone paleothermometry. *Geochimica et Cosmochimica Acta*, 175, 168–180. Available at: https://doi.org/10.1016/j.gca.2015.10.031.

Daniels, W.C., Castañeda, I.S., Salacup, J.M., Habicht, M.H., Lindberg, K.R. & Brigham-Grette, J. (2022) Archaeal lipids reveal climate-driven changes in microbial ecology at Lake El'gygytgyn (Far East Russia) during the Plio-Pleistocene. *Journal of Quaternary Science*, 37, 900–914. Available at: https://doi.org/10.1002/jqs.3347.

D'Anjou, R.M., Bradley, R.S., Balascio, N.L. & Finkelstein, D.B. (2012) Climate impacts on human settlement and agricultural activities in northern Norway revealed through sediment biogeochemistry. *Proceedings of the National Academy of Sciences*, 109, 20332–20337. Available at: https://doi.org/10.1073/pnas.1212730109

Davies, A.L., Harrault, L., Milek, K., McClymont, E.L., Dallimer, M., Hamilton, A. *et al*. (2022) A multiproxy approach to long-term herbivore grazing dynamics in peatlands based on pollen, coprophilous fungi and faecal biomarkers. *Palaeogeography, Palaeoclimatology, Palaeoecology*, 598, 111032, Available at: https://doi.org/10.1016/j.palaeo.2022.111032.

Davies, K.L., Pancost, R.D., Edwards, M.E., Walter Anthony, K.M., Langdon, P.G. & Chaves Torres, L. (2016) Diploptene δ_{13}C values from contemporary thermokarst lake sediments show complex spatial variation. *Biogeosciences*, 13, 2611–2621. Available at: https://doi.org/10.5194/bg-13-2611-2016

De Bar, M.W., Stolwijk, D.J., McManus, J.F., Sinninghe Damsté, J.S. & Schouten, S. (2018) A Late Quaternary climate record based on long-chain diol proxies from the Chilean margin. *Climate of the Past*, 14, 1783–1803. Available at: https://doi.org/10.5194/cp-14-1783-2018

De Bar, M.W., Weiss, G., Yildiz, C., Rampen, S.W., Lattaud, J., Bale, N.J. *et al*. (2020) Global temperature calibration of the Long chain Diol Index in marine surface sediments. *Organic Geochemistry*, 142, 103983, Available at: https://doi.org/10.1016/j.orggeochem.2020.103983.

De Jonge, C., Hopmans, E.C., Zell, C.I., Kim, J.H., Schouten, S. & Sinninghe Damsté, J.S. (2014) Occurrence and abundance of 6-methyl branched glycerol dialkyl glycerol tetraethers in soils: Implications for palaeoclimate reconstruction. *Geochimica et Cosmochimica Acta*, 141, 97–112. Available at: https://doi.org/10.1016/j.gca.2014.06.013

De Jonge, C., Stadnitskaia, A., Fedotov, A. & Sinninghe Damsté, J.S. (2015) Impact of riverine suspended particulate matter on the branched glycerol dialkyl glycerol tetraether composition of lakes: The outflow of the Selenga River in Lake Baikal (Russia). *Organic Geochemistry*, 83-84, 241–252. Available at: https://doi.org/10.1016/j.orggeochem.2015.04.004

De Rosa, M., Esposito, E., Gambacorta, A., Nicolaus, B. & Bu'Lock, J.D. (1980) Effects of temperature on ether lipid composition of Caldariella acidophila. *Phytochemistry*, 19(5), 827–831. Available at: https://doi.org/10.1016/0031-9422(80)85120-X

Dearing Crampton-Flood, E., Tierney, J.E., Peterse, F., Kirkels, F.M.S.A. & Sinninghe Damsté, J.S. (2020) BayMBT: A Bayesian calibration model for branched glycerol dialkyl glycerol tetraethers in soils and peats. *Geochimica et Cosmochimica Acta*, 268, 142–159. Available at: https://doi.org/10.1016/j.gca.2019.09.043

Denis, D., Crosta, X., Barbara, L., Massé, G., Renssen, H., Ther, O. *et al*. (2010) Sea ice and wind variability during the Holocene in East Antarctica: insight on middle–high latitude coupling. *Quaternary Science Reviews*, 29, 3709–3719. Available at: https://doi.org/10.1016/j.quascirev.2010.08.007

Detlef, H., Belt, S.T., Sosdian, S.M., Smik, L., Lear, C.H., Hall, I.R. *et al*. (2018) Sea ice dynamics across the Mid-Pleistocene transition in the Bering Sea. *Nature Communications*, 9, 941, Available at: https://doi.org/10.1038/s41467-018-02845-5.

Diefendorf, A.F. & Freimuth, E.J. (2017) Extracting the most from terrestrial plant-derived n-alkyl lipids and their carbon isotopes from the sedimentary record: A review. *Organic Geochemistry*, 103, 1–21. Available at: https://doi.org/10.1016/j.orggeochem.2016.10.016

Ding, S., Bale, N.J., Hopmans, E.C., Villanueva, L., Arts, M.G.I., Schouten, S. *et al*. (2021) Lipidomics of Environmental Microbial Communities. II: Characterization Using Molecular Networking and Information Theory. *Frontiers in Microbiology*, 12, 659315, Available at: https://doi.org/10.3389/fmicb.2021.659315.

Dong, L., Li, Z. & Jia, G. (2019) Archaeal ammonia oxidation plays a part in late Quaternary nitrogen cycling in the South China Sea. *Earth and Planetary Science Letters*, 509, 38–46. Available at: https://doi.org/10.1016/j.epsl.2018.12.023

Dubois, N. & Jacob, J. (2016) Molecular Biomarkers of Anthropic Impacts in Natural Archives: A Review. *Frontiers in Ecology and Evolution*, 4, 92. Available at: https://doi.org/10.3389/fevo.2016.00092

Duda, M.P., Hargan, K.E., Michelutti, N., Blais, J.M., Grooms, C., Gilchrist, H.G. *et al*. (2021) Reconstructing Long-Term Changes in Avian Populations Using Lake Sediments: Opening a Window Onto the Past. *Frontiers in Ecology and Evolution*, 9, 698175. Available at: https://doi.org/10.3389/fevo.2021.698175

Eglinton, G. & Calvin, M. (1967) Chemical Fossils. *Scientific American*, 216, 32–43. Available at: https://doi.org/10.1038/scientificamerican0167-32

Eglinton, G. & Hamilton, R.J. (1967) Leaf Epicuticular Waxes: The waxy outer surfaces of most plants display a wide diversity of fine structure and chemical constituents. *Science*, 156, 1322–1335. Available at: https://doi.org/10.1126/science.156.3780.1322

Eglinton, T.I., Aluwihare, L.I., Bauer, J.E., Druffel, E.R.M. & McNichol, A.P. (1996) Gas Chromatographic Isolation of Individual Compounds from Complex Matrices for Radiocarbon Dating. *Analytical Chemistry*, 68, 904–912. Available at: https://doi.org/10.1021/ac9508513

Eglinton, T.I., Galy, V.V., Hemingway, J.D., Feng, X., Bao, H., Blattmann, T.M. *et al*. (2021) Climate control on terrestrial biospheric carbon turnover. *Proceedings of the National Academy of Sciences*, 118(8), e2011585118, Available at: https://doi.org/10.1073/pnas.2011585118.

Eley, Y.L. & Hren, M.T. (2018) Reconstructing vapor pressure deficit from leaf wax lipid molecular distributions. *Scientific Reports*, 8(1), 3967, Available at: https://doi.org/10.1038/s41598-018-21959-w.

Elias, V.O., Simoneit, B.R.T., Cordeiro, R.C. & Turcq, B. (2001) Evaluating levoglucosan as an indicator of biomass burning in Carajαs, Amazônia: a comparison to the charcoal record. *Geochimica et Cosmochimica Acta*, 65, 267–272. Available at: https://doi.org/10.1016/S0016-7037(00)00522-6

Elliott Arnold, T., Hillman, A.L., McGrath, S.J., Abbott, M.B., Werne, J.P., Hutchings, J. & Arkush, E.N. (2021) Fecal stanol ratios indicate shifts in camelid pastoralism in the highlands of Peru across a

4,000-year lacustrine sequence. *Quaternary Science Reviews*, 270. https://doi.org/10.1016/j.quascirev.2021.107193

Englebrecht, A.C. & Sachs, J.P. (2005) Determination of sediment provenance at drift sites using hydrogen isotopes and unsaturation ratios in alkenones. *Geochimica et Cosmochimica Acta*, 69(17), 4253–4265. Available at: https://doi.org/10.1016/j.gca.2005.04.011

Epstein, B.L., D'Hondt, S. & Hargraves, P.E. (2001) The possible metabolic role of C37 alkenones in Emiliania huxleyi. *Organic Geochemistry*, 32(6), 867–875. Available at: https://doi.org/10.1016/S0146-6380(01)00026-2

Erdem, Z., Lattaud, J., Erk, M.R., Mezger, E., Reichart, G.J., Lückge, A. *et al.* (2021) Applicability of the Long Chain Diol Index (LDI) as a Sea Surface Temperature Proxy in the Arabian Sea. *Paleoceanography and Paleoclimatology*, 36(12), 4255. Available at: https://doi.org/10.1029/2021PA004255

Etourneau, J., Collins, L.G., Willmott, V., Kim, J.H., Barbara, L., Leventer, A. *et al.* (2013) Holocene climate variations in the western Antarctic Peninsula: evidence for sea ice extent predominantly controlled by changes in insolation and ENSO variability. *Climate of the Past*, 9, 1431–1446. Available at: https://doi.org/10.5194/cp-9-1431-2013

Evershed, R.P. (2008) Organic residue analysis in archaeology: the archaeological biomarker revolution. *Archaeometry*, 50, 895–924. Available at: https://doi.org/10.1111/j.1475-4754.2008.00446.x

Fabbri, D., Torri, C., Simoneit, B.R.T., Marynowski, L., Rushdi, A.I. & Fabiańska, M.J. (2009) Levoglucosan and other cellulose and lignin markers in emissions from burning of Miocene lignites. *Atmospheric Environment*, 43(14), 2286–2295. Available at: https://doi.org/10.1016/j.atmosenv.2009.01.030

Fahl, K. & Stein, R. (1999) Biomarkers as organic-carbon-source and environmental indicators in the Late Quaternary Arctic Ocean: problems and perspectives. *Marine Chemistry*, 63, 293–309. Available at: https://doi.org/10.1016/S0304-4203(98)00068-1

Feakins, S.J., Wu, M.S., Ponton, C. & Tierney, J.E. (2019) Biomarkers reveal abrupt switches in hydroclimate during the last glacial in southern California. *Earth and Planetary Science Letters*, 515, 164–172. Available at: https://doi.org/10.1016/j.epsl.2019.03.024

Feng, X., Vonk, J.E., van Dongen, B.E., van Dongen, B.E., Gustafsson, Ö., Semiletov, I.P. *et al.* (2013) Differential mobilization of terrestrial carbon pools in Eurasian Arctic river basins. *Proceedings of the National Academy of Sciences*, 110, 14168–14173. Available at: https://doi.org/10.1073/pnas.1307031110

Ficken, K.J., Li, B., Swain, D.L. & Eglinton, G. (2000) An n-alkane proxy for the sedimentary input of submerged/floating freshwater aquatic macrophytes. *Organic Geochemistry*, 31, 745–749. Available at: https://doi.org/10.1016/S0146-6380(00)00081-4.

Fietz, S., Huguet, C., Bendle, J., Escala, M., Gallacher, C., Herfort, L. *et al.* (2012) Co-variation of crenarchaeol and branched GDGTs in globally-distributed marine and freshwater sedimentary archives. *Global and Planetary Change*, 92–93, 275–285. Available at: https://doi.org/10.1016/j.gloplacha.2012.05.020

Foster, L.C., Pearson, E.J., Juggins, S., Hodgson, D.A., Saunders, K.M., Verleyen, E. *et al.* (2016) Development of a regional glycerol dialkyl glycerol tetraether (GDGT)–temperature calibration for Antarctic and sub-Antarctic lakes. *Earth and Planetary Science Letters*, 433, 370–379. Available at: https://doi.org/10.1016/j.epsl.2015.11.018

Galy, V. & Eglinton, T. (2011) Protracted storage of biospheric carbon in the Ganges–Brahmaputra basin. *Nature Geoscience*, 4(12), 843–847. Available at: https://doi.org/10.1038/ngeo1293

Gaskell, S.J. & Eglinton, G. (1975) Rapid hydrogenation of sterols in a contemporary lacustrine sediment. *Nature*, 254(5497), 209–211. Available at: https://doi.org/10.1038/254209b0

Griepentrog, M., De Wispelaere, L., Bauters, M., Bodé, S., Hemp, A., Verschuren, D. *et al.* (2019) Influence of plant growth form, habitat and season on leaf-wax n-alkane hydrogen-isotopic signatures in equatorial East Africa. *Geochimica et Cosmochimica Acta*, 263, 122–139. Available at: https://doi.org/10.1016/j.gca.2019.08.004

Günther, F., Thiele, A., Biskop, S., Mäusbacher, R., Haberzettl, T., Yao, T. *et al.* (2016) Late quaternary hydrological changes at Tangra Yumco, Tibetan Plateau: a compound-specific isotope-based quantification of lake level changes. *Journal of Paleolimnology*, 55, 369–382. Available at: https://doi.org/10.1007/s10933-016-9887-1

Guo, F., Gao, M., Dong, J., Sun, J., Hou, G., Liu, S. *et al.* (2022) The first high resolution PAH record of industrialization over the past 200 years in Liaodong Bay, northeastern China. *Water Research*, 224, 119103, Available at: https://doi.org/10.1016/j.watres.2022.119103.

Hargan, K.E., Gilchrist, H.G., Clyde, N.M.T., Iverson, S.A., Forbes, M.R., Kimpe, L.E. *et al.* (2019) Multicentury perspective assessing the sustainability of the historical harvest of seaducks. *Proceedings of the National Academy of Sciences*, 116, 8425–8430. Available at: https://doi.org/10.1073/pnas.1814057116

Harning, D.J., Curtin, L., Geirsdóttir, Á., D'Andrea, W.J., Miller, G.H. & Sepúlveda, J. (2020) Lipid Biomarkers Quantify Holocene Summer Temperature and Ice Cap Sensitivity in Icelandic Lakes. *Geophysical Research Letters*, 47, e2019GL085728. Available at: https://doi.org/10.1029/2019GL085728

Harrault, L., Milek, K., Jardé, E., Jeanneau, L., Derrien, M. & Anderson, D.G. (2019) Faecal biomarkers can distinguish specific mammalian species in modern and past environments. *PLoS One*, 14, e0211119. Available at: https://doi.org/10.1371/journal.pone.0211119

Harris, P.G. & Maxwell, J.R. (1995) A novel method for the rapid determination of chlorin concentrations at high stratigraphic resolution in marine sediments. *Organic Geochemistry*, 23, 853–856. Available at: https://doi.org/10.1016/0146-6380(95)80007-E

Harris, P.G., Zhao, M., Rosell-Melé, A., Tiedemann, R., Sarnthein, M. & Maxwell, J.R. (1996) Chlorin accumulation rate as a proxy for Quaternary marine primary productivity. *Nature*, 383, 63–65. Available at: https://doi.org/10.1038/383063a0

He, D., Simoneit, B.R.T., Cloutier, J.B. & Jaffé, R. (2018) Early diagenesis of triterpenoids derived from mangroves in a subtropical estuary. *Organic Geochemistry*, 125, 196–211. Available at: https://doi.org/10.1016/j.orggeochem.2018.09.005

He, Y., Wang, H., Meng, B., Liu, H., Zhou, A., Song, M. *et al.* (2020) Appraisal of alkenone- and archaeal ether-based salinity indicators in mid-latitude Asian lakes. *Earth and Planetary Science Letters*, 538, Article 116236, Available at: https://doi.org/10.1016/j.epsl.2020.116236.

He, Y., Zhao, C., Wang, Z., Wang, H., Song, M., Liu, W. *et al.* (2013) Late Holocene coupled moisture and temperature changes on the northern Tibetan Plateau. *Quaternary Science Reviews*, 80(2013), 47–57. Available at: https://doi.org/10.1016/j.quascirev.2013.08.017

Hedges, J.I., Ertel, J.R. & Leopold, E.B. (1982) Lignin geochemistry of a Late Quaternary sediment core from Lake Washington. *Geochimica et Cosmochimica Acta*, 46, 1869–1877. Available at: https://doi.org/10.1016/0016-7037(82)90125-9

Hefter, J., Naafs, B.D.A. & Zhang, S. (2017) Tracing the source of ancient reworked organic matter delivered to the North Atlantic Ocean during Heinrich Events. *Geochimica et Cosmochimica Acta*, 205, 211–225. Available at: https://doi.org/10.1016/j.gca.2017.02.008

Heidke, I., Scholz, D. & Hoffmann, T. (2019) Lignin oxidation products as a potential proxy for vegetation and environmental changes in speleothems and cave drip water – a first record from the Herbstlabyrinth, central Germany. *Climate of the Past*, 15, 1025–1037. Available at: https://doi.org/10.5194/cp-15-1025-2019

Hepp, J., Tuthorn, M., Zech, R., Mügler, I., Schlütz, F., Zech, W. *et al.* (2015) Reconstructing lake evaporation history and the isotopic composition of precipitation by a coupled δ18O–δ2H biomarker approach. *Journal of Hydrology*, 529, 622–631. Available at: https://doi.org/10.1016/j.jhydrol.2014.10.012

Herbert, T.D., Peterson, L.C., Lawrence, K.T. & Liu, Z. (2010) Tropical Ocean Temperatures Over the Past 3.5 Million Years. *Science*, 328, 1530–1534. Available at: https://doi.org/10.1126/science.1185435

Hodgson, D., Vyverman, W., Verleyen, E., LEAVITT, P., SABBE, K., SQUIER, A. *et al.* (2005) Late Pleistocene record of elevated UV radiation in an Antarctic lake. *Earth and Planetary Science Letters*, 236, 765–772. Available at: https://doi.org/10.1016/j.epsl.2005.05.023

Hodgson, D.A., McMinn, A., Kirkup, H., Cremer, H., Gore, D., Melles, M. *et al.* (2003) Colonization, succession, and extinction of marine floras during a glacial cycle: A case study from the Windmill Islands (east Antarctica) using biomarkers: late Quaternary marine floras. *Paleoceanography*, 18, n/a. Available at: https://doi.org/10.1029/2002PA000775

Hoff, U., Rasmussen, T.L., Stein, R., Ezat, M.M. & Fahl, K. (2016) Sea ice and millennial-scale climate variability in the Nordic seas 90 kyr ago to present. *Nature Communications*, 7, 12247, Available at: https://doi.org/10.1038/ncomms12247.

Holtvoeth, J., Whiteside, J.H., Engels, S., Freitas, F.S., Grice, K., Greenwood, P. *et al.* (2019) The paleolimnologist's guide to compound-specific stable isotope analysis – An introduction to principles and applications of CSIA for Quaternary lake sediments. *Quaternary Science Reviews*, 207, 101–133. Available at: https://doi.org/10.1016/j.quascirev.2019.01.001

Hopmans, E.C., Weijers, J.W.H., Schefuß, E., Herfort, L., Sinninghe Damsté, J.S. & Schouten, S. (2004) A novel proxy for terrestrial organic matter in sediments based on branched and isoprenoid tetraether lipids. *Earth and Planetary Science Letters*, 224, 107–116. Available at: https://doi.org/10.1016/j.epsl.2004.05.012

Huang, X., Wang, C., Zhang, J., WIESENBERG, G.L.B., ZHANG, Z. & XIE, S. (2011) Comparison of free lipid compositions between roots and leaves of plants in the Dajiuhu Peatland, central China. *Geochemical Journal*, 45, 365–373. Available at: https://doi.org/10.2343/geochemj.1.0129,2011

Huang, Y., Shuman, B., Wang, Y. & Webb, T. (2004) Hydrogen isotope ratios of individual lipids in lake sediments as novel tracers of climatic and environmental change: a surface sediment test. *Journal of Paleolimnology*, 31, 363–375. Available at: https://doi.org/10.1023/B:JOPL.0000021855.80535.13

Huang, Y., Shuman, B., Wang, Y., Webb, T., Grimm, E.C. & Jacobson, G.L. (2006) Climatic and environmental controls on the variation of C3 and C4 plant abundances in central Florida for the past 62,000 years. *Palaeogeography, Palaeoclimatology, Palaeoecology*, 237, 428–435. Available at: https://doi.org/10.1016/j.palaeo.2005.12.014

Huguet, C., Routh, J., Fietz, S., Lone, M.A., Kalpana, M.S., Ghosh, P. *et al.* (2018) Temperature and Monsoon Tango in a Tropical Stalagmite: Last Glacial-Interglacial Climate Dynamics. *Scientific Reports*, 8, 5386, Available at: https://doi.org/10.1038/s41598-018-23606-w.

Inglis, G.N., Bhattacharya, T., Hemingway, J.D., Hollingsworth, E.H., Feakins, S.J. & Tierney, J.E. (2022) Biomarker Approaches for Reconstructing Terrestrial Environmental Change. *Annual Review of Earth and Planetary Sciences*, 50, 369–394. Available at: https://doi.org/10.1146/annurev-earth-032320-095943

Inglis, G.N., Naafs, B.D.A., Zheng, Y., McClymont, E.L., Evershed, R.P. & Pancost, R.D. (2018) Distributions of geohopanoids in peat: Implications for the use of hopanoid-based proxies in natural archives. *Geochimica et Cosmochimica Acta*, 224, 249–261. Available at: https://doi.org/10.1016/j.gca.2017.12.029

Inglis, G.N. & Tierney, J.E. (2020) *The TEX86 Paleotemperature Proxy*, 1st ed. Cambridge University Press. Available at: https://doi.org/10.1017/9781108846998

Innes, H.E., Bishop, A.N., Head, I.M. & Farrimond, P. (1997) Preservation and diagenesis of hopanoids in Recent lacustrine sediments of Priest Pot, England. *Organic Geochemistry*, 26(9), 565–576. Available at: https://doi.org/10.1016/S0146-6380(97)00017-X

Jacob, J., Disnar, J.-R., Arnaud, F. et al (2008a) Millet cultivation history in the French Alps as evidenced by a sedimentary molecule. *Journal of Archaeological Science*, 35, 814–820. Available at: https://doi.org/10.1016/j.jas.2007.06.006

Jacob, J., Disnar, J.-R., Bardoux, G. et al (2008b) Carbon isotope evidence for sedimentary miliacin as a tracer of Panicum miliaceum (broomcorn millet) in the sediments of Lake le Bourget (French Alps). *Organic Geochemistry*, 39, 1077–1080. Available at: https://doi.org/10.1016/j.orggeochem.2008.04.003

Jaffé, R., Mead, R., Hernandez, M.E., Peralba, M.C. & DiGuida, O.A. (2001) Origin and transport of sedimentary organic matter in two subtropical estuaries: a comparative, biomarker-based study. *Organic Geochemistry*, 32(4), 507–526. Available at: https://doi.org/10.1016/S0146-6380(00)00192-3

Jeffrey, S.W., Mantoura, R.F.C. & Wright, S.W. (1997) Eds. Phytoplankton pigments in oceanography (1997, Eds.): 261-282.

Jessen, G.L., Lichtschlag, A., Ramette, A., Pantoja, S., Rossel, P.E., Schubert, C.J. *et al.* (2017) Hypoxia causes preservation of labile organic matter and changes seafloor microbial community composition (Black Sea). *Science Advances*, 3(2), e1601897, Available at: https://doi.org/10.1126/sciadv.1601897.

Jetter, R., Kunst, L. & Samuels, A.L. (2006) Composition of plant cuticular waxes. *Annual plant reviews volume 23: Biology of the plant cuticle*, 45–181.

Johnson, K.M., McKay, R.M., Etourneau, J., Jiménez-Espejo, F.J., Albot, A., Riesselman, C.R. *et al.* (2021) Sensitivity of Holocene East Antarctic productivity to subdecadal variability set by sea ice. *Nature Geoscience*, 14, 762–768. Available at: https://doi.org/10.1038/s41561-021-00816-y

Kahmen, A., Schefuß, E. & Sachse, D. (2013) Leaf water deuterium enrichment shapes leaf wax n-alkane δD values of angiosperm plants I: Experimental evidence and mechanistic insights. *Geochimica et Cosmochimica Acta*, 111, 39–49. Available at: https://doi.org/10.1016/j.gca.2012.09.003

Kalpana, M.S., Routh, J., Fietz, S., Lone, M.A. & Mangini, A. (2021) Sources, Distribution and Paleoenvironmental Application of Fatty Acids in Speleothem Deposits From Krem Mawmluh, Northeast India. *Frontiers in Earth Science*, 9, 687376, Available at: https://doi.org/10.3389/feart.2021.687376.

Karp, A.T., Holman, A.I., Hopper, P., Grice, K. & Freeman, K.H. (2020) Fire distinguishers: Refined interpretations of polycyclic aromatic hydrocarbons for paleo-applications. *Geochimica et Cosmochimica Acta*, 289, 93–113. Available at: https://doi.org/10.1016/j.gca.2020.08.024

Kasper, S., van der Meer, M.T.J., Mets, A., Zahn, R., Sinninghe Damsté, J.S. & Schouten, S. (2014) Salinity changes in the Agulhas leakage area recorded by stable hydrogen isotopes of C_{37} alkenones during Termination I and II. *Climate of the Past*, 10, 251–260. Available at: https://doi.org/10.5194/cp-10-251-2014

Katrantsiotis, C., Norström, E., Smittenberg, R.H., Salonen, J.S., Plikk, A. & Helmens, K. (2021) Seasonal variability in temperature trends and atmospheric circulation systems during the Eemian (Last Interglacial) based on n-alkanes hydrogen isotopes from Northern Finland. *Quaternary Science Reviews*, 273, 107250, Available at: https://doi.org/10.1016/j.quascirev.2021.107250.

Keenan, B., Imfeld, A., Johnston, K., Breckenridge, A., Gélinas, Y. & Douglas, P.M.J. (2021) Molecular evidence for human population change associated with climate events in the Maya lowlands. *Quaternary Science Reviews*, 258, 106904, Available at: https://doi.org/10.1016/j.quascirev.2021.106904.

Kehelpannala, C., Rupasinghe, T.W.T., Hennessy, T., Bradley, D., Ebert, B. & Roessner, U. (2020) A comprehensive comparison of four methods for extracting lipids from Arabidopsis tissues. *Plant Methods*, 2020 Dec 3 16(1), 155, Available at: https://doi.org/10.1186/s13007-020-00697-z.

Kemp, A.C., Vane, C.H., Kim, A.W., Dutton, C.L., Subalusky, A.L., Kemp, S.K. *et al.* (2022) Fecal steroids as a potential tool for conservation paleobiology in East Africa. *Biodiversity and Conservation*, 31, 183–209. Available at: https://doi.org/10.1007/s10531-021-02328-y

Killops, S.D. & Killops, V.J. (2013) *Introduction to Organic Geochemistry*, 2nd Edition. Wiley-Blackwell. p. 408

Kim, J.-H., van der Meer, J., Schouten, S., Helmke, P., Willmott, V., Sangiorgi, F. *et al.* (2010) New indices and calibrations derived from the distribution of crenarchaeal isoprenoid tetraether lipids: Implications for past sea surface temperature reconstructions. *Geochimica et Cosmochimica Acta*, 74, 4639–4654. Available at: https://doi.org/10.1016/j.gca.2010.05.027

Kirchgeorg, T., Schüpbach, S., Kehrwald, N., McWethy, D.B. & Barbante, C. (2014) Method for the determination of specific molecular markers of biomass burning in lake sediments. *Organic Geochemistry*, 71, 1–6. Available at: https://doi.org/10.1016/j.orggeochem.2014.02.014

Kjellman, S.E., Schomacker, A., Thomas, E.K., Håkansson, L., Duboscq, S., Cluett, A.A. *et al.* (2020) Holocene precipitation seasonality in northern Svalbard: Influence of sea ice and regional ocean surface conditions. *Quaternary Science Reviews*, 240, 106388, Available at: https://doi.org/10.1016/j.quascirev.2020.106388.

Knies, J., Cabedo-Sanz, P., Belt, S.T., Baranwal, S., Fietz, S. & Rosell-Melé, A. (2014) The emergence of modern sea ice cover in the Arctic Ocean. *Nature Communications*, 5, 5608, Available at: https://doi.org/10.1038/ncomms6608.

Koch, B.P., Souza Filho, P.W.M., Behling, H., Cohen, M.C.L., Kattner, G., Rullkötter, J. *et al.* (2011) Triterpenols in mangrove sediments as

a proxy for organic matter derived from the red mangrove (Rhizophora mangle). *Organic Geochemistry*, 42, 62–73. Available at: https://doi.org/10.1016/j.orggeochem.2010.10.007

Kornilova, O. & Rosell-Melé, A. (2003) Application of microwave-assisted extraction to the analysis of biomarker climate proxies in marine sediments. *Organic Geochemistry*, 34, 1517–1523. Available at: https://doi.org/10.1016/S0146-6380(03)00155-4

Krentscher, C., Dubois, N., Camperio, G., Prebble, M. & Ladd, S.N. (2019) Palmitone as a potential species-specific biomarker for the crop plant taro (Colocasia esculenta Schott) on remote Pacific islands. *Organic Geochemistry*, 132, 1–10. Available at: https://doi.org/10.1016/j.orggeochem.2019.03.006

Kuo, L.-J., Herbert, B.E. & Louchouarn, P. (2008) Can levoglucosan be used to characterize and quantify char/charcoal black carbon in environmental media? *Organic Geochemistry*, 39(10), 1466–1478. Available at: https://doi.org/10.1016/j.orggeochem.2008.04.026

Kuo, L.-J., Louchouarn, P. & Herbert, B.E. (2011) Influence of combustion conditions on yields of solvent-extractable anhydrosugars and lignin phenols in chars: Implications for characterizations of biomass combustion residues. *Chemosphere*, 85, 797–805. Available at: https://doi.org/10.1016/j.chemosphere.2011.06.074

Kusch, S. & Rush, D. (2022) Revisiting the precursors of the most abundant natural products on Earth: A look back at 30+ years of bacteriohopanepolyol (BHP) research and ahead to new frontiers. *Organic Geochemistry*, 172, 104469, Available at: https://doi.org/10.1016/j.orggeochem.2022.104469.

Kusch, S., Winterfeld, M., Mollenhauer, G., Höfle, S.T., Schirrmeister, L., Schwamborn, G. *et al.* (2019) Glycerol dialkyl glycerol tetraethers (GDGTs) in high latitude Siberian permafrost: Diversity, environmental controls, and implications for proxy applications. *Organic Geochemistry*, 136, 103888, Available at: https://doi.org/10.1016/j.orggeochem.2019.06.009.

Ladd, S.N. & Sachs, J.P. (2015) Influence of salinity on hydrogen isotope fractionation in Rhizophora mangroves from Micronesia. *Geochimica et Cosmochimica Acta*, 168, 206–221. Available at: https://doi.org/10.1016/j.gca.2015.07.004

Lamb, H.H. (1977) Climatic History and the Future (Climate: Present, Past and Future, vol. 2; Methuen.

Lamping, N., Müller, J., Esper, O., Hillenbrand, C.D., Smith, J.A. & Kuhn, G. (2020) Highly branched isoprenoids reveal onset of deglaciation followed by dynamic sea-ice conditions in the western Amundsen Sea, Antarctica. *Quaternary Science Reviews*, 228, 106103, Available at: https://doi.org/10.1016/j.quascirev.2019.106103.

Lang, D.C., Bailey, I., Wilson, P.A., Beer, C.J., Bolton, C.T., Friedrich, O. *et al.* (2014) The transition on North America from the warm humid Pliocene to the glaciated Quaternary traced by eolian dust deposition at a benchmark North Atlantic Ocean drill site. *Quaternary Science Reviews*, 93, 125–141. Available at: https://doi.org/10.1016/j.quascirev.2014.04.005

Larson, E.A., Afolabi, A., Zheng, J. & Ojeda, A.S. (2022) Sterols and sterol ratios to trace fecal contamination: pitfalls and potential solutions. *Environmental Science and Pollution Research*, Jul 29(35), 53395–53402. Available at: https://doi.org/10.1007/s11356-022-19611-2

Lattaud, J., Balzano, S., van der Meer, M.T.J., Villanueva, L., Hopmans, E.C., Sinninghe Damsté, J.S. *et al.* (2021) Sources and seasonality of long-chain diols in a temperate lake (Lake Geneva). *Organic Geochemistry*, 156, 104223, Available at: https://doi.org/10.1016/j.orggeochem.2021.104223.

Lavrieux, M., Jacob, J., Disnar, J.-R., Bréheret, J.G., Le Milbeau, C., Miras, Y. *et al.* (2013) Sedimentary cannabinol tracks the history of hemp retting. *Geology*, 41, 751–754. Available at: https://doi.org/10.1130/G34073.1

Leavitt, P.R. (1993) A review of factors that regulate carotenoid and chlorophyll deposition and fossil pigment abundance. *Journal of Paleolimnology*, 9, 109–127. Available at: https://doi.org/10.1007/BF00677513

Leeming, R., Ball, A., Ashbolt, N. & Nichols, P. (1996) Using faecal sterols from humans and animals to distinguish faecal pollution in receiving waters. *Water Research*, 30, 2893–2900. Available at: https://doi.org/10.1016/S0043-1354(96)00011-5

Li, X., Wang, C., Huang, J., Hu, C. & Xie, S. (2011) Seasonal variation of fatty acids from drip water in Heshang Cave, central China. *Applied Geochemistry*, 26, 341–347. Available at: https://doi.org/10.1016/j.apgeochem.2010.12.007

Lima, A.L.C., Farrington, J.W. & Reddy, C.M. (2005) Combustion-Derived Polycyclic Aromatic Hydrocarbons in the Environment—A Review. *Environmental Forensics*, 6, 109–131. Available at: https://doi.org/10.1080/15275920590952739

Liu, J. (2021) Seasonality of the altitude effect on leaf wax n-alkane distributions, hydrogen and carbon isotopes along an arid transect in the Qinling Mountains. *Science of the Total Environment*, 778, 146272, Available at: https://doi.org/10.1016/j.scitotenv.2021.146272.

Liu, J., Zhao, J., He, D., Huang, X., Jiang, C., Yan, H. *et al.* (2022) Effects of plant types on terrestrial leaf wax long-chain n-alkane biomarkers: Implications and paleoapplications. *Earth-Science Reviews*, 235, 104248, Available at: https://doi.org/10.1016/j.earscirev.2022.104248.

Liu, W., Liu, Z., Fu, M. & An, Z. (2008) Distribution of the C37 tetra-unsaturated alkenone in Lake Qinghai, China: A potential lake salinity indicator. *Geochimica et Cosmochimica Acta*, 72(3), 988–997. Available at: https://doi.org/10.1016/j.gca.2007.11.016

Liu, W., Liu, Z., Wang, H., He, Y., Wang, Z. & Xu, L. (2011) Salinity control on long-chain alkenone distributions in lake surface waters and sediments of the northern Qinghai-Tibetan Plateau, China. *Geochimica et Cosmochimica Acta*, 75(7), 1693–1703. Available at: https://doi.org/10.1016/j.gca.2010.10.029

Liu, W. & Yang, H. (2008) Multiple controls for the variability of hydrogen isotopic compositions in higher plant *n*-alkanes from modern ecosystems. *Global Change Biology*, 14, 2166–2177. Available at: https://doi.org/10.1111/j.1365-2486.2008.01608.x

Liu, W., Yang, H. & Li, L. (2006) Hydrogen isotopic compositions of n-alkanes from terrestrial plants correlate with their ecological life forms. *Oecologia*, 150(2), 330–338. Available at: https://doi.org/10.1007/s00442-006-0494-0

Liu, W.G., Yang, H., Wang, H.Y. et al (2015) Carbon isotope composition of long chain leaf wax n-alkanes in lake sediments: A dual indicator of paleoenvironment in the Qinghai-Tibet Plateau. *Organic Geochemistry*, 83–84, 190–201. Available at: https://doi.org/10.1016/j.orggeochem.2015.03.017.

Loakes, K.L., Ryves, D.B., Lamb, H.F., Schäbitz, F., Dee, M., Tyler, J.J. *et al.* (2018) Late Quaternary climate change in the north-eastern highlands of Ethiopia: A high resolution 15,600 year diatom and pigment record from Lake Hayk. *Quaternary Science Reviews*, 202, 166–181. Available at: https://doi.org/10.1016/j.quascirev.2018.09.005

Longo, W.M., Theroux, S., Giblin, A.E., Zheng, Y., Dillon, J.T. & Huang, Y. (2016) Temperature calibration and phylogenetically distinct distributions for freshwater alkenones: Evidence from northern Alaskan lakes. *Geochimica et Cosmochimica Acta*, 180, 177–196. Available at: https://doi.org/10.1016/j.gca.2016.02.019

Loomis, S.E., Russell, J.M., Heureux, A.M., D'Andrea, W.J. & Sinninghe Damsté, J.S. (2014) Seasonal variability of branched glycerol dialkyl glycerol tetraethers (brGDGTs) in a temperate lake system. *Geochimica et Cosmochimica Acta*, 144, 173–187. Available at: https://doi.org/10.1016/j.gca.2014.08.027

Loomis, S.E., Russell, J.M., Ladd, B., Street-Perrott, F.A. & Sinninghe Damsté, J.S. (2012) Calibration and application of the branched GDGT temperature proxy on East African lake sediments. *Earth and Planetary Science Letters*, 357-358, 277–288. Available at: https://doi.org/10.1016/j.epsl.2012.09.031

Lopes dos Santos, R.A., De Deckker, P., Hopmans, E.C. et al (2013b) Abrupt vegetation change after the Late Quaternary megafaunal extinction in southeastern Australia. *Nature Geosci*, 6, 627–631. Available at: https://doi.org/10.1038/ngeo1856

Lopes dos Santos, R.A., Spooner, M.I., Barrows, T.T. et al (2013a) Comparison of organic ($U^{K'}_{37}$, TEX $^{H}_{86}$, LDI) and faunal proxies (foraminiferal assemblages) for reconstruction of late Quaternary sea surface temperature variability from offshore southeastern Australia: SST from offshore Southeastern Australia. *Paleoceanography*, 28, 377–387. Available at: https://doi.org/10.1002/palo.20035

Lu, H., Zhu, L. & Zhu, N. (2009) Polycyclic aromatic hydrocarbon emission from straw burning and the influence of combustion parameters. *Atmospheric Environment*, 43(4), 978–983. Available at: https://doi.org/10.1016/j.atmosenv.2008.10.02

Lupien, R.L., Russell, J.M., Pearson, E.J., Castañeda, I.S., Asrat, A., Foerster, V. *et al*. (2022) Orbital controls on eastern African hydroclimate in the Pleistocene. *Scientific Reports*, 12, 3170, Available at: https://doi.org/10.1038/s41598-022-06826-z.

Mackay, H., Davies, K.L., Robertson, J., Roy, L., Bull, I.D., Whitehouse, N.J. *et al*. (2020) Characterising life in settlements and structures: Incorporating faecal lipid biomarkers within a multiproxy case study of a wetland village. *Journal of Archaeological Science*, 121, 105202, Available at: https://doi.org/10.1016/j.jas.2020.105202.

Madureira, L.A.S., van Kreveld, S.A., Eglinton, G., Conte, M.H., Ganssen, G., van Hinte, J.E. *et al*. (1997) Late Quaternary high-resolution biomarker and other sedimentary climate proxies in a Northeast Atlantic Core. *Paleoceanography*, 12, 255–269. Available at: https://doi.org/10.1029/96PA03120

Magill, C.R., Ashley, G.M. & Freeman, K.H. (2013) Ecosystem variability and early human habitats in eastern Africa. *Proceedings of the National Academy of Sciences*, 110(4), 1167–1174. Available at: https://doi.org/10.1073/pnas.1206276110

Mallorquí, N., Arellano, J.B., Borrego, C.M. & Garcia-Gil, L.J. (2005) Signature pigments of green sulfur bacteria in lower Pleistocene deposits from the Banyoles lacustrine area (Spain). *Journal of Paleolimnology*, 34, 271–280. Available at: https://doi.org/10.1007/s10933-005-3731-3

Maloney, A.E., Richey, J.N., Nelson, D.B., Hing, S.N., Sear, D.A., Hassall, J.D. *et al*. (2022) Contrasting Common Era climate and hydrology sensitivities from paired lake sediment dinosterol hydrogen isotope records in the South Pacific Convergence Zone. *Quaternary Science Reviews*, 281, 107421, Available at: https://doi.org/10.1016/j.quascirev.2022.107421.

Manley, A., Collins, A.L., Joynes, A., Mellander, P.E. & Jordan, P. (2020) Comparing Extraction Methods for Biomarker Steroid Characterisation from Soil and Slurry. *Water, Air, and Soil Pollution*, 231(10), 524, Available at: https://doi.org/10.1007/s11270-020-04871-w.

MARGO Project Members. (2005) Constraints on the magnitude and patterns of ocean cooling at the Last Glacial Maximum. *Nature Geosci*, 2, 127–132. Available at: https://doi.org/10.1038/ngeo411

Marino, G., Rohling, E.J., Rijpstra, W.I.C., Sangiorgi, F., Schouten, S. & Damsté, J.S.S. (2007) Aegean Sea as driver of hydrographic and ecological changes in the eastern Mediterranean. *Geology*, 35, 675. Available at: https://doi.org/10.1130/G23831A.1

Martínez-Garcia, A., Rosell-Melé, A., Geibert, W., Gersonde, R., Masqué, P., Gaspari, V. *et al*. (2009) Links between iron supply, marine productivity, sea surface temperature, and CO2 over the last 1.1 Ma. *Paleoceanography*, 24, n/a. Available at: https://doi.org/10.1029/2008PA001657

Martínez-Garcia, A., Rosell-Melé, A., Jaccard, S.L., Geibert, W., Sigman, D.M. & Haug, G.H. (2011) Southern Ocean dust–climate coupling over the past four million years. *Nature*, 476, 312–315. Available at: https://doi.org/10.1038/nature10310

Martínez-Garcia, A., Rosell-Melé, A., McClymont, E.L., Gersonde, R. & Haug, G.H. (2010) Subpolar Link to the Emergence of the Modern Equatorial Pacific Cold Tongue. *Science*, 328, 1550–1553. Available at: https://doi.org/10.1126/science.1184480

Martínez-Sosa, P., Tierney, J.E., Stefanescu, I.C., Crampton-Flood, E.D., Shuman, B.N., & Routson, C. (2021) *A global Bayesian temperature calibration for lacustrine brGDGTs*. Available at: https://doi.org/10.1594/PANGAEA.931169

Martrat, B., Grimalt, J.O., Shackleton, N.J., de Abreu, L., Hutterli, M.A. & Stocker, T.F. (2007) Four Climate Cycles of Recurring Deep and Surface Water Destabilizations on the Iberian Margin. *Science*, 317, 502–507. Available at: https://doi.org/10.1126/science.1139994

Massa, C., Beilman, D.W., Nichols, J.E. & Timm, O.E. (2021) Central Pacific hydroclimate over the last 45,000 years: Molecular-isotopic evidence from leaf wax in a Hawai'i peatland. *Quaternary Science Reviews*, 253, 106744, Available at: https://doi.org/10.1016/j.quascirev.2020.106744.

Massé, G., Belt, S.T., Crosta, X., Schmidt, S., Snape, I., Thomas, D.N. *et al*. (2011) Highly branched isoprenoids as proxies for variable sea ice conditions in the Southern Ocean. *Antarctic Science*, 23, 487–498. Available at: https://doi.org/10.1017/S0954102011000381

Masson-Delmotte, V., Zhai, P., Pirani, A. *et al*. (2021) *Climate Change 2021: The Physical Science Basis. Contribution of Working Group I to the Sixth Assessment Report of the Intergovernmental Panel on Climate Change*. Cambridge, United Kingdom and New York, NY, USA: Cambridge University Press. Available at: https://doi.org/10.1017/9781009157896

McClymont, E.L., Bentley, M.J., Hodgson, D.A., Spencer-Jones, C.L., Wardley, T., West, M.D. *et al*. (2022) Summer sea-ice variability on the Antarctic margin during the last glacial period reconstructed from snow petrel (*Pagodroma nivea*) stomach-oil deposits. *Climate of the Past*, 18, 381–403. Available at: https://doi.org/10.5194/cp-18-381-2022

McClymont, E.L., Bingham, E.M., Nott, C.J., Chambers, F.M., Pancost, R.D. & Evershed, R.P. (2011) Pyrolysis GC–MS as a rapid screening tool for determination of peat-forming plant composition in cores from ombrotrophic peat. *Organic Geochemistry*, 42, 1420–1435. Available at: https://doi.org/10.1016/j.orggeochem.2011.07.004

McClymont, E.L., Ganeshram, R.S., Pichevin, L.E., Talbot, H.M., van Dongen, B.E., Thunell, R.C. *et al*. (2012) Sea-surface temperature records of Termination 1 in the Gulf of California: Challenges for seasonal and interannual analogues of tropical Pacific climate change: Gulf of California termination 1. *Paleoceanography*, 27(2), n/a. Available at: https://doi.org/10.1029/2011PA002226

McClymont, E.L., Martínez-Garcia, A. & Rosell-Melé, A. (2007) Benefits of freeze-drying sediments for the analysis of total chlorins and alkenone concentrations in marine sediments. *Organic Geochemistry*, 38, 1002–1007. Available at: https://doi.org/10.1016/j.orggeochem.2007.01.006

McClymont, E.L., Mauquoy, D., Yeloff, D. et al (2008a) The disappearance of Sphagnum imbricatum from Butterburn Flow. *The Holocene*, 18, 991–1002. Available at: https://doi.org/10.1177/0959683608093537

McClymont, E.L., Rosell-Melé, A., Giraudeau, J., Pierre, C. & Lloyd, J.M. (2005) Alkenone and coccolith records of the mid-Pleistocene in the south-east Atlantic: Implications for the U37K′ index and South African climate. *Quaternary Science Reviews*, 24, 1559–1572. Available at: https://doi.org/10.1016/j.quascirev.2004.06.024

McClymont, E.L., Rosell-Melé, A., Haug, G., & Lloyd, J.M. (2008b) Expansion of subarctic water masses in the north Atlantic and Pacific Oceans and implications for mid-Pleistocene ice-sheet growth. *Paleoceanography*, 23, PA4214. Available at: https://doi.org/10.1029/2008PA001622

McClymont, E.L., Sosdian, S.M., Rosell-Melé, A. & Rosenthal, Y. (2013) Pleistocene sea-surface temperature evolution: Early cooling, delayed glacial intensification, and implications for the mid-Pleistocene climate transition. *Earth-Science Reviews*, 123, 173–193. Available at: https://doi.org/10.1016/j.earscirev.2013.04.006

McGowan, S. (2007) Pigments in sediments of aquatic environments, *Encyclopedia of Quaternary Science*, 2007. Elsevier, Amsterdam. pp. 2062–2074

McGowan, S. (2013) Paleolimnology - Pigment Studies. In: Elias, S.A. & Mock, C.J., (Eds.) *Encyclopedia of Quaternary Science*, Second Edition. Amsterdam: Elsevier. pp. 326–338. https://doi.org/10.1016/B0-444-52747-8/00247-7

Meckler, A.N., Vonhof, H. & Martínez-García, A. (2021) Temperature Reconstructions Using Speleothems. *Elements*, 17, 101–106. Available at: https://doi.org/10.2138/gselements.17.2.101

Meyers, P.A. (2003) Applications of organic geochemistry to paleolimnological reconstructions: a summary of examples from the Laurentian Great Lakes. *Organic Geochemistry*, 34, 261–289. Available at: https://doi.org/10.1016/S0146-6380(02)00168-7

Mochida, M., Kawamura, K., Fu, P. & Takemura, T. (2010) Seasonal variation of levoglucosan in aerosols over the western North Pacific and its assessment as a biomass-burning tracer. *Atmospheric Environment*, 44(29), 3511–3518. Available at: https://doi.org/10.1016/j.atmosenv.2010.06.017

Müller, J., Massé, G., Stein, R. & Belt, S.T. (2009) Variability of sea-ice conditions in the Fram Strait over the past 30,000 years. *Nature Geoscience*, 2, 772–776. Available at: https://doi.org/10.1038/ngeo665

Müller, J., Romero, O., Cowan, E.A., McClymont, E.L., Forwick, M., Asahi, H. *et al*. (2018) Cordilleran ice-sheet growth fueled primary

productivity in the Gulf of Alaska, northeast Pacific Ocean. *Geology*, 46(4), 307–310. Available at: https://doi.org/10.1130/G39904.1

Müller, P.J., Kirst, G., Ruhland, G., von Storch, I. & Rosell-Melé, A. (1998) Calibration of the alkenone paleotemperature index U37K′ based on core-tops from the eastern South Atlantic and the global ocean (60°N-60°S). *Geochimica et Cosmochimica Acta*, 62, 1757–1772. Available at: https://doi.org/10.1016/S0016-7037(98)00097-0

Muñoz, S.E., Porter, T.J., Bakkelund, A., Nusbaumer, J., Dee, S.G., Hamilton, B. *et al.* (2020) Lipid Biomarker Record Documents Hydroclimatic Variability of the Mississippi River Basin During the Common Era. *Geophysical Research Letters*, 47, e2020GL087237. Available at: https://doi.org/10.1029/2020GL087237

Naafs, B.D.A., Gallego-Sala, A.V., Inglis, G.N. & Pancost, R.D. (2017) Refining the global branched glycerol dialkyl glycerol tetraether (brGDGT) soil temperature calibration. *Organic Geochemistry*, 106, 48–56. Available at: https://doi.org/10.1016/j.orggeochem.2017.01.009

Naafs, B.D.A., Hefter, J., Acton, G., Haug, G.H., Martínez-Garcia, A., Pancost, R. *et al.* (2012) Strengthening of North American dust sources during the late Pliocene (2.7Ma). *Earth and Planetary Science Letters*, 317–318, 8–19. Available at: https://doi.org/10.1016/j.epsl.2011.11.026

Naafs, B.D.A., Hefter, J., Grützner, J. & Stein, R. (2013) Warming of surface waters in the mid-latitude North Atlantic during Heinrich events: HIGH SSTs DURING HEINRICH EVENTS. *Paleoceanography*, 28, 153–163. Available at: https://doi.org/10.1029/2012PA002354

Naafs, B.D.A., Inglis, G.N., Blewett, J., McClymont, E.L., Lauretano, V., Xie, S. *et al.* (2019) The potential of biomarker proxies to trace climate, vegetation, and biogeochemical processes in peat: A review. *Global and Planetary Change*, 179, 57–79. Available at: https://doi.org/10.1016/j.gloplacha.2019.05.006

Nakakuni, M., Dairiki, C., Kaur, G. & Yamamoto, S. (2017) Stanol to sterol ratios in late Quaternary sediments from southern California: An indicator for continuous variability of the oxygen minimum zone. *Organic Geochemistry*, 111, 126–135. Available at: https://doi.org/10.1016/j.orggeochem.2017.06.009

Nelson, D.B. & Sachs, J.P. (2014) The influence of salinity on D/H fractionation in dinosterol and brassicasterol from globally distributed saline and hypersaline lakes. *Geochimica et Cosmochimica Acta*, 133, 325–339. Available at: https://doi.org/10.1016/j.gca.2014.03.007

Nemiah Ladd, S. & Sachs, J.P. (2012) Inverse relationship between salinity and n-alkane δD values in the mangrove Avicennia marina. *Organic Geochemistry*, 48, 25–36. Available at: https://doi.org/10.1016/j.orggeochem.2012.04.009

Ngugi, C.C., Oyoo-Okoth, E., Gichuki, J., Gatune, C. & Mwangi-Kinyanjui, J. (2017) Fingerprints of upstream catchment land use in suspended particulate organic matter (SPOM) at the river discharge sites in Lake Victoria (Kenya): insights from element, stable isotope and lipid biomarker analysis. *Aquatic Sciences*, 79, 73–87. Available at: https://doi.org/10.1007/s00027-016-0480-5

Nicholl, J.A.L., Hodell, D.A., Naafs, B.D.A., Hillaire-Marcel, C., Channell, J.E.T. & Romero, O.E. (2012) A Laurentide outburst flooding event during the last interglacial period. *Nature Geoscience*, 5(12), 901–904. Available at: https://doi.org/10.1038/ngeo1622

Nichols, J.E. (2010) Procedures for extraction and purification of leaf wax biomarkers from peats. *Mires and Peats*, 7, Article 13, 1–7.

Nichols, J.E., Booth, R.K., Jackson, S.T., Pendall, E.G. & Huang, Y. (2006) Paleohydrologic reconstruction based on n-alkane distributions in ombrotrophic peat. *Organic Geochemistry*, 37, 1505–1513. Available at: https://doi.org/10.1016/j.orggeochem.2006.06.020

Nichols, J.E. & Huang, Y. (2012) Hydroclimate of the northeastern United States is highly sensitive to solar forcing. *Geophysical Research Letters*, 39, n/a. Available at: https://doi.org/10.1029/2011GL050720

Niedermeyer, E.M., Sessions, A.L., Feakins, S.J. & Mohtadi, M. (2014) Hydroclimate of the western Indo-Pacific Warm Pool during the past 24,000 years. *Proceedings of the National Academy of Sciences*, 111(26), 9402–9406. Available at: https://doi.org/10.1073/pnas.1323585111

Nishihara, M. & Koga, Y. (1987) Extraction and Composition of Polar Lipids from the Archaebacterium, Methanobacterium thermoautotrophicum: Effective Extraction of Tetraether Lipids by an Acidified Solvent 1. *The Journal of Biochemistry*, 101(4), 997–1005. Available at: https://doi.org/10.1093/oxfordjournals.jbchem.a121969

Norström, E., Katrantsiotis, C., Finné, M., Risberg, J., Smittenberg, R.H. & Bjursäter, S. (2018) Biomarker hydrogen isotope composition (δD) as proxy for Holocene hydroclimatic change and seismic activity in SW Peloponnese, Greece: δD AS PROXY FOR HYDROCLIMATE CHANGE. *Journal of Quaternary Science*, 33(5), 563–574. Available at: https://doi.org/10.1002/jqs.3036

Ohkouchi, N., Eglinton, T.I., Keigwin, L.D. & Hayes, J.M. (2002) Spatial and Temporal Offsets Between Proxy Records in a Sediment Drift. *Science*, 298(5596), 1224–1227. Available at: https://doi.org/10.1126/science.1075287

Orem, W.H., Colman, S.M. & Lerch, H.E. (1997) Lignin phenols in sediments of Lake Baikal, Siberia: application to paleoenvironmental studies. *Organic Geochemistry*, 27, 153–172. Available at: https://doi.org/10.1016/S0146-6380(97)00079-X

Oros, D.R., Simoneit, B.R.T. & (2001) Identification and emission factors of molecular tracers in organic aerosols from biomass burning Part 1. Temperate climate conifers. *Applied Geochemistry*, 16, 1513–1544. Available at: https://doi.org/10.1016/S0883-2927(01)00021-X

Ortiz, J.E., Gallego, J.L.R., Torres, T., Díaz-Bautista, A. & Sierra, C. (2010) Palaeoenvironmental reconstruction of Northern Spain during the last 8000calyr BP based on the biomarker content of the Roñanzas peat bog (Asturias). *Organic Geochemistry*, 41(5), 454–466. Available at: https://doi.org/10.1016/j.orggeochem.2010.02.003

Ourisson, G., Albrecht, P. & Rohmer, M. (1979) The hopanoids: palaeochemistry and biochemistry of a group of natural products. *Pure and Applied Chemistry*, 51(4), 709–729. Available at: https://doi.org/10.1351/pac197951040709

Pahnke, K., Sachs, J.P., Keigwin, L., Timmermann, A. & Xie, S.P. (2007) Eastern tropical Pacific hydrologic changes during the past 27,000 years from D/H ratios in alkenones. *Paleoceanography*, 22, n/a. Available at: https://doi.org/10.1029/2007PA001468

Pancost, R.D., Baas, M., van Geel, B. & Sinninghe Damsté, J.S. (2002) Biomarkers as proxies for plant inputs to peats: an example from a subboreal ombrotrophic bog. *Organic Geochemistry*, 33(7), 675–690. Available at: https://doi.org/10.1016/S0146-6380(02)00048-7

Pancost, R.D., Baas, M., van Geel, B. & Sinninghe Damsté, J.S. (2003) Response of an ombrotrophic bog to a regional climate event revealed by macrofossil, molecular and carbon isotopic data. *The Holocene*, 13, 921–932. Available at: https://doi.org/10.1191/0959683603hl674rp

Pancost, R.D., McClymont, E.L., Bingham, E.M., Roberts, Z., Charman, D.J., Hornibrook, E.R.C. *et al.* (2011) Archaeol as a methanogen biomarker in ombrotrophic bogs. *Organic Geochemistry*, 42, 1279–1287. Available at: https://doi.org/10.1016/j.orggeochem.2011.07.003

Pancost, R.D. & Sinninghe Damsté, J.S. (2003) Carbon isotopic compositions of prokaryotic lipids as tracers of carbon cycling in diverse settings: Chemical Geology, Vol. 195, 29–58. https://doi.org/10.1016/S0009-2541(02)00387-X.

Parkinson, C.L. (2019) A 40-y record reveals gradual Antarctic sea ice increases followed by decreases at rates far exceeding the rates seen in the Arctic. *Proceedings of the National Academy of Sciences*, 116, 14414–14423. Available at: https://doi.org/10.1073/pnas.1906556116

Past Interglacials Working Group of PAGES. (2016) Interglacials of the last 800,000 years. *Reviews of Geophysics*, 54, 162–219. Available at: https://doi.org/10.1002/2015RG000482

Patalano, R., Roberts, P., Boivin, N., Petraglia, M.D. & Mercader, J. (2021) Plant wax biomarkers in human evolutionary studies. *Evolutionary Anthropology: Issues, News, and Reviews*, 30, 385–398. Available at: https://doi.org/10.1002/evan.21921

Pearson, E.J., Juggins, S. & Farrimond, P. (2008) Distribution and significance of long-chain alkenones as salinity and temperature indicators in Spanish saline lake sediments. *Geochimica et Cosmochimica Acta*, 72, 4035–4046. Available at: https://doi.org/10.1016/j.gca.2008.05.052

Pérez-Angel, L.C., Sepúlveda, J., Molnar, P., Montes, C., Rajagopalan, B., Snell, K. *et al*. (2020) Soil and air temperature calibrations using branched GDGTs for the Tropical Andes of Colombia: Toward a pan-tropical calibration. *Geochemistry, Geophysics, Geosystems*, 21, e2020GC008941, Available at: https://doi.org/10.1029/2020GC008941.

Peters, K.E., Walters, C.C. & Moldowan, J.M. (2005) *The biomarker guide*, 2nd ed. Cambridge, UK; New York: Cambridge University Press. Available at: https://doi.org/10.1017/S0016756806212056

Peterse, F., Martínez-García, A., Zhou, B., Beets, C.J., Prins, M.A., Zheng, H. *et al*. (2014) Molecular records of continental air temperature and monsoon precipitation variability in East Asia spanning the past 130,000 years. *Quaternary Science Reviews*, 83, 76–82. Available at: https://doi.org/10.1016/j.quascirev.2013.11.001

Peterse, F., van der Meer, J., Schouten, S., Weijers, J.W.H., Fierer, N., Jackson, R.B. *et al*. (2012) Revised calibration of the MBT–CBT paleotemperature proxy based on branched tetraether membrane lipids in surface soils. *Geochimica et Cosmochimica Acta*, 96, 215–229. Available at: https://doi.org/10.1016/j.gca.2012.08.011

Petrick, B., McClymont, E.L., Littler, K., Rosell-Melé, A., Clarkson, M.O., Maslin, M. *et al*. (2018) Oceanographic and climatic evolution of the southeastern subtropical Atlantic over the last 3.5 Ma. *Earth and Planetary Science Letters*, 492, 12–21. Available at: https://doi.org/10.1016/j.epsl.2018.03.054

Petrick, B.F., McClymont, E.L., Marret, F. & van der Meer, M.T.J. (2015) Changing surface water conditions for the last 500 ka in the Southeast Atlantic: Implications for variable influences of Agulhas leakage and Benguela upwelling: Last 500 ka in the Southeast Atlantic. *Paleoceanography*, 30, 1153–1167. Available at: https://doi.org/10.1002/2015PA002787

Pitcher, A., Hopmans, E.C., Schouten, S. & Sinninghe Damsté, J.S. (2009) Separation of core and intact polar archaeal tetraether lipids using silica columns: Insights into living and fossil biomass contributions. *Organic Geochemistry*, 40(1), 12–19. Available at: https://doi.org/10.1016/j.orggeochem.2008.09.008

Plancq, J., McColl, J.L., Bendle, J.A., Seki, O., Couto, J.M., Henderson, A.C.G. *et al*. (2018) Genomic identification of the long-chain alkenone producer in freshwater Lake Toyoni, Japan: implications for temperature reconstructions. *Organic Geochemistry*, 125, 189–195. Available at: https://doi.org/10.1016/j.orggeochem.2018.09.011

Post-Beittenmiller, D. (1996) Biochemistry and Molecular Biology of Wax Production in Plants. *Annual Review of Plant Physiology and Plant Molecular Biology*, 47(1), 405–430. Available at: https://doi.org/10.1146/annurev.arplant.47.1.405

Powers, L., Werne, J.P., Vanderwoude, A.J., Sinninghe Damsté, J.S., Hopmans, E.C. & Schouten, S. (2010) Applicability and calibration of the TEX86 paleothermometer in lakes. *Organic Geochemistry*, 41(4), 404–413. Available at: https://doi.org/10.1016/j.orggeochem.2009.11.009

Powers, L.A. (2005) Large temperature variability in the southern African tropics since the Last Glacial Maximum. *Geophysical Research Letters*, 32, L08706, Available at: https://doi.org/10.1029/2004GL022014.

Poynter, J.G., Farrimond, P., Robinson, N. et al (1989) Aeolian-Derived Higher Plant Lipids in the Marine Sedimentary Record: Links with Palaeoclimate. In: Leinen, M., Sarnthein, M., (Eds.) *Paleoclimatology and Paleometeorology: Modern and Past Patterns of Global Atmospheric Transport*. Dordrecht: Springer Netherlands. pp. 435–462. https://doi.org/10.1007/978-94-009-0995-3_18

Prahl, F.G. & Wakeham, S.G. (1987) Calibration of unsaturation patterns in long-chain ketone compositions for palaeotemperature assessment. *Nature*, 330, 367–369. Available at: https://doi.org/10.1038/330367a0

Prost, K., Birk, J.J., Lehndorff, E., Gerlach, R. & Amelung, W. (2017) Steroid Biomarkers Revisited – Improved Source Identification of Faecal Remains in Archaeological Soil Material. *PLoS One*, 12, e0164882. Available at: https://doi.org/10.1371/journal.pone.0164882

Rach, O., Engels, S., Kahmen, A., Brauer, A., Martín-Puertas, C., van Geel, B. *et al*. (2017) Hydrological and ecological changes in western Europe between 3200 and 2000 years BP derived from lipid biomarker δD values in lake Meerfelder Maar sediments. *Quaternary Science Reviews*, 172, 44–54. Available at: https://doi.org/10.1016/j.quascirev.2017.07.019

Raja, M. & Rosell-Melé, A. (2021) Appraisal of sedimentary alkenones for the quantitative reconstruction of phytoplankton biomass. *Proceedings of the National Academy of Sciences*, 118(2), e2014787118. Available at: https://doi.org/10.1073/pnas.201478711

Ramdahl, T. (1983) Retene—a molecular marker of wood combustion in ambient air. *Nature*, 306(5943), 580–582. Available at: https://doi.org/10.1038/306580a0

Rampen, S.W., Datema, M., Rodrigo-Gámiz, M., Schouten, S., Reichart, G.J. & Sinninghe Damsté, J.S. (2014) Sources and proxy potential of long chain alkyl diols in lacustrine environments. *Geochimica et Cosmochimica Acta*, 144, 59–71. Available at: https://doi.org/10.1016/j.gca.2014.08.033

Rampen, S.W., Willmott, V., Kim, J.-H., Uliana, E., Mollenhauer, G., Schefuß, E. *et al*. (2012) Long chain 1,13- and 1,15-diols as a potential proxy for palaeotemperature reconstruction. *Geochimica et Cosmochimica Acta*, 84, 204–216. Available at: https://doi.org/10.1016/j.gca.2012.01.024

Randlett, M.-È., Coolen, M.J.L., Stockhecke, M., Pickarski, N., Litt, T., Balkema, C. *et al*. (2014) Alkenone distribution in Lake Van sediment over the last 270 ka: influence of temperature and haptophyte species composition. *Quaternary Science Reviews*, 104, 53–62. Available at: https://doi.org/10.1016/j.quascirev.2014.07.009

Reuss, N., Conley, D.J. & Bianchi, T.S. (2005) Preservation conditions and the use of sediment pigments as a tool for recent ecological reconstruction in four Northern European estuaries. *Marine Chemistry*, 95(3–4), 283–302. Available at: https://doi.org/10.1016/j.marchem.2004.10.002

Riaux-Gobin, C., Tréguer, P., Poulin, M. & Vétion, G. (2000) Nutrients, algal biomass and communities in land-fast ice and seawater off Adélie Land (Antarctica). *Antarctic Science*, 12(2), 160–171. Available at: https://doi.org/10.1017/S0954102000000213

Ribeiro, S., Limoges, A., Massé, G., Johansen, K.L., Colgan, W., Weckström, K. *et al*. (2021) Vulnerability of the North Water ecosystem to climate change. *Nature Communications*, 12, 4475, Available at: https://doi.org/10.1038/s41467-021-24742-0.

Richter, H. & Howard, J.B. (2000) Formation of polycyclic aromatic hydrocarbons and their growth to soot—a review of chemical reaction pathways. *Progress in Energy and Combustion Science*, 26(4), 565–608. Available at: https://doi.org/10.1016/S0360-1285(00)00009-5

Richter, N., Russell, J.M., Garfinkel, J. & Huang, Y. (2021) Winter–spring warming in the North Atlantic during the last 2000 years: evidence from southwest Iceland. *Climate of the Past*, 17, 1363–1383. Available at: https://doi.org/10.5194/cp-17-1363-2021

Rodrigo-Gámiz, M., García-Alix, A., Jiménez-Moreno, G., Ramos-Román, M.J., Camuera, J., Toney, J.L. *et al*. (2022) Paleoclimate reconstruction of the last 36 kyr based on branched glycerol dialkyl glycerol tetraethers in the Padul palaeolake record (Sierra Nevada, southern Iberian Peninsula). *Quaternary Science Reviews*, 281, 107434, Available at: https://doi.org/10.1016/j.quascirev.2022.107434.

Rohmer, M., Bisseret, P. & Neunlist, S. (1992) The hopanoids, prokaryotic triterpenoids and precursors of ubiquitous molecular fossils. In: Moldowan, J.M., Albrecht, P. & Philp, R.P., (Eds.) *Biological Markers in Sediments and Petroleum*. London: Prentice Hall. pp. 1–17.

Romero-Viana, L., Kienel, U. & Sachse, D. (2012) Lipid biomarker signatures in a hypersaline lake on Isabel Island (Eastern Pacific) as a proxy for past rainfall anomaly (1942–2006 AD). *Palaeogeography, Palaeoclimatology, Palaeoecology*, 350–352. 49–61. Available at: https://doi.org/10.1016/j.palaeo.2012.06.011

Ronkainen, T., McClymont, E.L., Väliranta, M. & Tuittila, E.S. (2013) The n-alkane and sterol composition of living fen plants as a potential tool for palaeoecological studies. *Organic Geochemistry*, 59, 1–9. Available at: https://doi.org/10.1016/j.orggeochem.2013.03.005

Ronkainen, T., Väliranta, M., Mcclymont, E., BIASI, C., SALONEN, S., FONTANA, S. *et al*. (2015) A combined biogeochemical and palaeobotanical approach to study permafrost environments and

past dynamics. *Journal of Quaternary Science*, 30, 189–200. Available at: https://doi.org/10.1002/jqs.2763

Rontani, J.-F., Smik, L. & Belt, S.T. (2019) Autoxidation of the sea ice biomarker proxy IPSO25 in the near-surface oxic layers of Arctic and Antarctic sediments. *Organic Geochemistry*, 129, 63–76. Available at: https://doi.org/10.1016/j.orggeochem.2019.02.002

Rosell-Melé, A. (1998) Interhemispheric appraisal of the value of alkenone indices as temperature and salinity proxies in high-latitude locations. *Paleoceanography*, 13, 694–703. Available at: https://doi.org/10.1029/98PA02355

Rosell-Melé, A., Balestra, B., Kornilova, O., Mcclymont, E.L., Russell, M., Monechi, S. *et al.* (2011) Alkenones and coccoliths in ice-rafted debris during the Last Glacial Maximum in the North Atlantic: implications for the use of $U^{K}_{37}{}'$ as a sea surface temperature proxy. *Journal of Quaternary Science*, 26, 657–664. Available at: https://doi.org/10.1002/jqs.1488

Rosell-Melé, A., Maslin, M.A., Maxwell, J.R. & Schaeffer, P. (1997) Biomarker evidence for "Heinrich" events. *Geochimica et Cosmochimica Acta*, 61, 1671–1678. Available at: https://doi.org/10.1016/S0016-7037(97)00046-X

Rosell-Melé, A. & McClymont, E.L. (2007) Chapter Eleven Biomarkers as Paleoceanographic Proxies. In: Hillaire–Marcel, C. & De Vernal, A., (eds) *Developments in Marine Geology*. Elsevier (Proxies in Late Cenozoic Paleoceanography). pp. 441–490. https://doi.org/10.1016/S1572-5480(07)01016-0

Rousseau, L., Keraudren, B., Pèpe, C., Laurent, M. & Blanc, J.J. (1995) Sterols as biogeochemical markers in pliocene sediments and their potential application for the identification of marine facies. *Quaternary Science Reviews*, 14, 605–608. Available at: https://doi.org/10.1016/0277-3791(95)00019-L

Ruan, Y., Mohtadi, M., Dupont, L.M., Hebbeln, D., Kaars, S., Hopmans, E.C. *et al.* (2020) Interaction offire, vegetation, and climate in tropical ecosystems: Amultiproxy study over the past 22,000 years. *Global Biogeochemical Cycles*, 34, e2020GB006677, Available at: https://doi.org/10.1029/2020GB006677.

Rull, V., Sacristán-Soriano, O., Sànchez-Melsió, A., Borrego, C.M. & Vegas-Vilarrúbia, T. (2022) Bacterial phylogenetic markers in lake sediments provide direct evidence for historical hemp retting. *Quaternary Science Reviews*, 295, 107803, Available at: https://doi.org/10.1016/j.quascirev.2022.107803.

Rush, D., Sinninghe Damsté, J.S., Poulton, S.W., Thamdrup, B., Garside, A.L., Acuña González, J. *et al.* (2014) Anaerobic ammonium-oxidising bacteria: A biological source of the bacteriohopanetetrol stereoisomer in marine sediments. *Geochimica et Cosmochimica Acta*, 140, 50–64. Available at: https://doi.org/10.1016/j.gca.2014.05.014

Russell, J.M., Hopmans, E.C., Loomis, S.E., Liang, J. & Sinninghe Damsté, J.S. (2018) Distributions of 5- and 6-methyl branched glycerol dialkyl glycerol tetraethers (brGDGTs) in East African lake sediment: Effects of temperature, pH, and new lacustrine paleotemperature calibrations. *Organic Geochemistry*, 117, 56–69. Available at: https://doi.org/10.1016/j.orggeochem.2017.12.003

Sachse, D., Billault, I., Bowen, G.J., Chikaraishi, Y., Dawson, T.E., Feakins, S.J. *et al.* (2012) Molecular Paleohydrology: Interpreting the Hydrogen-Isotopic Composition of Lipid Biomarkers from Photosynthesizing Organisms. *Annual Review of Earth and Planetary Sciences*, 40, 221–249. Available at: https://doi.org/10.1146/annurev-earth-042711-105535

Sachse, D., Gleixner, G., Wilkes, H. & Kahmen, A. (2010) Leaf wax n-alkane δD values of field-grown barley reflect leaf water δD values at the time of leaf formation. *Geochimica et Cosmochimica Acta*, 74, 6741–6750. Available at: https://doi.org/10.1016/j.gca.2010.08.033

Sachse, D., Radke, J. & Gleixner, G. (2004) Hydrogen isotope ratios of recent lacustrine sedimentary n-alkanes record modern climate variability. *Geochimica et Cosmochimica Acta*, 68, 4877–4889. Available at: https://doi.org/10.1016/j.gca.2004.06.004

Sachse, D., Radke, J. & Gleixner, G. (2006) δD values of individual n-alkanes from terrestrial plants along a climatic gradient – Implications for the sedimentary biomarker record. *Organic Geochemistry*, 37, 469–483. Available at: https://doi.org/10.1016/j.orggeochem.2005.12.003

Sachse, D. & Sachs, J.P. (2008) Inverse relationship between D/H fractionation in cyanobacterial lipids and salinity in Christmas Island saline ponds. *Geochimica et Cosmochimica Acta*, 72, 793–806. Available at: https://doi.org/10.1016/j.gca.2007.11.022.

Sadatzki, H., Maffezzoli, N., Dokken, T.M., Simon, M.H., Berben, S.M.P., Fahl, K. *et al.* (2020) Rapid reductions and millennial-scale variability in Nordic Seas sea ice cover during abrupt glacial climate changes. *Proceedings of the National Academy of Sciences*, 117(47), 29478–29486. Available at: https://doi.org/10.1073/pnas.2005849117

Saini, J., Günther, F., Aichner, B., Mischke, S., Herzschuh, U., Zhang, C. *et al.* (2017) Climate variability in the past ~19,000 yr in NE Tibetan Plateau inferred from biomarker and stable isotope records of Lake Donggi Cona. *Quaternary Science Reviews*, 157, 129–140. Available at: https://doi.org/10.1016/j.quascirev.2016.12.023

Sánchez-Montes, M.L., McClymont, E.L., Lloyd, J.M., Müller, J., Cowan, E.A. & Zorzi, C. (2020) Late Pliocene Cordilleran Ice Sheet development with warm northeast Pacific sea surface temperatures. *Climate of the Past*, 16, 299–313. Available at: https://doi.org/10.5194/cp-16-299-2020

Sánchez-Montes, M.L., Romero, O.E., Cowan, E.A., Müller, J., Moy, C.M., Lloyd, J.M. *et al.* (2022) Plio-Pleistocene Ocean Circulation Changes in the Gulf of Alaska and Its Impacts on the Carbon and Nitrogen Cycles and the Cordilleran Ice Sheet Development. *Paleoceanography and Paleoclimatology*, 37, e2021PA004341. Available at: https://doi.org/10.1029/2021PA004341

Sarkar, S., Prasad, S., Wilkes, H., Riedel, N., Stebich, M., Basavaiah, N. *et al.* (2015) Monsoon source shifts during the drying mid-Holocene: Biomarker isotope based evidence from the core 'monsoon zone' (CMZ) of India. *Quaternary Science Reviews*, 123, 144–157. Available at: https://doi.org/10.1016/j.quascirev.2015.06.020

Sauer, P.E., Eglinton, T.I., Hayes, J.M., Schimmelmann, A. & Sessions, A.L. (2001) Compound-specific D/H ratios of lipid biomarkers from sediments as a proxy for environmental and climatic conditions. *Geochimica et Cosmochimica Acta*, 65(2), 213–222. Available at: https://doi.org/10.1016/S0016-7037(00)00520-2

Schefuß, E., Schouten, S., Jansen, J.H.F. & Sinninghe Damsté, J.S. (2003) African vegetation controlled by tropical sea surface temperatures in the mid-Pleistocene period. *Nature*, 422, 418–421. Available at: https://doi.org/10.1038/nature01500

Schefuß, E., Schouten, S., Schneider, R.R. et al (2005) Climatic controls on central African hydrology during the past 20,000 years. *Nature*, 437, 1003–1006. Available at: https://doi.org/10.1038/nature03945

Schmidt, T., Kramell, A.E., Oehler, F., Kluge, R., Demske, D., Tarasov, P.E. *et al.* (2020) Identification and quantification of cannabinol as a biomarker for local hemp retting in an ancient sedimentary record by HPTLC-ESI-MS. *Analytical and Bioanalytical Chemistry*, 412(11), 2633–2644. Available at: https://doi.org/10.1007/s00216-020-02492-0

Schmittner, A., Urban, N.M., Shakun, J.D., Mahowald, N.M., Clark, P.U., Bartlein, P.J. *et al.* (2011) Climate Sensitivity Estimated from Temperature Reconstructions of the Last Glacial Maximum. *Science*, 334(6061), 1385–1388. Available at: https://doi.org/10.1126/science.1203513

Schouten, S., Hopmans, E.C., Rosell-Melé, A., Pearson, A., Adam, P., Bauersachs, T. *et al.* (2013) An interlaboratory study of TEX_{86} and BIT analysis of sediments, extracts and standard mixtures. *Geochemistry, Geophysics, Geosystems*, 14(12), 5263–5285. Available at: https://doi.org/10.1002/2013GC004904

Schouten, S., Hopmans, E.C., Schefuß, E. & Sinninghe Damsté, J.S. (2002) Distributional variations in marine crenarchaeotal membrane lipids: a new tool for reconstructing ancient sea water temperatures? *Earth and Planetary Science Letters*, 204, 265–274. Available at: https://doi.org/10.1016/S0012-821X(02)00979-2

Schouten, S., Ossebaar, J., Schreiber, K., Kienhuis, M.V.M., Langer, G., Benthien, A. *et al.* (2006) The effect of temperature, salinity and growth rate on the stable hydrogen isotopic composition of long chain alkenones produced by *Emiliania huxleyi* and *Gephyrocapsa oceanica*. *Biogeosciences*, 3, 113–119. Available at: https://doi.org/10.5194/bg-3-113-2006

Schreuder, L.T., Donders, T.H., Mets, A., Hopmans, E.C., Sinninghe Damsté, J. S., & Schouten, S. (2019a) Comparison of organic and palynological proxies for biomass burning and vegetation in a

lacustrine sediment record (Lake Allom, Fraser Island, Australia). *Organic Geochemistry*, 133, 10–19. Available at: https://doi.org/10.1016/j.orggeochem.2019.03.002.

Schreuder, L.T., Hopmans, E.C. & Castañeda, I.S. (2019b) Late Quaternary Biomass Burning in Northwest Africa and Interactions With Climate, Vegetation, and Humans. *Paleoceanography and Paleoclimatology*, 34, 153–163. Available at: https://doi.org/10.1029/2018PA003467

Schroeter, N., Lauterbach, S., Stebich, M., Kalanke, J., Mingram, J., Yildiz, C. *et al.* (2020) Biomolecular Evidence of Early Human Occupation of a High-Altitude Site in Western Central Asia During the Holocene. *Frontiers in Earth Science*, 8, 20. Available at: https://doi.org/10.3389/feart.2020.00020

Schüpbach, S., Kirchgeorg, T., Colombaroli, D., Beffa, G., Radaelli, M., Kehrwald, N.M. *et al.* (2015) Combining charcoal sediment and molecular markers to infer a Holocene fire history in the Maya Lowlands of Petén, Guatemala. *Quaternary Science Reviews*, 115, 123–131. Available at: https://doi.org/10.1016/j.quascirev.2015.03.004

Schwab, V.F. & Sachs, J.P. (2011) Hydrogen isotopes in individual alkenones from the Chesapeake Bay estuary. *Geochimica et Cosmochimica Acta*, 75(23), 7552–7565. Available at: https://doi.org/10.1016/j.gca.2011.09.031

Schwark, L., Zink, K. & Lechterbeck, J. (2002) Reconstruction of postglacial to early Holocene vegetation history in terrestrial Central Europe via cuticular lipid biomarkers and pollen records from lake sediments. *Geology*, 30(5), 463–466. Available at: https://doi.org/10.1130/0091-7613(2002)030<0463:ROPTEH>2.0.CO;2

Sear, D.A., Allen, M.S., Hassall, J.D., Maloney, A.E., Langdon, P.G., Morrison, A.E. *et al.* (2020) Human settlement of East Polynesia earlier, incremental, and coincident with prolonged South Pacific drought. *Proceedings of the National Academy of Sciences*, 117, 8813–8819. Available at: https://doi.org/10.1073/pnas.1920975117

Sefton, J., (2020) Evaluating mangrove proxies for quantitative relative sea-level reconstructions. PhD Thesis, Department of Geography, Durham University, Durham, U.K.

Segato, D., Villoslada Hidalgo, M.D.C., Edwards, R., Barbaro, E., Vallelonga, P., Kjær, H.A. *et al.* (2021) Five thousand years of fire history in the high North Atlantic region: natural variability and ancient human forcing. *Climate of the Past*, 17, 1533–1545. Available at: https://doi.org/10.5194/cp-17-1533-2021,2021

Seki, O., Meyers, P.A., Kawamura, K., Zheng, Y. & Zhou, W. (2009) Hydrogen isotopic ratios of plant wax n-alkanes in a peat bog deposited in northeast China during the last 16kyr. *Organic Geochemistry*, 40(6), 671–677. Available at: https://doi.org/10.1016/j.orggeochem.2009.03.007

Sessions, A.L. (2016) Factors controlling the deuterium contents of sedimentary hydrocarbons. *Organic Geochemistry*, 96, 43–64. Available at: https://doi.org/10.1016/j.orggeochem.2016.02.012

Sessions, A.L., Burgoyne, T.W., Schimmelmann, A. & Hayes, J.M. (1999) Fractionation of hydrogen isotopes in lipid biosynthesis. *Organic Geochemistry*, 30, 1193–1200. Available at: https://doi.org/10.1016/S0146-6380(99)00094-7

Sharifi, A., Pourmand, A., Canuel, E.A., Ferer-Tyler, E., Peterson, L.C., Aichner, B. *et al.* (2015) Abrupt climate variability since the last deglaciation based on a high-resolution, multi-proxy peat record from NW Iran: The hand that rocked the Cradle of Civilization? *Quaternary Science Reviews*, 123, 215–230. Available at: https://doi.org/10.1016/j.quascirev.2015.07.006

Shillito, L.-M., Whelton, H.L., Blong, J.C., Jenkins, D.L., Connolly, T.J. & Bull, I.D. (2020) Pre-Clovis occupation of the Americas identified by human fecal biomarkers in coprolites from Paisley Caves, Oregon. *Science Advances*, 6, eaba6404, Available at: https://doi.org/10.1126/sciadv.aba6404.

Shintani, T., Yamamoto, M. & Chen, M.-T. (2011) Paleoenvironmental changes in the northern South China Sea over the past 28,000years: A study of TEX86-derived sea surface temperatures and terrestrial biomarkers. *Journal of Asian Earth Sciences*, 40(6), 1221–1229. Available at: https://doi.org/10.1016/j.jseaes.2010.09.013

Simoneit, B.R.T. (2002) Biomass burning — a review of organic tracers for smoke from incomplete combustion. *Applied Geochemistry*, 17(3), 129–162. Available at: https://doi.org/10.1016/S0883-2927(01)00061-0

Simoneit, B.R.T., Schauer, J.J., Nolte, C.G., Oros, D.R., Elias, V.O., Fraser, M.P. *et al.* (1999) Levoglucosan, a tracer for cellulose in biomass burning and atmospheric particles. *Atmospheric Environment*, Vol. 33(2), 173–182. Available at: https://doi.org/10.1016/S1352-2310(98)00145-9

Simpson, I.A., Dockrill, S.J., Bull, I.D. & Evershed, R.P. (1998) Early Anthropogenic Soil Formation at Tofts Ness, Sanday, Orkney. *Journal of Archaeological Science*, 25(8), 729–746. Available at: https://doi.org/10.1006/jasc.1997.0216

Sinninghe Damsté, J.S., Ossebaar, J., Schouten, S. & Verschuren, D. (2012) Distribution of tetraether lipids in the 25-ka sedimentary record of Lake Challa: extracting reliable TEX86 and MBT/CBT palaeotemperatures from an equatorial African lake. *Quaternary Science Reviews*, 50, 43–54. Available at: https://doi.org/10.1016/j.quascirev.2012.07.001

Sinninghe Damsté, J.S., Rijpstra, W.I.C., Coolen, M.J.L., Schouten, S. & Volkman, J.K. (2007) Rapid sulfurisation of highly branched isoprenoid (HBI) alkenes in sulfidic Holocene sediments from Ellis Fjord, Antarctica. *Organic Geochemistry*, 38(1), 128–139. Available at: https://doi.org/10.1016/j.orggeochem.2006.08.003

Sinninghe Damsté, J.S., Schouten, S. & van Duin, A.C.T. (2001) Isorenieratene derivatives in sediments: possible controls on their distribution. *Geochimica et Cosmochimica Acta*, 65, 1557–1571. Available at: https://doi.org/10.1016/S0016-7037(01)00549-X

Sinninghe Damsté, J.S., Verschuren, D., Ossebaar, J., Blokker, J., van Houten, R., van der Meer, M.T.J. *et al.* (2011) A 25,000-year record of climate-induced changes in lowland vegetation of eastern equatorial Africa revealed by the stable carbon-isotopic composition of fossil plant leaf waxes. *Earth and Planetary Science Letters*, 302, 236–246. Available at: https://doi.org/10.1016/j.epsl.2010.12.025

Sinninghe Damsté, J.S., Weber, Y., Zopfi, J., Lehmann, M.F. & Niemann, H. (2022) Distributions and sources of isoprenoidal GDGTs in Lake Lugano and other central European (peri-)alpine lakes: Lessons for their use as paleotemperature proxies. *Quaternary Science Reviews*, 277, 107352, Available at: https://doi.org/10.1016/j.quascirev.2021.107352.

Sistiaga, A., Mallol, C., Galván, B. & Summons, R.E. (2014) The Neanderthal Meal: A New Perspective Using Faecal Biomarkers. *PLoS One*, 9(6), e101045. Available at: https://doi.org/10.1371/journal.pone.0101045

Smith, F.A. & Freeman, K.H. (2006) Influence of physiology and climate on δD of leaf wax n-alkanes from C3 and C4 grasses. *Geochimica et Cosmochimica Acta*, 70(5), 1172–1187. Available at: https://doi.org/10.1016/j.gca.2005.11.006

Smith, J.A., Callard, L., Bentley, M.J., Jamieson, S.S.R., Sánchez-Montes, M.L., Lane, T.P. *et al.* (2023) Holocene history of the 79° N ice shelf reconstructed from epishelf lake and uplifted glaciomarine sediments. *The Cryosphere*, 17(3), 1247–1270. Available at: https://doi.org/10.5194/tc-17-1247-2023

Song, M., Zhou, A., He, Y., Zhao, C., Wu, J., Zhao, Y. *et al.* (2016) Environmental controls on long-chain alkenone occurrence and compositional patterns in lacustrine sediments, northwestern China. *Organic Geochemistry*, 91, 43–53. Available at: https://doi.org/10.1016/j.orggeochem.2015.10.009

Spencer-Jones, C.L., McClymont, E.L., Bale, N.J., Hopmans, E.C., Schouten, S., Müller, J. *et al.* (2021) Archaeal intact polar lipids in polar waters: a comparison between the Amundsen and Scotia seas. *Biogeosciences*, 18, 3485–3504. Available at: https://doi.org/10.5194/bg-18-3485-2021

Spencer-Jones, C.L., Wagner, T. & Talbot, H.M. (2017) A record of aerobic methane oxidation in tropical Africa over the last 2.5 Ma. *Geochimica et Cosmochimica Acta*, 218, 27–39. Available at: https://doi.org/10.1016/j.gca.2017.08.042

Stein, R., Fahl, K., Schade, I., Manerung, A., Wassmuth, S., Niessen, F. *et al.* (2017) Holocene variability in sea ice cover, primary production, and Pacific-Water inflow and climate change in the Chukchi and East Siberian Seas (Arctic Ocean): HOLOCENE SEA ICE CHANGES IN THE CHUKCHI AND EAST SIBERIAN SEAS. *Journal of Quaternary Science*, 32, 362–379. Available at: https://doi.org/10.1002/jqs.2929

Stein, R., Hefter, J., Grützner, J., Voelker, A. & Naafs, B.D.A. (2009) Variability of surface water characteristics and Heinrich-like events

in the Pleistocene midlatitude North Atlantic Ocean: Biomarker and XRD records from IODP Site U1313 (MIS 16-9): NORTH ATLANTIC PALEOCEANOGRAPHY. *Paleoceanography*, 24, n/a. Available at: https://doi.org/10.1029/2008PA001639

Stockhecke, M., Bechtel, A., Peterse, F., Guillemot, T. & Schubert, C.J. (2021) Temperature, precipitation, and vegetation changes in the Eastern Mediterranean over the last deglaciation and Dansgaard-Oeschger events. *Palaeogeography, Palaeoclimatology, Palaeoecology*, 577, 110535, Available at: https://doi.org/10.1016/j.palaeo.2021.110535.

Stogiannidis, E. & Laane, R. (2015) Source Characterization of Polycyclic Aromatic Hydrocarbons by Using Their Molecular Indices: An Overview of Possibilities. In: Whitacre, D.M., (ed.) *Reviews of Environmental Contamination and Toxicology*. Cham: Springer International Publishing (Reviews of Environmental Contamination and Toxicology). pp. 49–133. https://doi.org/10.1007/978-3-319-10638-0_2

Sun, S., Meyer, V.D., Dolman, A.M., Winterfeld, M., Hefter, J., Dummann, W. *et al*. (2020) ^{14}C Blank Assessment in Small-Scale Compound-Specific Radiocarbon Analysis of Lipid Biomarkers and Lignin Phenols. *Radiocarbon*, 62(1), 207–218. Available at: https://doi.org/10.1017/RDC.2019.108

Talbot, H.M. & Farrimond, P. (2007) Bacterial populations recorded in diverse sedimentary biohopanoid distributions. *Organic Geochemistry*, 38, 1212–1225. Available at: https://doi.org/10.1016/j.orggeochem.2007.04.006

Talbot, H.M., Handley, L., Spencer-Jones, C.L., Dinga, B.J., Schefuß, E., Mann, P.J. *et al*. (2014) Variability in aerobic methane oxidation over the past 1.2Myrs recorded in microbial biomarker signatures from Congo fan sediments. *Geochimica et Cosmochimica Acta*, 133, 387–401. Available at: https://doi.org/10.1016/j.gca.2014.02.035

Talbot, H.M., McClymont, E.L., Inglis, G.N. et al (2016) Origin and preservation of bacteriohopanepolyol signatures in Sphagnum peat from Bissendorfer Moor (Germany). *Organic Geochemistry*, 97, 95–110. Available at: https://doi.org/10.1016/j.orggeochem.2016.04.011

Talbot, H.M., Watson, D.F., Pearson, E.J. & Farrimond, P. (2003) Diverse biohopanoid compositions of non-marine sediments. *Organic Geochemistry*, 34, 1353–1371. Available at: https://doi.org/10.1016/S0146-6380(03)00159-1

Tamalavage, A.E., van Hengstum, P.J., Louchouarn, P., Fall, P.L., Donnelly, J.P., Albury, N.A. *et al*. (2020) Plant wax evidence for precipitation and vegetation change from a coastal sinkhole lake in the Bahamas spanning the last 3000 years. *Organic Geochemistry*, 150, 104120, Available at: https://doi.org/10.1016/j.orggeochem.2020.104120.

Tan, Z., Wu, C., Han, Y., Zhang, Y., Mao, L., Li, D. *et al*. (2020) Fire history and human activity revealed through poly cyclic aromatic hydrocarbon (PAH) records at archaeological sites in the middle reaches of the Yellow River drainage basin, China. *Palaeogeography, Palaeoclimatology, Palaeoecology*, 560, 110015, Available at: https://doi.org/10.1016/j.palaeo.2020.110015.

Tareq, S.M., Tanaka, N. & Ohta, K. (2004) Biomarker signature in tropical wetland: lignin phenol vegetation index (LPVI) and its implications for reconstructing the paleoenvironment. *Science of the Total Environment*, 324, 91–103. Available at: https://doi.org/10.1016/j.scitotenv.2003.10.020

Tesi, T., Belt, S.T., Gariboldi, K., Muschitiello, F., Smik, L., Finocchiaro, F. *et al*. (2020) Resolving sea ice dynamics in the north-western Ross Sea during the last 2.6 ka: From seasonal to millennial timescales. *Quaternary Science Reviews*, 237, 106299, Available at: https://doi.org/10.1016/j.quascirev.2020.106299.

Tesi, T., Muschitiello, F., Mollenhauer, G., Miserocchi, S., Langone, L., Ceccarelli, C. *et al*. (2021) Rapid Atlantification along the Fram Strait at the beginning of the 20th century. *Science Advances*, 7, eabj2946, Available at: https://doi.org/10.1126/sciadv.abj2946.

Theroux, S., D'Andrea, W.J., Toney, J., Amaral-Zettler, L. & Huang, Y. (2010) Phylogenetic diversity and evolutionary relatedness of alkenone-producing haptophyte algae in lakes: Implications for continental paleotemperature reconstructions. *Earth and Planetary Science Letters*, 300, 311–320. Available at: https://doi.org/10.1016/j.epsl.2010.10.009

Theroux, S., Huang, Y., Toney, J.L., Andersen, R., Nyren, P., Bohn, R. *et al*. (2020) Successional blooms of alkenone-producing haptophytes in Lake George, North Dakota: Implications for continental paleoclimate reconstructions. *Limnology and Oceanography*, 65, 413–425. Available at: https://doi.org/10.1002/lno.11311

Thomas, C.L., Jansen, B., van Loon, E.E. & Wiesenberg, G.L.B. (2021) Transformation of *n*-alkanes from plant to soil: a review. *SOIL*, 7, 785–809. Available at: https://doi.org/10.5194/soil-7-785-2021

Tierney, J.E., Poulsen, C.J., Montañez, I.P., Bhattacharya, T., Feng, R., Ford, H.L. *et al*. (2020) Past climates inform our future. *Science*, 370, eaay3701, Available at: https://doi.org/10.1126/science.aay3701.

Tierney, J.E., Russell, J.M. & Huang, Y. (2010) A molecular perspective on Late Quaternary climate and vegetation change in the Lake Tanganyika basin, East Africa. *Quaternary Science Reviews*, 29, 787–800. Available at: https://doi.org/10.1016/j.quascirev.2009.11.030

Tierney, J.E. & Tingley, M.P. (2014) A Bayesian, spatially-varying calibration model for the TEX86 proxy. *Geochimica et Cosmochimica Acta*, 127, 83–106. Available at: https://doi.org/10.1016/j.gca.2013.11.026

Tierney, J.E. & Tingley, M.P. (2018) BAYSPLINE: A New Calibration for the Alkenone Paleothermometer. *Paleoceanography and Paleoclimatology*, 33, 281–301. Available at: https://doi.org/10.1002/2017PA003201

Toney, J.L., Huang, Y., Fritz, S.C., Baker, P.A., Grimm, E. & Nyren, P. (2010) Climatic and environmental controls on the occurrence and distributions of long chain alkenones in lakes of the interior United States. *Geochimica et Cosmochimica Acta*, 74, 1563–1578. Available at: https://doi.org/10.1016/j.gca.2009.11.021

Trigui, Y., Wolf, D., Sahakyan, L., Hovakimyan, H., Sahakyan, K., Zech, R. *et al*. (2019) First Calibration and Application of Leaf Wax *n*-Alkane Biomarkers in Loess-Paleosol Sequences and Modern Plants and Soils in Armenia. *Geosciences*, 9(6), 263. Available at: https://doi.org/10.3390/geosciences9060263

Turich, C. & Freeman, K.H. (2011) Archaeal lipids record paleosalinity in hypersaline systems. *Organic Geochemistry*, 42(9), 1147–1157. Available at: https://doi.org/10.1016/j.orggeochem.2011.06.002

Vachula, R.S., Huang, Y., Longo, W.M., Dee, S.G., Daniels, W.C. & Russell, J.M. (2019) Evidence of Ice Age humans in eastern Beringia suggests early migration to North America. *Quaternary Science Reviews*, 205, 35–44. Available at: https://doi.org/10.1016/j.quascirev.2018.12.003

Vachula, R.S., Karp, A.T., Denis, E.H., Balascio, N.L., Canuel, E.A. & Huang, Y. (2022) Spatially calibrating polycyclic aromatic hydrocarbons (PAHs) as proxies of area burned by vegetation fires: Insights from comparisons of historical data and sedimentary PAH fluxes. *Palaeogeography, Palaeoclimatology, Palaeoecology*, 596, 110995, Available at: https://doi.org/10.1016/j.palaeo.2022.110995.

van der Meer, M.T.J., Baas, M., Rijpstra, W.I.C., Marino, G., Rohling, E.J., Sinninghe Damsté, J.S. *et al*. (2007) Hydrogen isotopic compositions of long-chain alkenones record freshwater flooding of the Eastern Mediterranean at the onset of sapropel deposition. *Earth and Planetary Science Letters*, 262, 594–600. Available at: https://doi.org/10.1016/j.epsl.2007.08.014

van der Meer, M.T.J., Sangiorgi, F., Baas, M., Brinkhuis, H., Sinninghe Damsté, J.S. & Schouten, S. (2008) Molecular isotopic and dinoflagellate evidence for Late Holocene freshening of the Black Sea. *Earth and Planetary Science Letters*, 267(3–4), 426–434. Available at: https://doi.org/10.1016/j.epsl.2007.12.001

van der Bilt, W.G.M., D'Andrea, W.J., Oppedal, L.T., Bakke, J., Bjune, A.E. & Zwier, M. (2022) Stable Southern Hemisphere westerly winds throughout the Holocene until intensification in the last two millennia. *Communications Earth & Environment*, 3, 186, Available at: https://doi.org/10.1038/s43247-022-00512-8.

van Geel, B., Aptroot, A., Baittinger, C., Birks, H.H., Bull, I.D., Cross, H.B. *et al*. (2008) The ecological implications of a Yakutian mammoth's last meal. *Quaternary Research*, 69(3), 361–376. Available at: https://doi.org/10.1016/j.yqres.2008.02.004

Versteegh, G.J.M., Schefuß, E., Dupont, L., Marret, F., Sinninghe Damsté, J.S. & Jansen, J.H.F. (2004) Taraxerol and Rhizophora pollen as proxies for tracking past mangrove ecosystems. *Geochimica et Cosmochimica Acta*, 68, 411–422. Available at: https://doi.org/10.1016/S0016-7037(03)00456-3

Volkman, J.K. (1986) A review of sterol markers for marine and terrigenous organic matter. *Organic Geochemistry*, 9(2), 83–99. Available at: https://doi.org/10.1016/0146-6380(86)90089-6

Vorrath, M.-E., Müller, J., Rebolledo, L., Cárdenas, P., Shi, X., Esper, O. *et al.* (2020) Sea ice dynamics in the Bransfield Strait, Antarctic Peninsula, during the past 240 years: a multi-proxy intercomparison study. *Climate of the Past*, 16, 2459–2483. Available at: https://doi.org/10.5194/cp-16-2459-2020

Wakeham, S.G. (1989) Reduction of stenols to stanols in particulate matter at oxic–anoxic boundaries in sea water. *Nature*, 342, 787–790. Available at: https://doi.org/10.1038/342787a0

Wakeham, S.G., Hedges, J.I., Lee, C., Peterson, M.L. & Hernes, P.J. (1997) Compositions and transport of lipid biomarkers through the water column and surficial sediments of the equatorial Pacific Ocean. *Deep Sea Research Part II: Topical Studies in Oceanography*, 44(9), 2131–2162. Available at: https://doi.org/10.1016/S0967-0645(97)00035-0

Wakeham, S.G., Schaffner, C. & Giger, W. (1980) Polycyclic aromatic hydrocarbons in Recent lake sediments—I. Compounds having anthropogenic origins. *Geochimica et Cosmochimica Acta*, 44(3), 403–413. Available at: https://doi.org/10.1016/0016-7037(80)90040-X

Wang, C., Bendle, J.A., Greene, S.E. et al (2019a) Speleothem biomarker evidence for a negative terrestrial feedback on climate during Holocene warm periods. *Earth and Planetary Science Letters*, 525, 115754, Available at: https://doi.org/10.1016/j.epsl.2019.115754.

Wang, C., Bendle, J.A., Yang, H., Yang, Y., Hardman, A., Yamoah, A. *et al.* (2021a) Global calibration of novel 3-hydroxy fatty acid based temperature and pH proxies. *Geochimica et Cosmochimica Acta*, 302, 101–119. Available at: https://doi.org/10.1016/j.gca.2021.03.010

Wang, J., Chen, L., Li, L., He, J., Chen, J., Jiang, C. *et al.* (2014) Preliminary identification of palaeofloods with the alkane ratio C31/C17 and their potential link to global climate changes. *Scientific Reports*, 4, 6502, Available at: https://doi.org/10.1038/srep06502.

Wang, J., Wang, Y., Wang, X. & Sun, L. (2007) Penguins and vegetations on Ardley Island, Antarctica: evolution in the past 2,400 years. *Polar Biology*, 30, 1475–1481. Available at: https://doi.org/10.1007/s00300-007-0308-9

Wang, K.J., Huang, Y., Majaneva, M. et al (2021b) Group 2i Isochrysidales produce characteristic alkenones reflecting sea ice distribution. *Nature Communications*, 12(1), 15, Available at: https://doi.org/10.1038/s41467-020-20187-z.

Wang, K.J., O'Donnell, J.A., Longo, W.M. et al (2019b) Group I alkenones and Isochrysidales in the world's largest maar lakes and their potential paleoclimate applications. *Organic Geochemistry*, 138, 103924, Available at: https://doi.org/10.1016/j.orggeochem.2019.103924.

Wang, M., Zheng, Z., Man, M., Hu, J. & Gao, Q. (2017) Branched GDGT-based paleotemperature reconstruction of the last 30,000years in humid monsoon region of Southeast China. *Chemical Geology*, 463, 94–102. Available at: https://doi.org/10.1016/j.chemgeo.2017.05.014

Wang, M., Zong, Y., Zheng, Z. et al (2018) Utility of brGDGTs as temperature and precipitation proxies in subtropical China. *Scientific Reports*, 8(1), 194, Available at: https://doi.org/10.1038/s41598-017-17964-0.

Wang, Y.V., Larsen, T., Leduc, G., Andersen, N., Blanz, T. & Schneider, R.R. (2013) What does leaf wax δD from a mixed C3/C4 vegetation region tell us? *Geochimica et Cosmochimica Acta*, 111, 128–139. Available at: https://doi.org/10.1016/j.gca.2012.10.016

Warnock, J.P., Bauersachs, T., Kotthoff, U., Brandt, H.T. & Andrén, E. (2018) Holocene environmental history of the Ångermanälven Estuary, northern Baltic Sea. *Boreas*, 47, 593–608. Available at: https://doi.org/10.1111/bor.12281

Watson, B.I., Williams, J.W., Russell, J.M., Jackson, S.T., Shane, L. & Lowell, T.V. (2018) Temperature variations in the southern Great Lakes during the last deglaciation: Comparison between pollen and GDGT proxies. *Quaternary Science Reviews*, 182, 78–92. Available at: https://doi.org/10.1016/j.quascirev.2017.12.011

Weckström, K., Massé, G., Collins, L.G., Hanhijärvi, S., Bouloubassi, I., Sicre, M.A. *et al.* (2013) Evaluation of the sea ice proxy IP25 against observational and diatom proxy data in the SW Labrador Sea. *Quaternary Science Reviews*, 79, 53–62. Available at: https://doi.org/10.1016/j.quascirev.2013.02.012

Weijers, J.W.H., Schouten, S., van den Donker, J.C., Hopmans, E.C. & Sinninghe Damsté, J.S. (2007) Environmental controls on bacterial tetraether membrane lipid distribution in soils. *Geochimica et Cosmochimica Acta*, 71(3), 703–713. Available at: https://doi.org/10.1016/j.gca.2006.10.003

White, A.J., Stevens, L.R., Lorenzi, V., Munoz, S.E., Lipo, C.P. & Schroeder, S. (2018) An evaluation of fecal stanols as indicators of population change at Cahokia, Illinois. *Journal of Archaeological Science*, 93, 129–134. Available at: https://doi.org/10.1016/j.jas.2018.03.009

White, A.J., Stevens, L.R., Lorenzi, V., Munoz, S.E., Schroeder, S., Cao, A. *et al.* (2019) Fecal stanols show simultaneous flooding and seasonal precipitation change correlate with Cahokia's population decline. *Proceedings of the National Academy of Sciences*, 116(12), 5461–5466. Available at: https://doi.org/10.1073/pnas.1809400116

White, D.M., Garland, D.S., Beyer, L. & Yoshikawa, K. (2004) Pyrolysis-GC/MS fingerprinting of environmental samples. *Journal of Analytical and Applied Pyrolysis*, 71(1), 107–118. Available at: https://doi.org/10.1016/S0165-2370(03)00101-3

Wolhowe, M.D., Prahl, F.G., Probert, I. & Maldonado, M. (2009) Growth phase dependent hydrogen isotopic fractionation in alkenone-producing haptophytes. *Biogeosciences*, 6, 1681–1694. Available at: https://doi.org/10.5194/bg-6-1681-2009

Xiao, X., Zhao, M., Knudsen, K.L., Sha, L., Eiríksson, J., Gudmundsdóttir, E. *et al.* (2017) Deglacial and Holocene sea–ice variability north of Iceland and response to ocean circulation changes. *Earth and Planetary Science Letters*, 472, 14–24. Available at: https://doi.org/10.1016/j.epsl.2017.05.006

Xie, S., Nott, C.J., Avsejs, L.A., Volders, F., Maddy, D., Chambers, F.M. *et al.* (2000) Palaeoclimate records in compound-specific δD values of a lipid biomarker in ombrotrophic peat. *Organic Geochemistry*, 31(10), 1053–1057. Available at: https://doi.org/10.1016/S0146-6380(00)00116-9

Xie, S., Yi, Y., Huang, J., Hu, C., Cai, Y., Collins, M. *et al.* (2003) Lipid distribution in a subtropical southern China stalagmite as a record of soil ecosystem response to paleoclimate change. *Quaternary Research*, 60, 340–347. Available at: https://doi.org/10.1016/j.yqres.2003.07.010

Yamamoto, Y., Ajioka, T. & Yamamoto, M. (2016) Climate reconstruction based on GDGT-based proxies in a paleosol sequence in Japan: Postdepositional effect on the estimation of air temperature. *Quaternary International*, 397, 380–391. Available at: https://doi.org/10.1016/j.quaint.2014.12.009

Yamane, M., Yokoyama, Y., Miyairi, Y., Suga, H., Matsuzaki, H., Dunbar, R.B. *et al.* (2014) Compound-Specific ^{14}C Dating of IODP Expedition 318 Core U1357A Obtained Off the Wilkes Land Coast, Antarctica. *Radiocarbon*, 56(3), 1009–1017. Available at: https://doi.org/10.2458/56.17773

Yang, H., Pagani, M., Briggs, D.E.G., Equiza, M.A., Jagels, R., Leng, Q. *et al.* (2009) Carbon and hydrogen isotope fractionation under continuous light: implications for paleoenvironmental interpretations of the High Arctic during Paleogene warming. *Oecologia*, 160, 461–470. Available at: https://doi.org/10.1007/s00442-009-1321-1

Yang, H., Pancost, R.D., Dang, X., Zhou, X., Evershed, R.P., Xiao, G. *et al.* (2014) Correlations between microbial tetraether lipids and environmental variables in Chinese soils: Optimizing the paleo-reconstructions in semi-arid and arid regions. *Geochimica et Cosmochimica Acta*, 126, 49–69. Available at: https://doi.org/10.1016/j.gca.2013.10.041

Yang, Y., Wang, C., Bendle, J.A., Yu, X., Gao, C., Lü, X. *et al.* (2020) A new sea surface temperature proxy based on bacterial 3-hydroxy fatty acids. *Organic Geochemistry*, 141, 103975, Available at: https://doi.org/10.1016/j.orggeochem.2020.103975.

Yao, Y., Zhao, J., Vachula, R.S., Liao, S., Li, G., Pearson, E.J. *et al.* (2022) Phylogeny, alkenone profiles and ecology of Isochrysidales subclades in saline lakes: Implications for paleosalinity and paleotemperature reconstructions. *Geochimica et Cosmochimica Acta*, 317, 472–487. Available at: https://doi.org/10.1016/j.gca.2021.11.001

Zennaro, P., Kehrwald, N., McConnell, J.R., Schüpbach, S., Maselli, O.J., Marlon, J. *et al.* (2014) Fire in ice: two millennia of boreal forest fire history from the Greenland NEEM ice core. *Climate of the Past*, 10, 1905–1924. Available at: https://doi.org/10.5194/cp-10-1905-2014

Zhang, Z., Sachs, J.P. & Marchetti, A. (2009) Hydrogen isotope fractionation in freshwater and marine algae: II. Temperature and nitrogen limited growth rate effects. *Organic Geochemistry*, 40(3), 428–439. Available at: https://doi.org/10.1016/j.orggeochem.2008.11.002

Zhang, Z., Zhao, M., Eglinton, G., LU, H. & HUANG, C. (2006) Leaf wax lipids as paleovegetational and paleoenvironmental proxies for the Chinese Loess Plateau over the last 170kyr. *Quaternary Science Reviews*, 25, 575–594. Available at: https://doi.org/10.1016/j.quascirev.2005.03.009

Zhao, M., Mercer, J.L., Eglinton, G., Higginson, M.J. & Huang, C.Y. (2006) Comparative molecular biomarker assessment of phytoplankton paleoproductivity for the last 160kyr off Cap Blanc, NW Africa. *Organic Geochemistry*, 37, 72–97. Available at: https://doi.org/10.1016/j.orggeochem.2005.08.022

Zheng, Y., Fang, Z., Fan, T., Liu, Z., Wang, Z., Li, Q. *et al.* (2019) Operation of the boreal peatland methane cycle across the past 16 k.y. *Geology*, 48(1), 82–86. Available at: https://doi.org/10.1130/G46709.1

Zheng, Y., Pancost, R.D., Naafs, B.D.A., Li, Q., Liu, Z. & Yang, H. (2018) Transition from a warm and dry to a cold and wet climate in NE China across the Holocene. *Earth and Planetary Science Letters*, 493, 36–46. Available at: https://doi.org/10.1016/j.epsl.2018.04.019

Zheng, Y., Singarayer, J.S., Cheng, P., Yu, X., Liu, Z., Valdes, P.J. *et al.* (2014) Holocene variations in peatland methane cycling associated with the Asian summer monsoon system. *Nature Communications*, 5, 4631, Available at: https://doi.org/10.1038/ncomms5631.

Zheng, Y., Zhou, W., Meyers, P.A. & Xie, S. (2007) Lipid biomarkers in the Zoigê-Hongyuan peat deposit: Indicators of Holocene climate changes in West China. *Organic Geochemistry*, 38(11), 1927–1940. Available at: https://doi.org/10.1016/j.orggeochem.2007.06.012

Zhou, W., Zheng, Y., Meyers, P.A., Jull, A.J.T. & Xie, S. (2010) Postglacial climate-change record in biomarker lipid compositions of the Hani peat sequence, Northeastern China. *Earth and Planetary Science Letters*, 294(1-2), 37–46. Available at: https://doi.org/10.1016/j.epsl.2010.02.035

Zindorf, M., Rush, D., Jaeger, J., Mix, A., Penkrot, M.L., Schnetger, B. *et al.* (2020) Reconstructing oxygen deficiency in the glacial Gulf of Alaska: Combining biomarkers and trace metals as paleo-redox proxies. *Chemical Geology*, 558, 119864. Available at 425 https://doi.org/10.1016/j.chemgeo.2020.119864,2020

Zocatelli, R., Lavrieux, M., Guillemot, T., Chassiot, L., Le Milbeau, C. & Jacob, J. (2017) Fecal biomarker imprints as indicators of past human land uses: Source distinction and preservation potential in archaeological and natural archives. *Journal of Archaeological Science*, 81, 79–89. Available at: https://doi.org/10.1016/j.jas.2017.03.010